CSA Engineering, Inc.
Engineering Consultants in Applied Mechanics

560 San Antonio Road Suite 101 Palo Alto, California 94306 (415) 494-7351

30-FT. FREE DROP TESTS OF A QUARTER-SCALE MODEL 2000 TRANSPORT PACKAGE

Submitted To:

GENERAL ELECTRIC COMPANY VALLECITOS NUCLEAR CENTER, PLEASANTON, CA

Report No. 87-08-01

August 1987

CSA Engineering, Inc.
Engineering Consultants in Applied Mechanics

This report describes a series of 30-foot, free drop tests performed on a 1/4-scale model of a General Electric Model 2000 Transport Package. The work was performed for General Electric Vallecitos Nuclear Center under Purchase Order No. 205-87C338.

Prepared by: 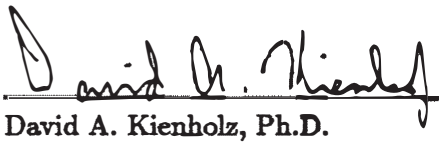

David A. Kienholz, Ph.D.
Principal Engineer

Bradley R. Allen
Engineer

Contents

1. Introduction and Summary **1**

2. Objectives **1**

3. Test Article **2**
3.1 Scaling Relations 6

4. Instrumentation **8**
4.1 Acceleration Measurements 8
4.2 Force Distribution Measurements 11
4.3 Photography 13
4.4 Deformation Measurements 15

5. Procedure **16**

6. Results **19**
6.1 Head-On Drop 19
6.1.1 Acceleration Data and High-Speed Photography 19
6.1.2 Pressure- Sensing Film 24
6.1.3 Cask and Overpack Deformation Measurements 26
6.2 Side Drop 28
6.2.1 Acceleration Data and High-Speed Photography 28
6.2.2 Pressure-Sensing Film 35
6.2.3 Cask and Overpack Deformation Measurements 35
6.3 CG-Over-Corner Drop 35
6.3.1 Acceleration Data and High-Speed Photography 35
6.3.2 Pressure- Sensing Film 42
6.3.3 Cask and Overpack Deformation Measurements 42

7. Summary and Conclusions **44**

List of Figures

1 Quarter-scale model of Model 2000 Transport Package showing accelerometer locations for drop tests 2
2 Model 2000 Transport Package details 3
3 Overpack weldments 4
4 Assembled package 5
5 Accelerometers mounted inside the cask 9
6 Accelerometers mounted outside the overpack 10
7 Accelerometer signal processing 11
8 Apparatus for testing response speed of pressure sensing film 12
9 Pressure-sensing film being applied to cask 14
10 Measurement of toroid profile 15
11 Drop test orientations 16
12 Package rigged for side drop 17
13 Head-on drop, vertical acceleration 20
14 Head-on drop, frames taken at 2.12 millisecond intervals 21
15 Overplot of cask and overpack acceleration, head-on drop 22
16 Toroid deformation caused by head-on drop 23
17 Time integral of cask vertical acceleration, head-on drop 24
18 Pressure-sensing film from head-on drop 25
19 Gage numbering for inspection of overpack top toroid 26
20 Side drop, vertical acceleration 30
21 Side drop, frames taken at 2.13 millisecond intervals 31
22 Overpack weldments separating after impact, side drop 32
23 Package after side drop 33
24 Time integral of cask vertical acceleration prior to cable fault, drop 34
25 Pressure-sensing film from side drop 36
26 Rigging for CG-over-corner drop 37
27 CG-over-corner drop vertical acceleration 38
28 CG-over-corner drop, frames taken at 2.16 millisecond intervals 39
29 Deformation of overpack produced by CG-over-corner drop 40
30 Time integral of cask vertical acceleration, CG-over-corner drop 41
31 Pressure-sensing film from CG-over-corner drop 43

1. INTRODUCTION AND SUMMARY

The General Electric Company Vallecitos Nuclear Center (GEVNC) designs and tests containers for shipping radioactive materials. These shielded containers must meet stringent safety requirements, including a 30-foot free drop onto a hard, unyielding horizontal surface. The package must withstand this drop without functional damage to the inner cask containing the radioactive payload.

CSA Engineering, Inc., was retained to perform a series of drop tests of 1/4-scale replicas of the Model 2000 transport package. Performed at the GEVNC facility on June 10, 11, and 14, 1987, the design and execution of the tests are governed by GE procurement specification 22A9367 (Rev. 2), dated June 8, 1987. This report documents the objectives, methods, results and conclusions of the tests.

Drop tests from three orientations were performed with no measurable deformation or other damage to the inner cask. Head-on and CG-over-corner drops were successfully completed with no unexpected results. Complete data on acceleration and internal load distribution were obtained for use in design verification.

An unexpected failure of the overpack bolted joint occurred when the cask was dropped on its side. The causes of the failure and requalification of the joint will be covered in a separate report.[2] The structural failure also caused the loss of some acceleration data. Nonetheless, a valid trace was obtained for the most important part of the impact event, including the portion during which plastic deformation of the overpack occurred and, probably, including the point of maximum vertical cask acceleration.

Subject to the above uncertainty in the side drop test, the maximum vertical accelerations recorded by sensors inside the cask for the head-on, side, and CG-over-corner drops were 408, 185, and 156 G's respectively.

2. OBJECTIVES

The objectives of the tests were to determine, for each of three drop orientations:

1. The damage, if any, suffered by the inner cask.
2. The vertical acceleration of the cask at impact.
3. The force distribution at impact between the inner cask and the outer protective overpack.

[2] Pomares, R. J., to be published

3. TEST ARTICLE

Figures 1 and 2 show the transport package in cross section with dimensions given for the 1/4-scale model. Figures 3 and 4 show the actual test article. The package is composed of two major assemblies: the inner cask and the outer protective overpack. The cask provides containment and radiation shielding for the payload. The overpack provides mechanical and thermal protection for the cask.

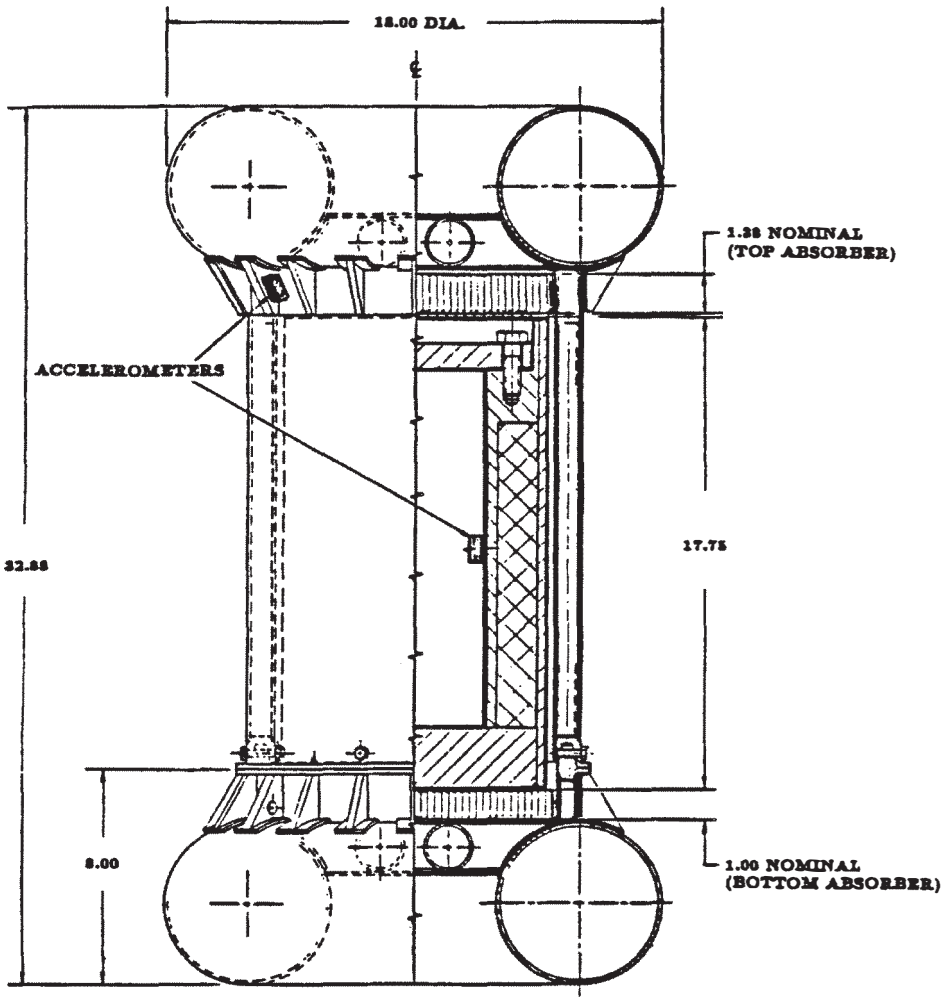

Figure 1. Quarter-scale model of Model 2000 Transport Package showing accelerometer locations for drop tests

The cask is essentially a thick-walled cylinder with a raised rim around the lid seal to protect this critical area. Of particular interest for this test are the impact-limiting features of the overpack. Constructed entirely of 304 stainless steel, it is composed of a double-walled cylindrical shell with identical toroidal shell "bumpers" at either end. Regardless of drop orientation, the initial impact will be taken by one of the toroids. They are designed to plastically deform and buckle inward at a specific load level and thus limit the acceleration of the cask. The cylindrical walls of the overpack are separated by tubular members running parallel to the cask axis. These are likewise designed to crush at a known load. Honeycomb "cushions" are provided between either end of the cask and the overpack for further impact limiting under axial acceleration.

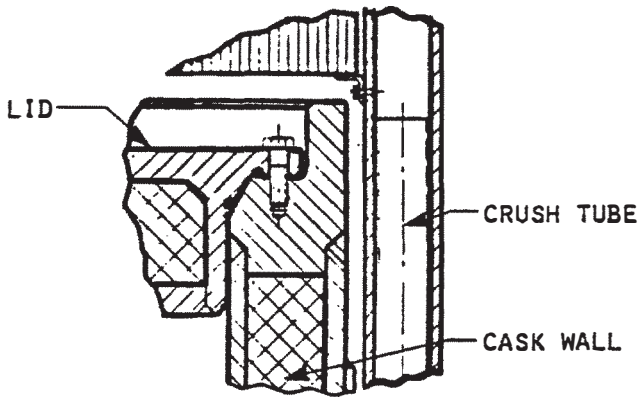

Lid Detail

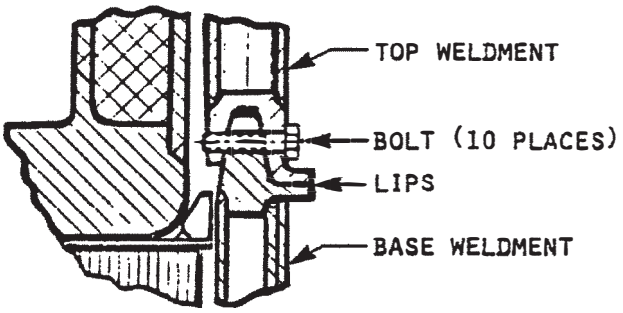

Joint Detail

Figure 2. Model 2000 Transport Package details

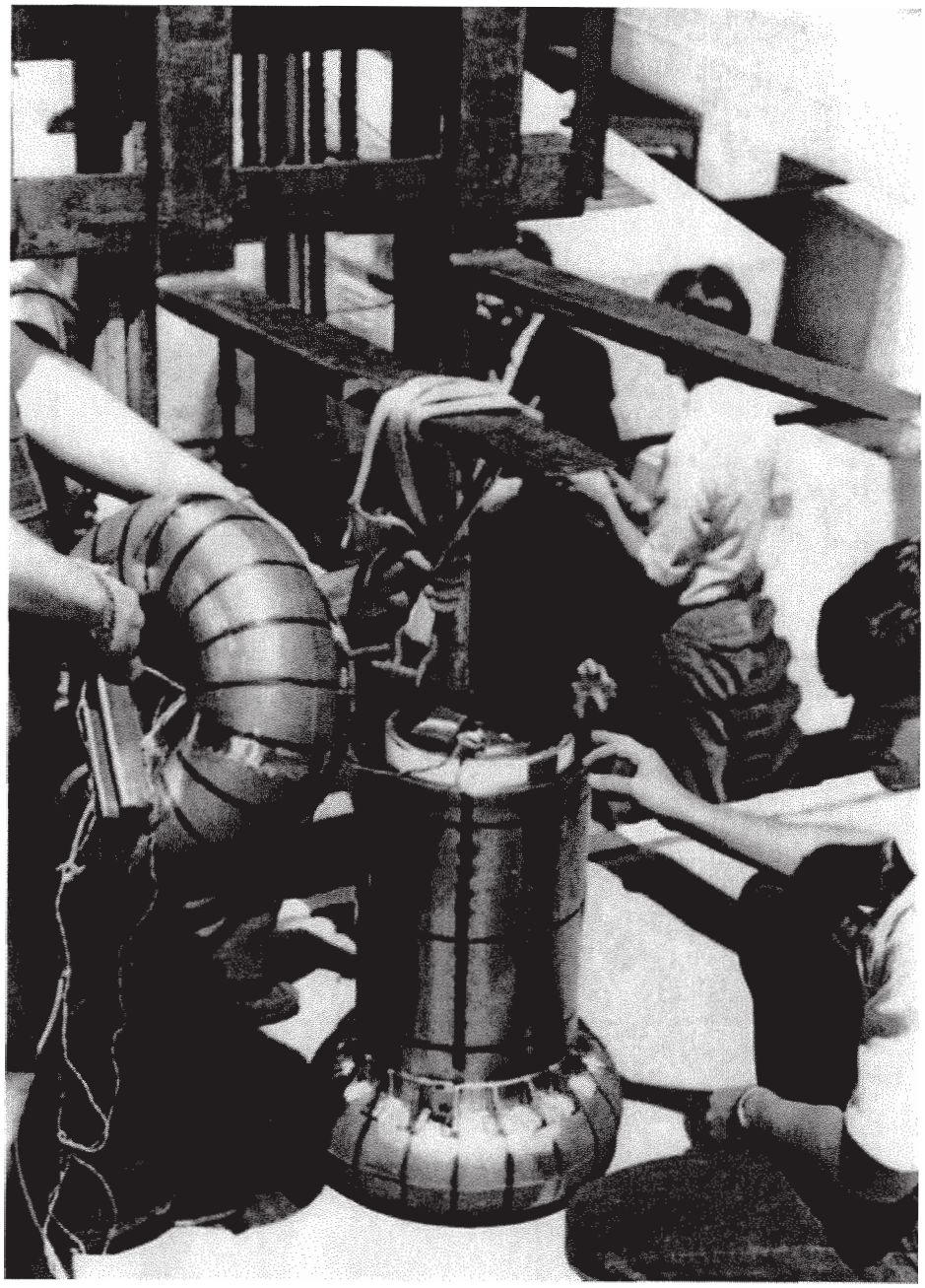

Figure 3. Overpack weldments

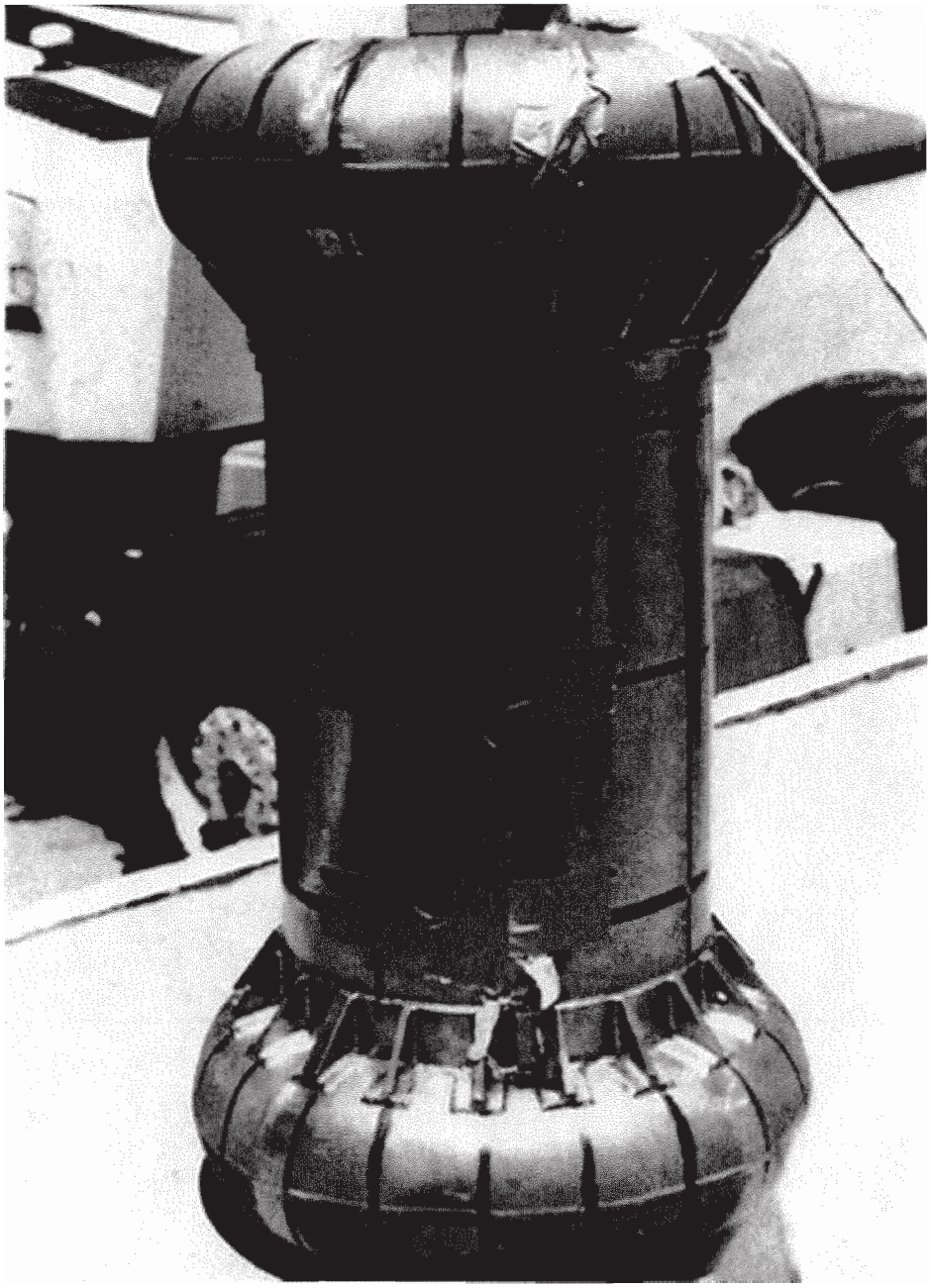

Figure 4 . Assembled package

The overpack is fabricated as two weldments bolted together at a lip joint running circumferentially around the cylinder just inboard of one toroid (see Figures 1 through 4). The smaller weldment is called the base and the larger is called the top. During normal assembly the cask is positioned, lid upwards, on the base and the top is lowered over it. The two weldments are joined at the lip seal by ten bolts, 1/4-inch in diameter for the scale model, inserted radially through the lips as shown in Figure 2.

The payload inside the cask was simulated by blocks of heavy metal, one attached to the lid and one to the floor. Weights of the package components are shown in Table 1.

Table 1: GE Model 2000 Transport Package Component Weights (lbm)

	Full-scale Prototype	1/4-Scale Model
Overpack	9,822	154
Cask	17,647	276
Payload (max.)	5,450	85
Total	32,919	515

One scale model cask and two scale model overpacks were fabricated for the tests. Two complete overpacks were required to insure that the initial impact in each of the three required drops occurred on an undeformed area.

3.1 Scaling Relations

The test article is a near-replica constructed at 1/4-scale. Table 2 shows the classical replica scaling relations for a model constructed of the same material as the full-scale prototype.

The scaling ratios of primary interest here are those for velocity, acceleration, and stress. Velocity scales independent of length. The drop height for the scale model is therefore the same as for a full-scale prototype in order to produce the correct impact velocity. Acceleration scales as $1/\lambda$. A measured value of a_{model} in the current model test therefore corresponds to $a_{model}/4$ for the prototype. Neglecting strain rate effects, stress scales independent of length. Yielding or rupture of material in the model therefore implies a similar result for the prototype.

Table 2: Scaling Relations

Assumptions

- Monolithic structure
- Same material for model and prototype
- Length ratio (model/prototype) = λ

Quantity	Model/Prototype Ratio	
	as function of λ	value for λ = 0.25
Length	λ	0.25
Mass or weight	λ^3	0.0156
Time	λ	0.25
Frequency	$1/\lambda$	4.00
Displacement	λ	0.25
Velocity	1	1.00
Acceleration	$1/\lambda$	4.00
Force	λ^2	0.0625
Moment	λ^3	0.0156
Stress	1	1.00
Strain	1	1.00
Stiffness	λ	0.25

4. Instrumentation

Several diverse types of instrumentation were utilized to sense and record the impact phenomena. These included:

1. Accelerometers with signals recorded on analog magnetic tape
2. Pressure-sensing film
3. High-speed film and videotape photography
4. Micrometers and dial gauge arrays

Details on each are given in this section.

4.1 Acceleration Measurements

Seven accelerometers were mounted on the package: four inside the cask and three on the outside of the overpack. Locations are shown in Figure 1. All were piezoelectric, integrated amplifier (voltage mode) devices with a time constant of 0.5 seconds or greater. A triaxial array mounted inside the cask sensed in the axial, radial, and tangential directions. An additional uniaxial sensor was mounted inside the cask sensing in a direction 29 degrees off the cask axis. Denoted as the cask oblique sensor, its purpose was to measure vertical acceleration of the cask during the CG-over-corner drop. All sensors inside the cask were miniature, general purpose accelerometers with a maximum usable range of 1000 G's. Figure 5 shows the transducers on their mounting block bonded to the inner surface of the cask.

The triaxial array outside the overpack was composed of three sensors mounted in a special machined block to sense in the axial, radial, and tangential directions. These miniature shock accelerometers have a usable range of 10,000 G's. The arrangement is shown in Figure 6.

An eighth accelerometer was mounted on the steel drop pad, several feet away from the impact point. Its output signal was to be used for a timing trigger during data processing. However it was found that using one of the package sensor signals with a small pre-trigger delay was both more reliable and more convenient. The pad accelerometer data was therefore not used.

A schematic of the accelerometer signal chain is shown in Figure 7. Signals were recorded on an instrumentation FM tape recorder for later replay and analysis. The most important signals (vertical acceleration of the cask and overpack) were recorded on two tape channels apiece with different gain settings to optimize the signal/noise ratio. One channel of each pair was ranged to

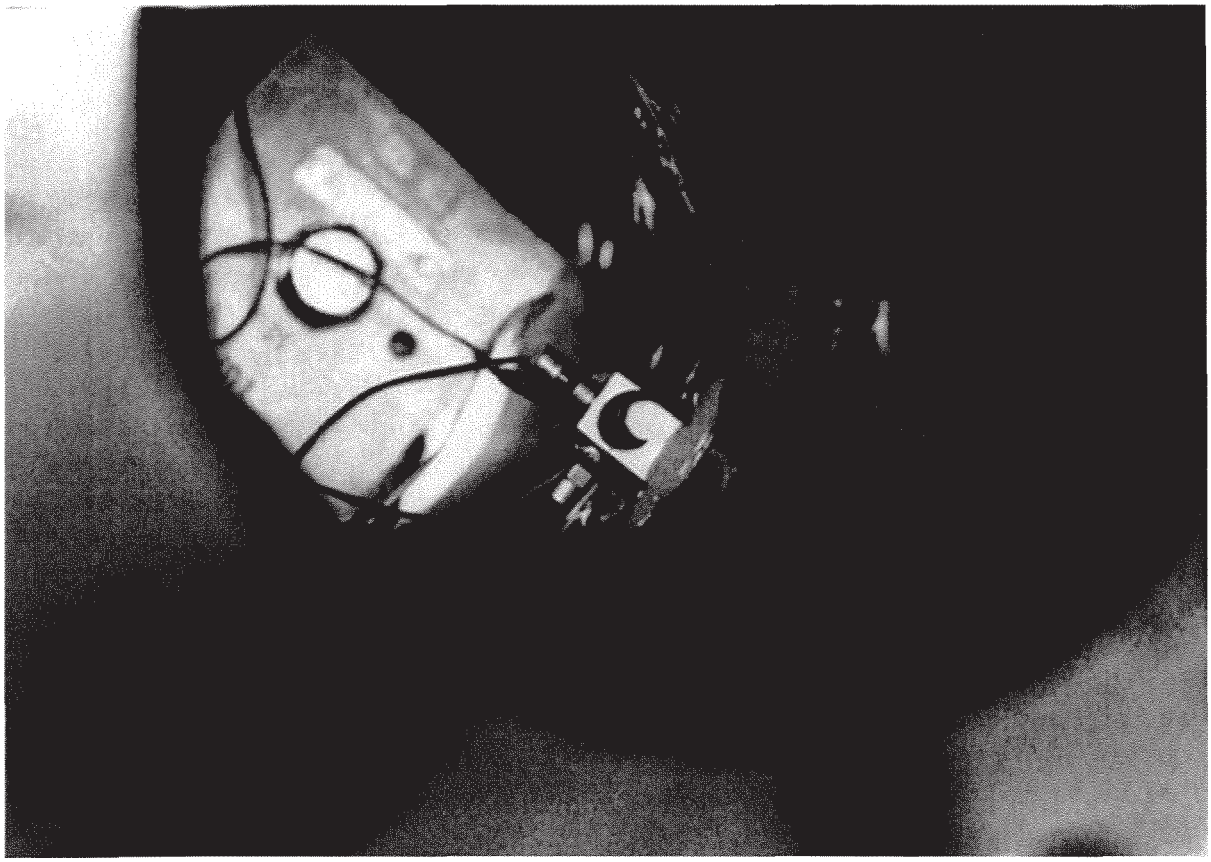

Figure 5. Accelerometers mounted inside the cask

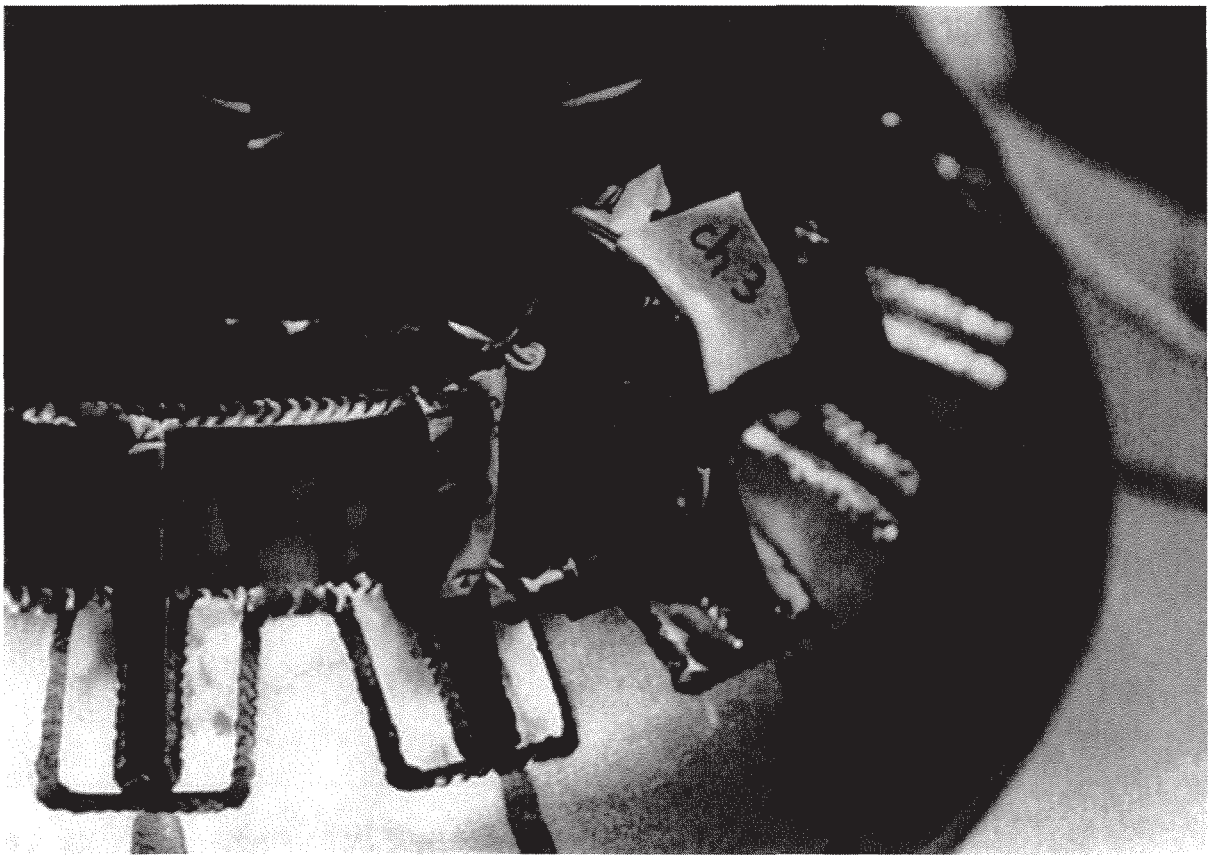

Figure 6. Accelerometers mounted outside the overpack

accommodate a signal level about 3 dB above the anticipated maximum and the other was set to provide about 9 dB of headroom. On playback, the channel from each pair whose signal came closest to full-scale without exceeding it was used for analysis.

The digital signal analyzer (Figure 7) provided analog-to-digital data conversion with a maximum sampling frequency of 102.4 kHz per channel. This was effectively increased even further for certain data records by replaying the tape at a speed lower than used for recording. Data was either displayed immediately on the real time display or passed via a DMA link to the main computer for further processing.

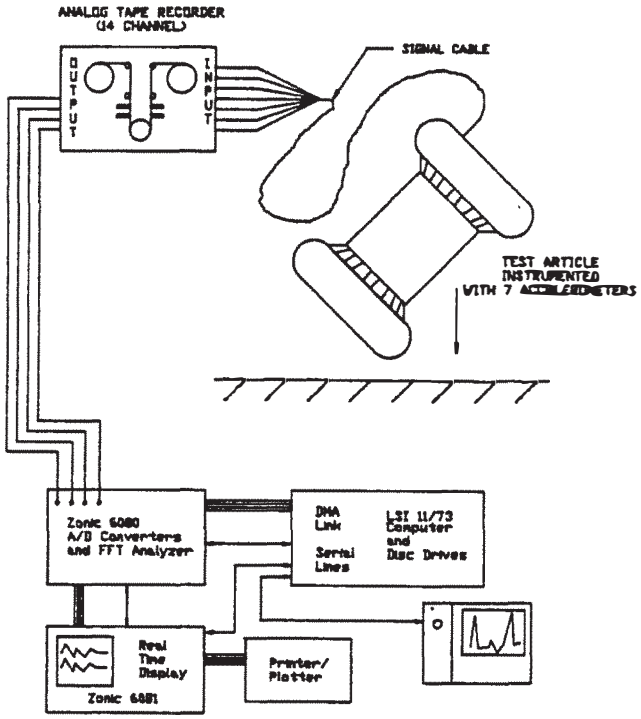

Figure 7. Accelerometer signal processing

4.2 Force Distribution Measurements

The distribution of force between the cask and overpack was determined by means of a pressure-sensing film on the cask exterior surface. The film undergoes a permanent color change from white to red when subjected to pressure. The color change is gradual with increasing pressure, allowing the approximate maximum pressure at any location to be determined by comparing

the exposed film to a calibrated color chart. More accurate reading is possible using a special densitometer. While somewhat subjective, the simpler comparison method was considered adequate for the present purpose.

The film provided a convenient method for determining the load distribution on the cask. It is available in several grades, each designed for a specific pressure range. The grade used for the drop test progresses from white to pink to red as the applied pressure is increased from 1000 to 3500 psi. Higher pressures have no effect, with the film simply retaining its maximum redness.

The film is normally used for static pressure measurements such as checking the flatness of mating surfaces of pipe flanges, cylinder heads, etc. Its manufacturer could not supply data on the time required for color change under sudden, impact loads. Therefore, a simple laboratory test was performed to assess its speed of response. Figure 8 shows the apparatus. Film specimens exposed at 2000 psi for a few hundred microseconds were compared to specimens exposed to the same pressure for two minutes. The specimens showed equal shades of red. It was concluded that the color change was effectively instantaneous.

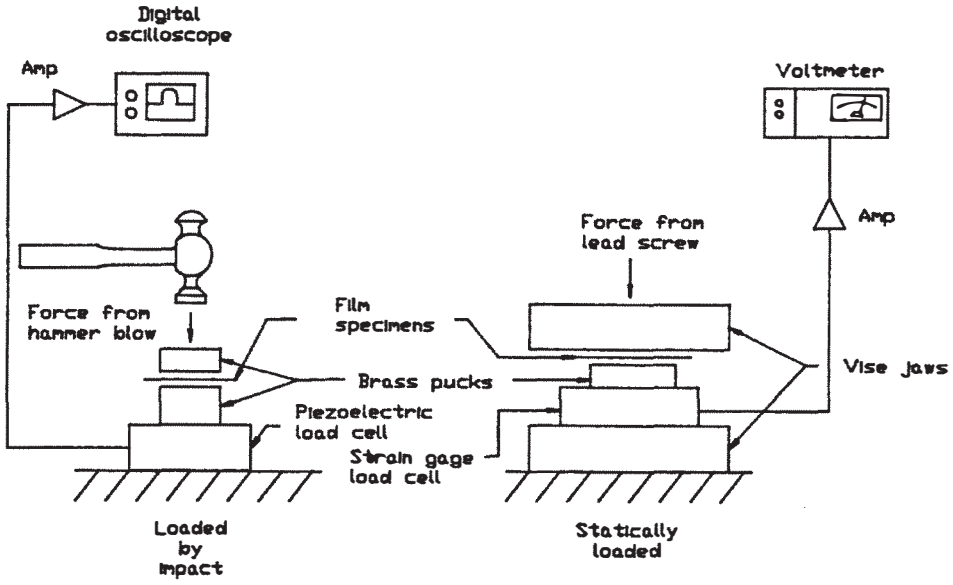

Figure 8. Apparatus for testing response speed of pressure sensing film

The film is composed of two separate layers, each resembling glossy paper with a total thickness is 0.008 inches. Under pressure, chemicals in the two layers react causing one layer to change color. It provides the pressure signature and the other layer is discarded.

Pieces were cut to fit the surfaces of the cask and held in place with adhesive tape as shown in Figure 9. A machined cover plate was located on the lid end of the cask to distribute the load over the entire surface of the circular honeycomb cushion. The film was placed between the cushion and the cover plate. Following each drop, the film was removed and the colored layer was annotated to become part of the permanent test record. Photographs in a later section show exposed film from each drop.

4.3 Photography

High-speed films were taken of each drop using two identical cameras viewing the scene from angles 90 degrees apart. Rated speed for the cameras was 500 frames/second.

A length scale and a time scale were located in the field of view of each camera, just behind the impact point. These scales, used in film interpretation, are shown later in photographs. Length scales were simply long rulers, graduated in inches and placed vertically in the field of view of each camera. Each time scale resembled a large clock with only one hand. The hand rotated clockwise at a measured speed of 3577 RPM. The time scales allowed accurate determination of frame rates, necessary for correlating the films with acceleration traces. Frame rates for the head-on, side, and CG-over-corner drop were 471.7, 469.5, and 463.0 frames/second respectively for the camera which produced the frames shown in this report.

A standard commercial videotape camera was also used to record the tests. By providing instant replay, it allowed the orientation of the package at impact to be verified immediately following each drop. Videotape was also used to document much of the test preparation.

Figure 9. Pressure-sensing film being applied to cask

4.4 Deformation Measurements

Micrometer measurements of the cask diameter were made at several axial locations before and after each drop to check for plastic deformation.

Since the top of one overpack was used for two drops (side and CG-over-corner), it was necessary to carefully record the damage due to the first to insure that the effects of the two were determined separately. The fixturing for these measurements, performed before and after each drop, is shown in Figure 10. The cask was mounted between centers in a large lathe and an array of dial gages was used to determine the deformation of the toroids at a number of relocatable positions. Plaster molds were also made of the deformed sections of the toroids.

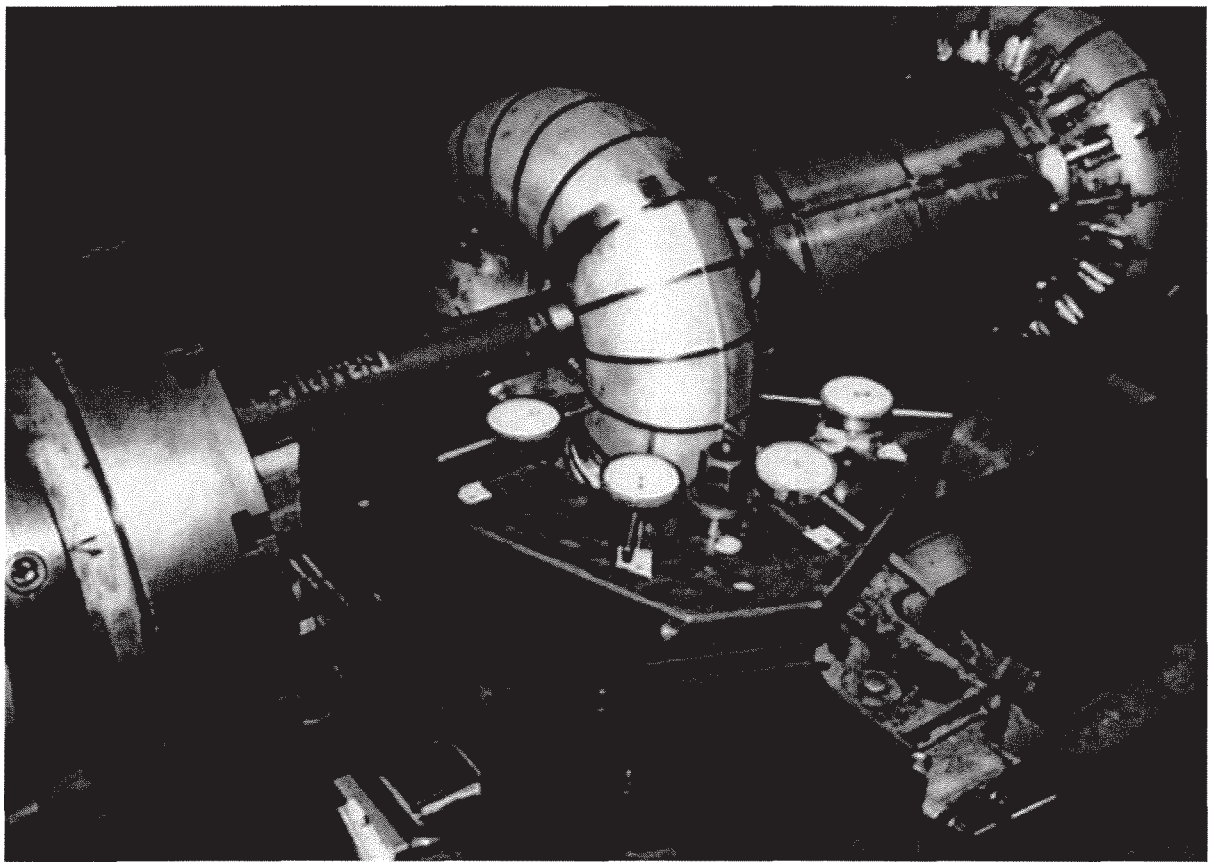

Figure 10. Measurement of toroid profile

5. PROCEDURE

Drop tests were performed for three different orientations of the cask. Depicted graphically in Figure 11, they are denoted in the order of performance as the head-on drop, the side drop, and the CG-over-corner drop. In the head-on and CG-over-corner drops, the cask lid and top of the overpack were oriented downwards to produce the worst-case load on the seal area of the cask.

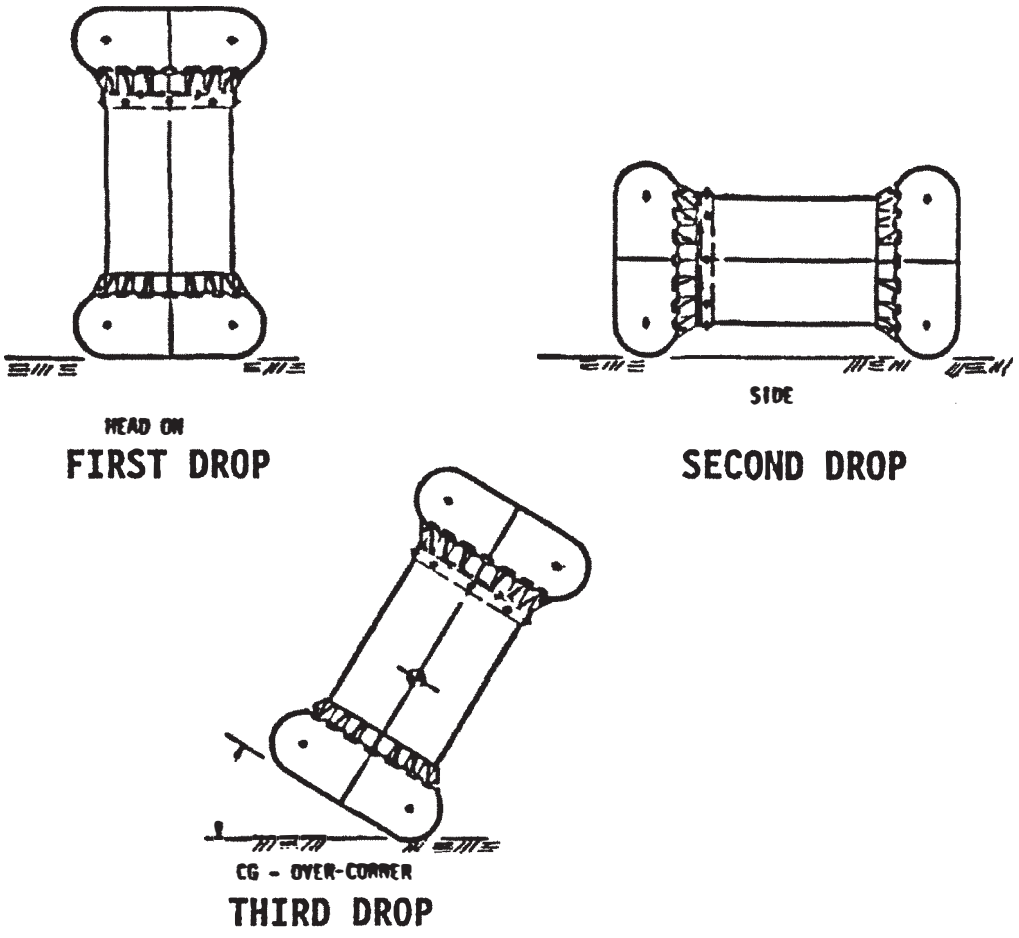

Figure 11. Drop test orientations

One cask and two complete overpack assemblies were fabricated. Overpack No. 1 was used for the head-on drop and No. 2 was used for the side drop. The CG-over-corner drop used the base of overpack No. 1 (still undamaged) and the top of overpack No. 2 with the package oriented such that the impact on the top occurred at an undamaged section.

Following the pre-drop dimensional inspection of the cask and overpack, the pressure sensing film was installed. The lateral sides and/or the lid end of the cask were covered, depending on the drop orientation. A cover plate was used between the lid end of the cask and the honeycomb cushion to distribute the load.

The cask and overpack were assembled, taking care to insure that the instrumentation cable was properly routed. The package was rigged for hoisting from the crane using an electromagnet and safety line. A magnet grip plate was secured to the overpack by a welded bracket which could be adjusted to obtain the correct orientation. Figure 12 shows the package rigged for the side drop. Special rigging was used for the CG-over-corner drop to balance the package over the contact point.

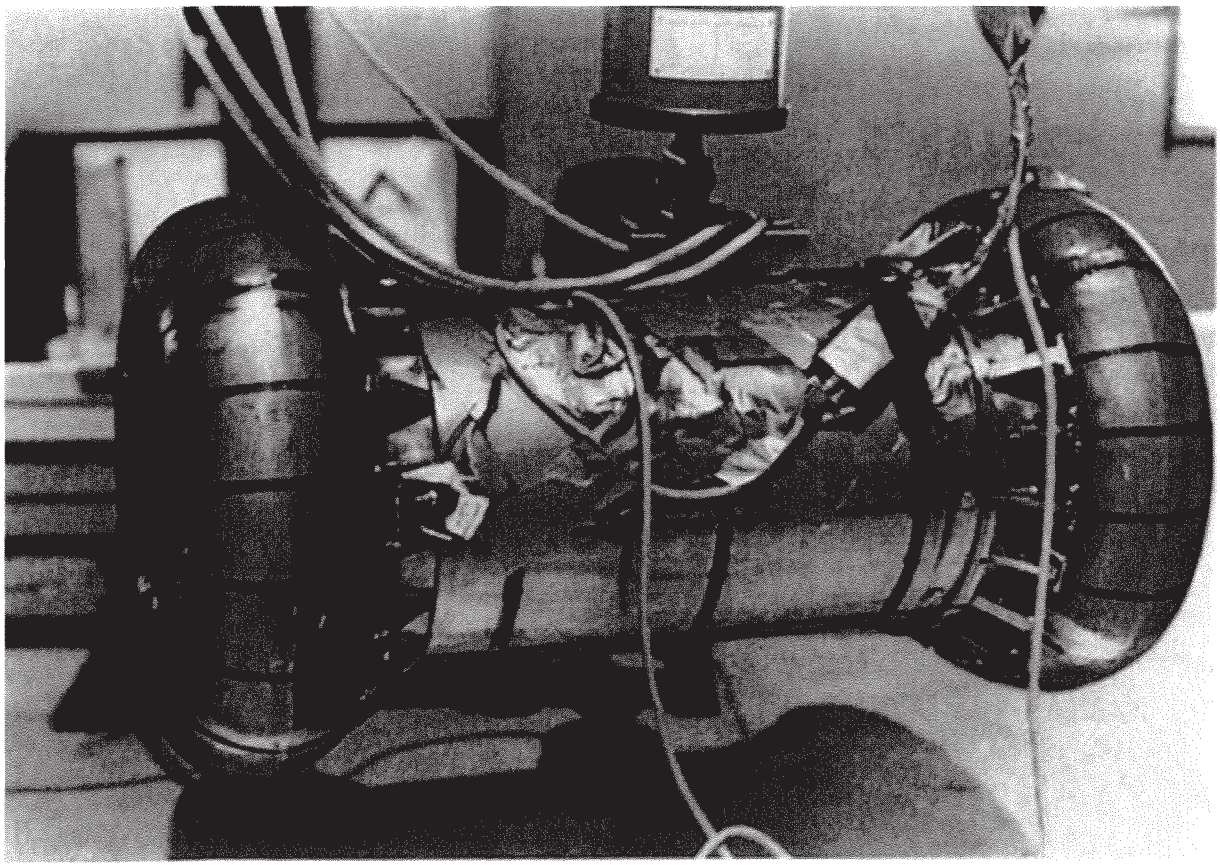

Figure 12. Package rigged for side drop

The package was hoisted by a mobile crane and the drop height was verified by a light, graduated chain hanging from the crane. The instrumentation cable was carefully routed and supported to prevent any interference with the free fall. The chain and safety line were removed just before the drop.

After a final check of all equipment, the tape recorder was started and voice-logged. The cameras were started and, after a one-second pause to allow them to reach speed, the polarity of the DC voltage to the electromagnet was reversed to release the package. Filming continued until the package came to rest.

Post-drop procedure included the following.

1. Data tapes were replayed to check signal ranging.
2. Pressure-sensing film was removed, inspected, annotated, and stored.
3. The cask and overpack were measured to determine the extent of plastic deformation.
4. Videotapes were replayed to check the package orientation at impact.

Detailed check lists were kept with each item initialed by the responsible individual after it was performed. These will become part of the final Product Quality Record.

6. RESULTS

Results of the drop tests are given in this section, organized by drop orientation.

6.1 Head-On Drop

6.1.1 Acceleration Data and High-Speed Photography

Figures 13 and 14 illustrates the impact event. The traces show the time history of vertical acceleration as measured by the axial accelerometers on the overpack and cask. The photographs are from the high-speed film, taken at a rate of 471.7 frames/second (2.12 milliseconds/frame). They are numbered in order of increasing time with zero being the frame closest to initial impact. The numbered vertical lines on the plot indicate the corresponding frame. The small markers along the bottom of each plot are spaced at 2.00 millisecond intervals.

Polarity of the vertical acceleration signal is not necessarily consistent between tests having different drop orientations. The sensors were simply installed in the most convenient way that provided correct alignment. Polarity was not considered important since the sense of the net velocity change, and thus the rigid-body component of acceleration at impact, was obviously known in advance.

Interpretation of the data from the head-on drop is straightforward. The acceleration seen by each sensor is composed of two parts. Low frequency components are present, corresponding to the rigid-body deceleration that produces the net change in velocity. A large number of high frequency components (ringing) are also produced by the resonant response of the vibration modes of the package. The low frequency portion, corresponding to a smoothed version of the trace, is of primary interest since it indicates the portion of the loading relevant to the package design.

Figure 15 shows the vertical acceleration of the cask and overpack plotted on the same scale. Peak acceleration of the cask is 408 G's, much lower than the 4853 G level experienced at the overpack sensor. The impact limiters greatly reduce the acceleration experienced by the cask.

Figure 16 shows the top toroid following the head-on drop. It has buckled inwards in an almost perfect axisymmetric pattern. The package rebounded almost straight up with negligible rotation and came to rest on the impact surface. These facts indicate that the accelerating force was essentially symmetric around the cask axis. The high-speed film showed a maximum rebound height at the overpack CG of 7.6 inches. The 408 G acceleration of the cask was the highest level seen in any of the three drops. This was as expected since the head-on drop distributed the crushing load over the largest portion of the toroid surface, thus producing the highest total force.

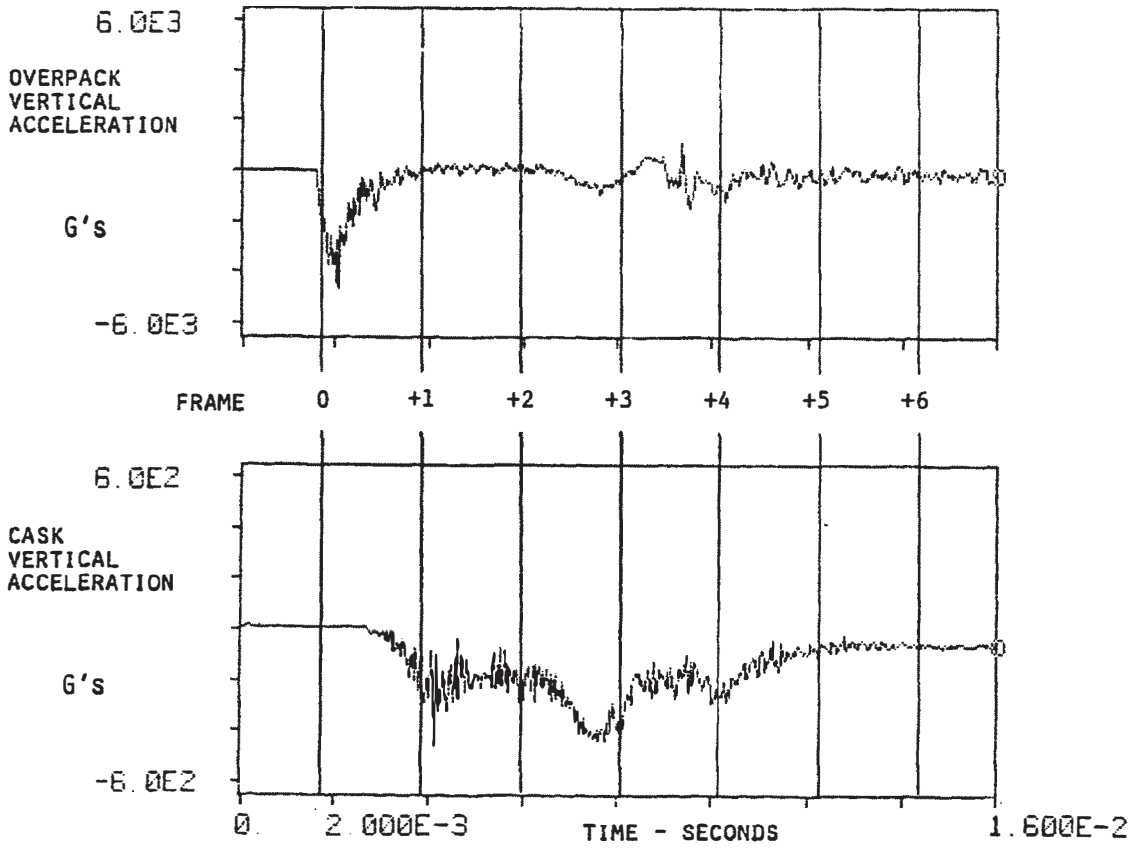

Figure 13. Head-on drop, vertical acceleration

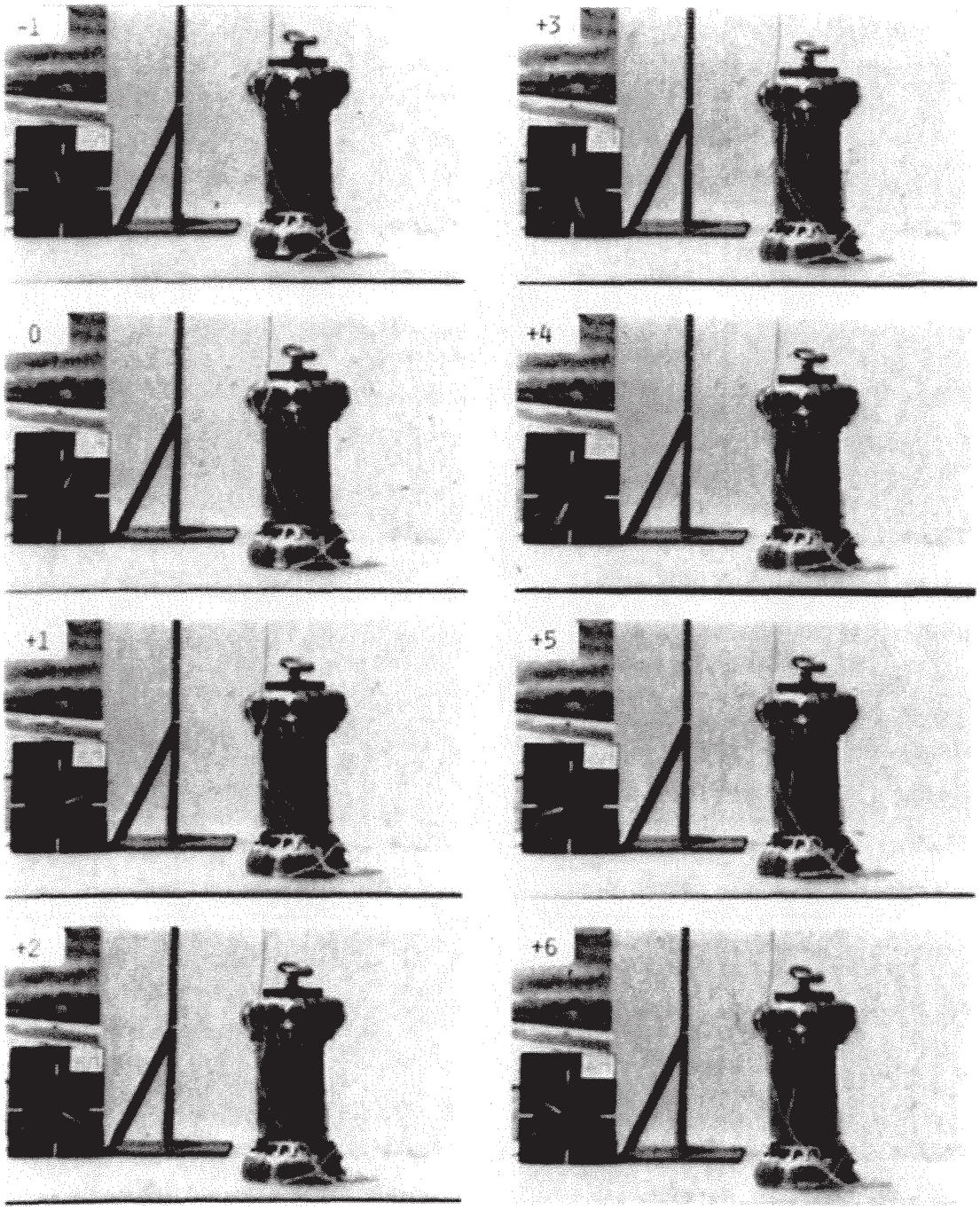

Figure 14. Head-on drop, frames taken at 2.12 millisecond intervals

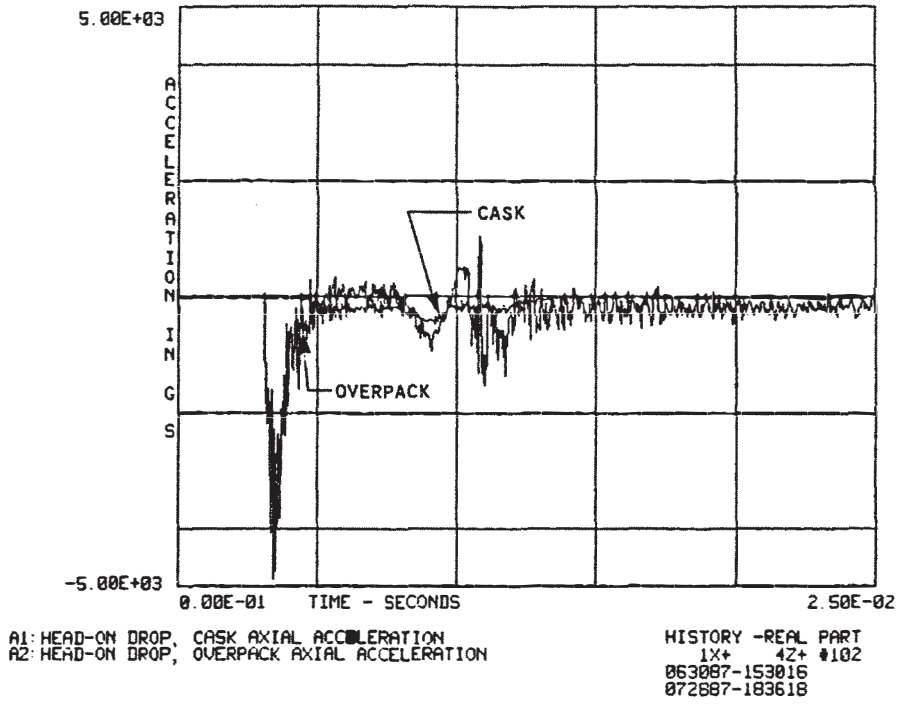

Figure 15. Overplot of cask and overpack acceleration, head-on drop

A smoothed version of the cask acceleration trace shows three distinct peaks. In Figure 13, these occur just after frame 1, just before frame 3, and just after frame 4. It is believed, based on analysis of the data from all three drops, that the first two peaks are typical of the nonlinear force-deflection characteristics of the toroid at large deformations. The momentary reduction in acceleration after the first peak probably occurs when the convex surface of the toroid is pushed through to present a concave surface over the impact area. The second, larger peak occurs as the crushing continues and this concave surface, now stiffer, is enlarged.

Figure 17 shows the time integral of the cask acceleration, computed as a forward sum over the digitized time history of Figure 15. The difference between initial and final values of the integral indicates the net velocity change. This calculation provides a check on the accuracy of the acceleration signal chain. The indicated velocity change must equal or exceed the initial impact velocity of 527 inches/second. The value of 645 inches/second indicated in Figure 17 is consistent with the observed rebound height.

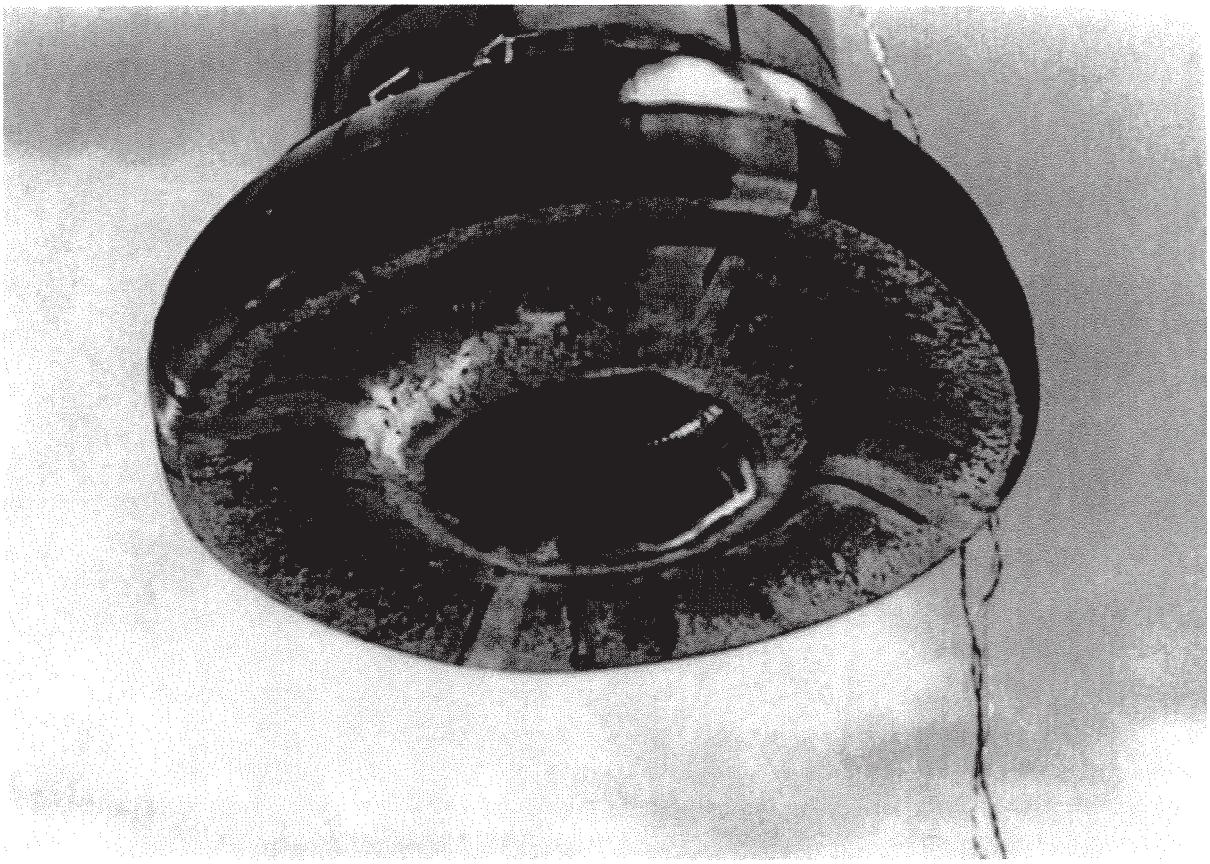

Figure 16. Toroid deformation caused by head-on drop

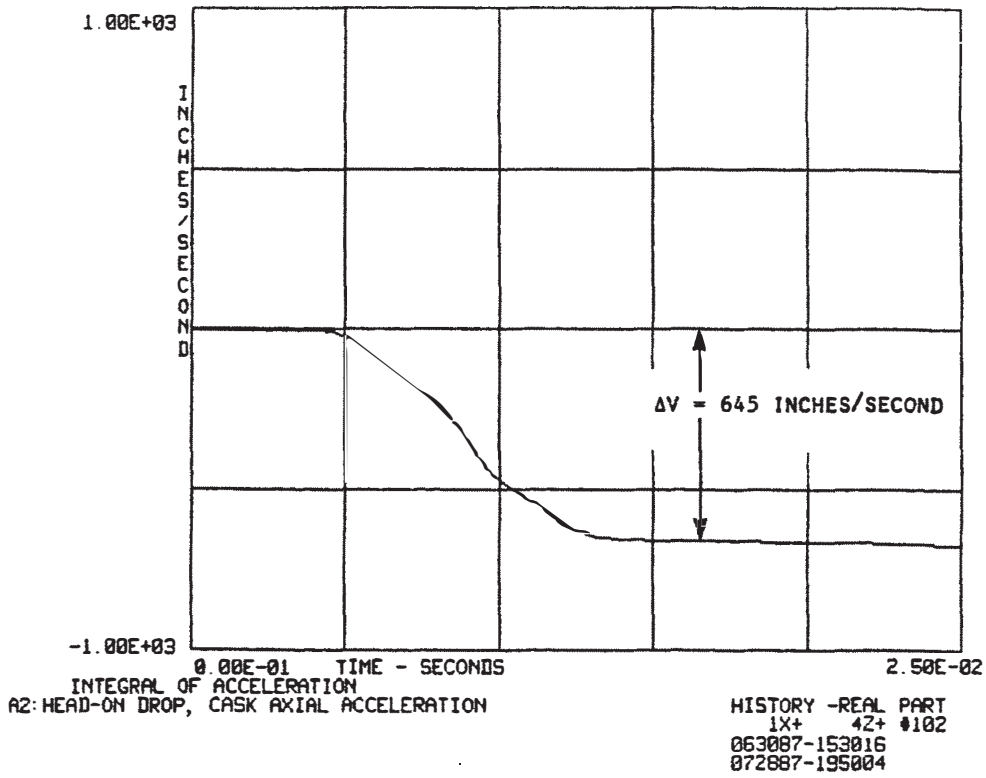

Figure 17. Time integral of cask vertical acceleration, head-on drop

6.1.2 Pressure-Sensing Film

Figure 18 shows the pressure sensing film after the head-on drop. The large rectangular piece, removed from the lateral sides of the cask, shows that significant pressure was applied in only a few small areas. The circular piece, removed from the cover plate on the lid end of the cask, shows an essentially axisymmetric pressure distribution. Most of the load was taken by a one-inch-wide band around the edge where the raised lip bears against the cover plate. This could occur only after the honeycomb cushion bottomed; until that point the cover plate and cushion would serve to distribute the load evenly. The film color near the rim indicates a peak pressure in excess of 3500 psi, consistent with the measured acceleration and weight of the cask.

The film color in the circular area inside the band is not quite uniform. Circular striations are visible, caused by tooling marks on the plate. This is not a defect of the film. It simply indicates the difficulty of producing a truly uniform pressure over the contact area between two hard surfaces.

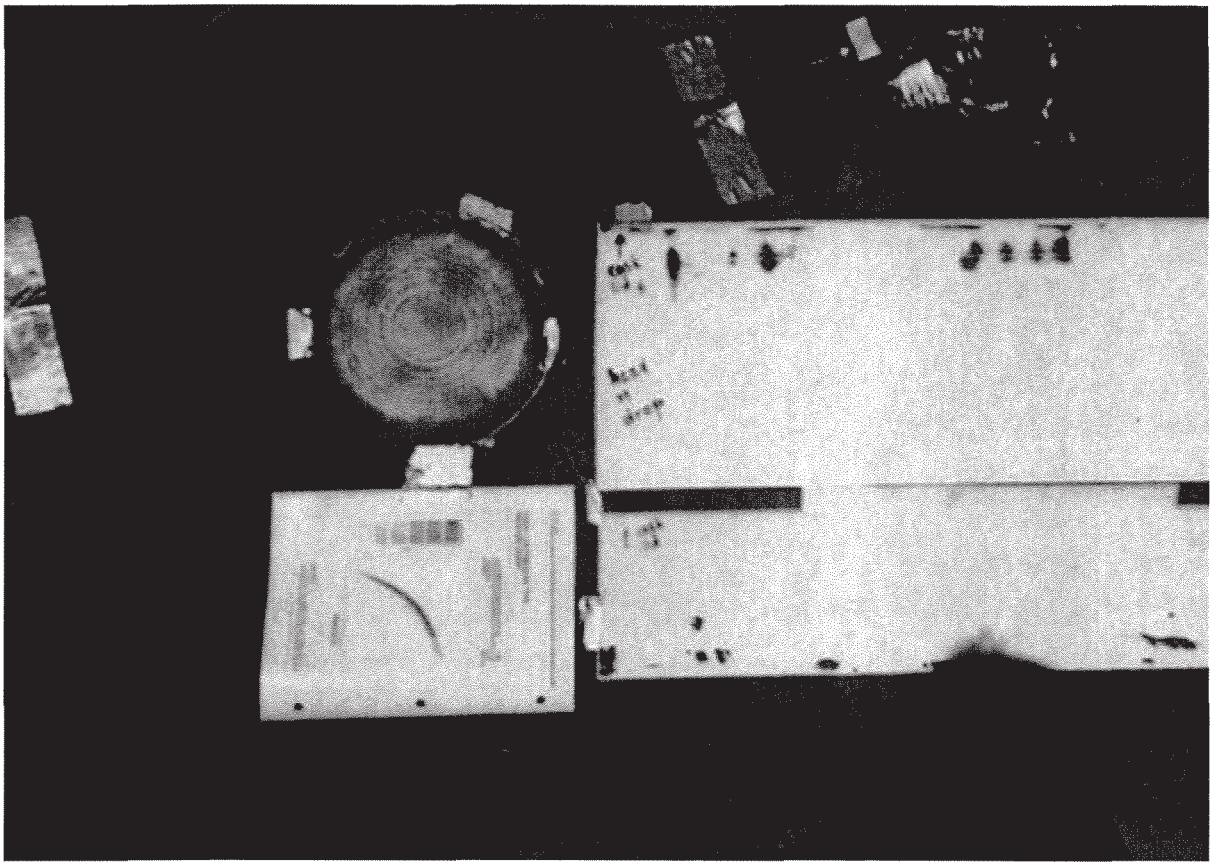

Figure 18. Pressure-sensing film from head-on drop

6.1.3 Cask and Overpack Deformation Measurements

Micrometer measurements were made of the cask diameter at a number of axial and azimuthal stations before and after the head-on drop. No change was found; no measurable plastic deformation of the cask had occurred.

Table 3 shows measurements of the deformed top toroid using the apparatus of Figure 10. Numbering of the dial gages is shown in Figure 19. Measurements of the toroid indicated that damage to it was localized to the impact area and was essentially axisymmetric.

The entire set of measurements made before and after the head-on drop is quite extensive and is documented in General Electric Inspection Report No. 6431, dated June 11, 1987. Data given here is excerpted from that report.

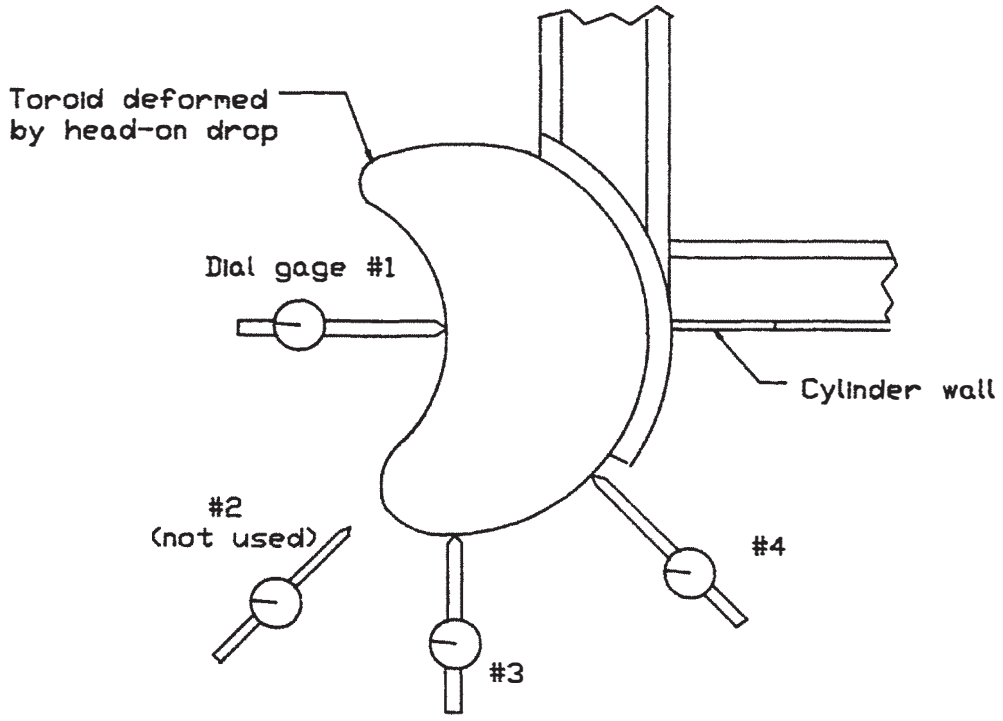

Figure 19. Gage numbering for inspection of overpack top toroid

Table 3. Deformation of top toroid due to head-on drop

Gauge / Azimuth (Degrees)	1	2*	3	4
0	2.115		-0.033	-0.001
90	2.009		-0.018	0.007
180	2.393		-0.063	-0.020
270	2.501		-0.063	0.002

*not used - deformation pattern did not produce meaningful readings (see Figure 19)

All reading in inches, positive values indicate inward deformation

6.2 Side Drop

An unexpected failure of the overpack occurred during the side drop. The bolted joint between the overpack top and base failed completely, shearing off all ten bolts and allowing the base to separate from the package. The cable carrying signals from the sensors inside the cask (routed through a hole in the overpack base) was broken almost instantaneously. As the two weldments separated, the cable connector was also pulled apart, causing loss of signal from the remaining accelerometers outside the overpack.

The causes of the overpack joint failure as well as its requalification will be discussed in a separate report.[2] The remainder of this subsection presents the data from the side drop test. The data suggests that, in spite of the failure, the acceleration record extends through the instant at which the peak value occurred.

6.2.1 Acceleration Data and High-Speed Photography

Figure 20 shows the time history of vertical acceleration as measured by the radial accelerometer inside the cask and the tangential accelerometer on the overpack. The photographs in Figure 21, taken at intervals of 2.13 milliseconds, show the critical time period between initial impact and loss of signal.

The high-speed films revealed that the package rotated slightly as it fell to strike the pad, top end first, with its axis inclined 10 degrees from the horizontal. This was probably caused either by a slight swinging of the package at the instant of release or a failure of the magnet to release uniformly over its entire surface. Implications of the contact angle for a side drop are considered in a separate report.[3]

Figures 20 and 21 contain much valuable information in spite of the fact that the instrumentation cable from the cask sensors was destroyed 11 milliseconds after the initial impact. Indicated on Figure 20 is the time interval during which crushing of the top toroid occurred. Following the initial impact at frame 0, the acceleration pattern shows a double peak, believed to be characteristic of the snap-through behavior of the toroid. The toroid on the overpack base strikes approximately 8 milliseconds later, after the crushing of the top toroid is complete. The second impact causes the vertical acceleration to again rise rapidly. The bolts break about 2 milliseconds later, releasing the base weldment which rotates outward and is propelled away from the package. Figure 22 shows a still photograph taken just after impact, with the base weldment in midair. Figure 23 shows the aftermath of the side drop.

[2]Ibid. [3]Ibid.

Based on the acceleration traces and the high-speed films, the signal cable is believed to have faulted 11 milliseconds after impact, between frames +5 and +6 of the film. This coincides approximately with the point in time when the joint flange of the overpack top struck the pad. The signal went low, indicating the cable had shorted. It later went high when the conductors parted completely. There is no certain way of determining the last instant at which the acceleration signal is accurate. The point indicated on Figure 20 is based on inspection of the signal itself and the high-speed film.

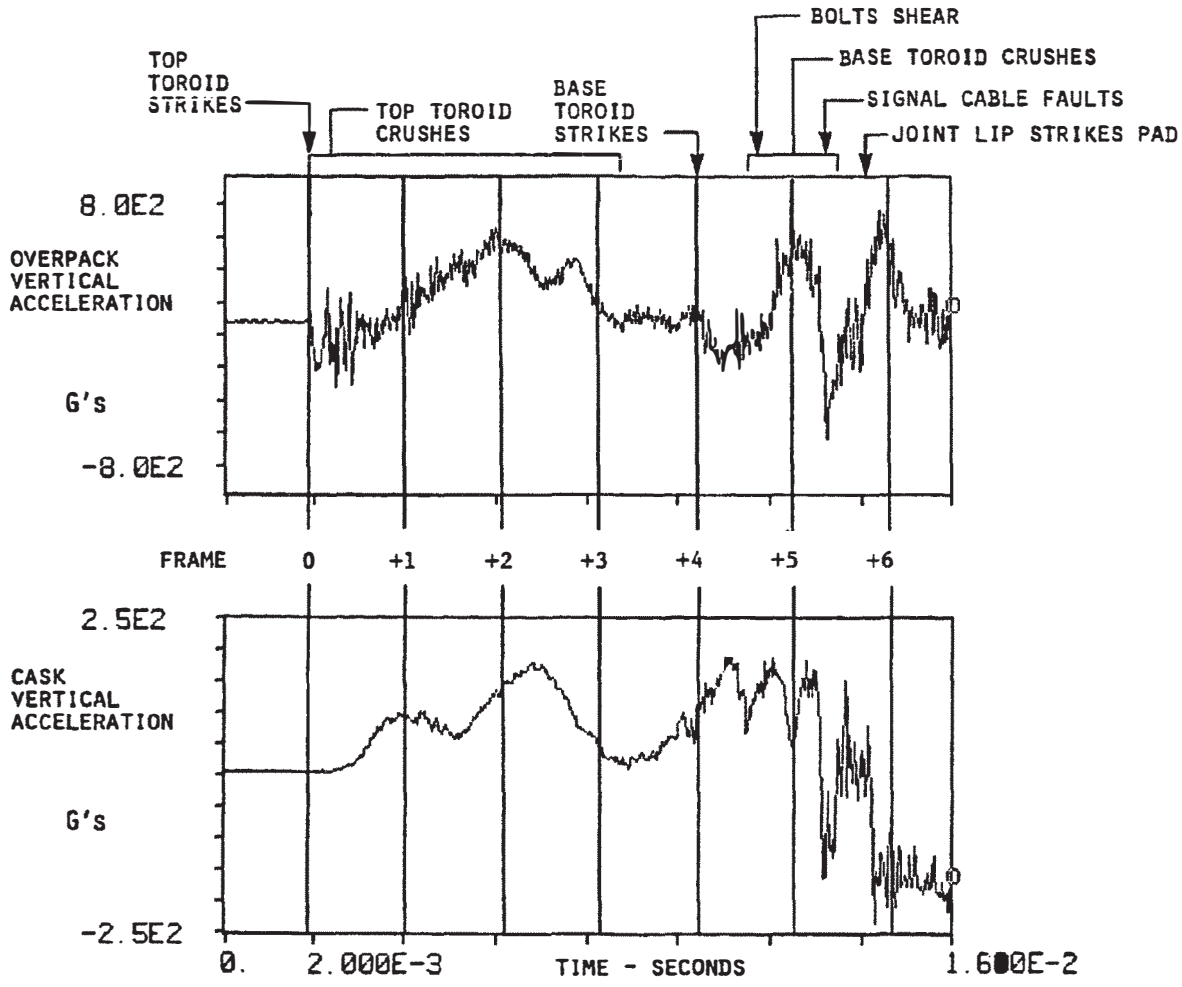

Figure 20. Side drop, vertical acceleration

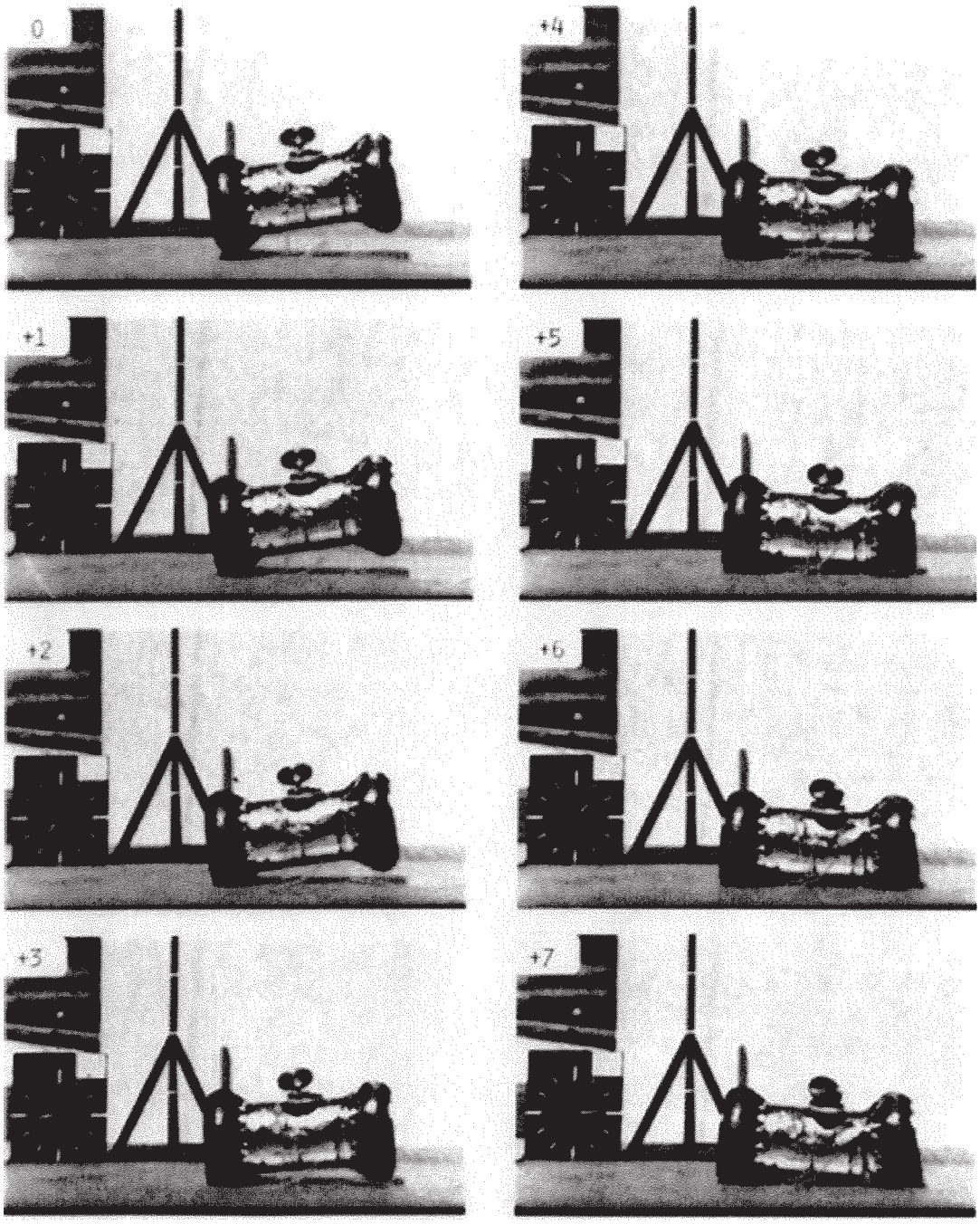

Figure 21. Side drop, frames taken at 2.13 millisecond intervals

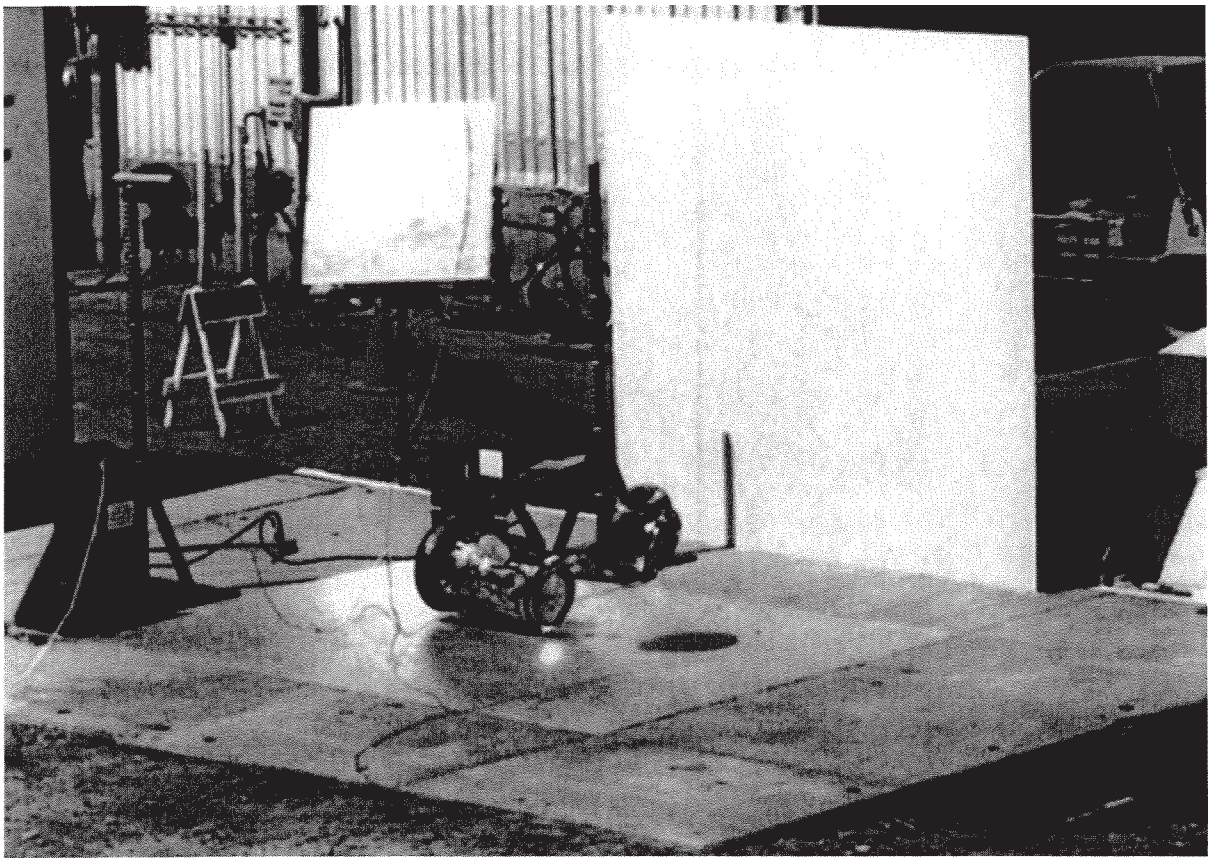

Figure 22. Overpack weldments separating after impact, side drop

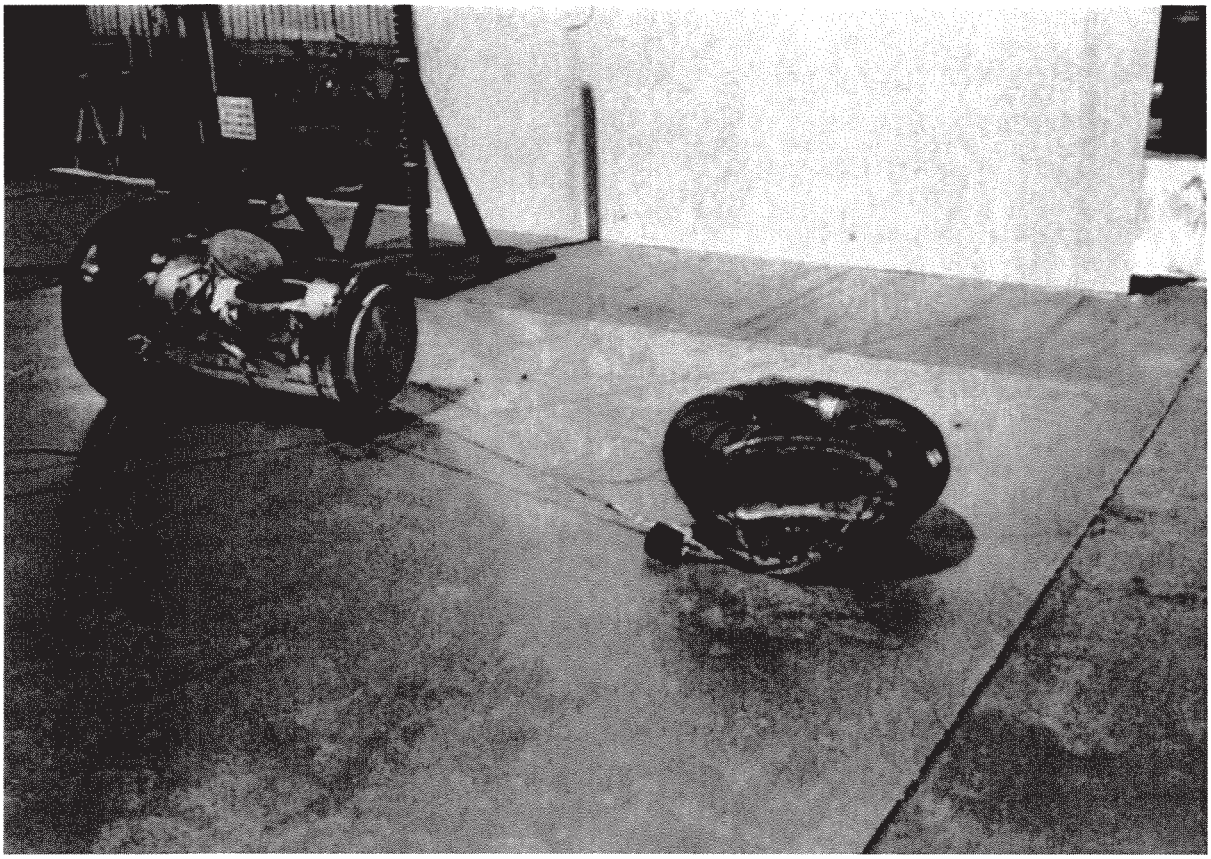

Figure 23. Package after side drop

It may be shown, however, that the important part of the impact event occurred prior to the indicated loss-of-signal point. Figure 24 shows the calculation of the net change in the cask vertical velocity between initial impact and the cable fault. The trace was zeroed from the fault point through the end of the record prior to integration. The result indicates that the cask had not come completely to rest when the signal was lost. The net velocity change up to that point was 379 inches/second. Since the impact velocity was 527 inches/second, the remaining velocity change was 527 - 379 = 148 inches/second. This corresponds to a free drop from 28 inches, an event unlikely to damage even an unprotected cask. Stated another way, since kinetic energy is proportional to velocity squared, the percent of the initial energy remaining when the signal was lost was only $(148/527)^2 \times 100$ =-7.9% of the initial value. In effect, the impact event was essentially over before the signal was lost.

Likewise, since the toroids were extensively deformed by the side drop (Figure 23) and this deformation could only have occurred while the sensing channel was still intact, the observed maximum acceleration of 185 G's is a reasonable estimate of the maximum that would have occurred if the bolted joint had not failed.

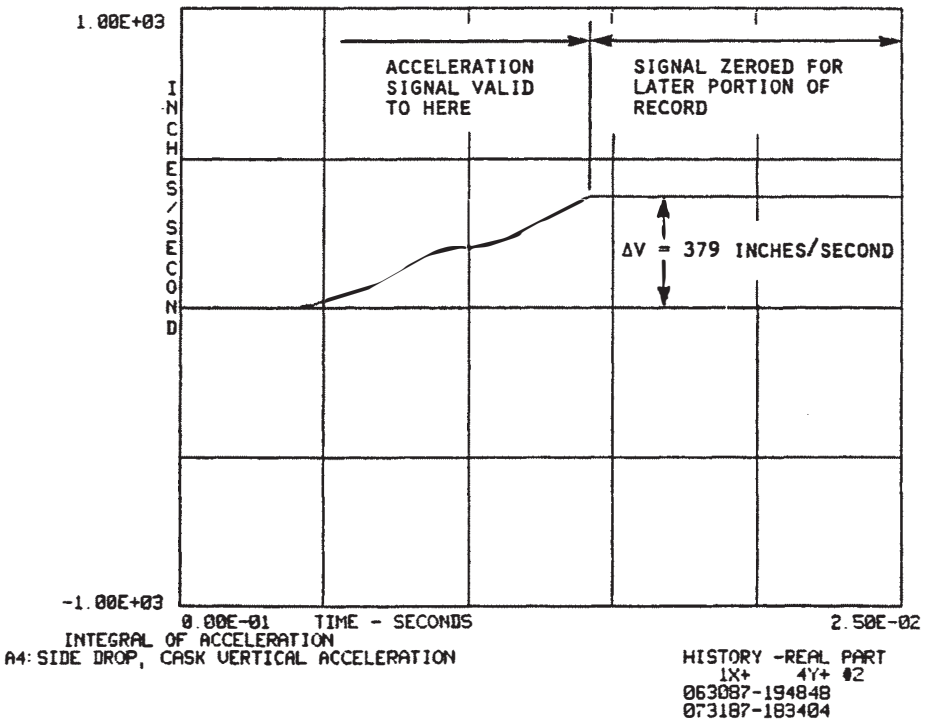

Figure 24. Time integral of cask vertical acceleration prior to cable fault, side drop

6.2.2 Pressure- Sensing Film

Figure 25 shows the pressure-sensing film after the side drop. The film was applied only to the lateral sides of the cask. It shows that the load tended to concentrate towards the ends of the cask, except for two narrow lines parallel to the cask axis. These localized areas of high pressure were caused by the crush tubes between the double walls of the overpack cylinder.

6.2.3 Cask and Overpack Deformation Measurements

Micrometer measurements were made of the cask diameter at a number of axial and azimuthal stations before and after the side drop. No change was found; no measurable plastic deformation of the cask had occurred.

Extensive measurements of the overpack before and after the side drop are given in General Electric Inspection Report No. 6430, dated June 12, 1987. The radial indentation of the top toroid (which struck the ground first) was found to be 3.18 inches in depth. Damage to the base toroid was slightly greater.

6.3 CG-Over-Corner Drop

For the final drop, the cask was oriented as shown in Figure 26. The orientation, with the cask axis 22 degrees off the vertical, positioned the package center-of-gravity directly over the impact point on the top toroid. This was verified by balancing the cask on the contact point. The angle proved to be slightly different from the calculated value of 29 degrees used in the design of the mounting block for the cask oblique accelerometer. The resulting 7 degree misalignment of the sensing axis was not considered significant since it reduced the acceleration signal by less than 1%.

The drop was performed without incident to conclude the test series.

6.3.1 Acceleration Data and High-Speed Photography

Figures 27 and 28 illustrate the impact event. The lower trace in Figure 27 shows the time history of cask acceleration in the vertical direction as sensed by the cask oblique accelerometer. The upper trace is from the overpack axial accelerometer and gives the vertical acceleration attenuated by about 7% due to the 22 degree misalignment of the sensor axis from vertical. The photographs in Figure 27 were taken at intervals of 2.16 milliseconds.

Upon striking the pad, the package rebounded in a direction roughly parallel to its axis while rotating counterclockwise (as seen in the view of Figure 28) in

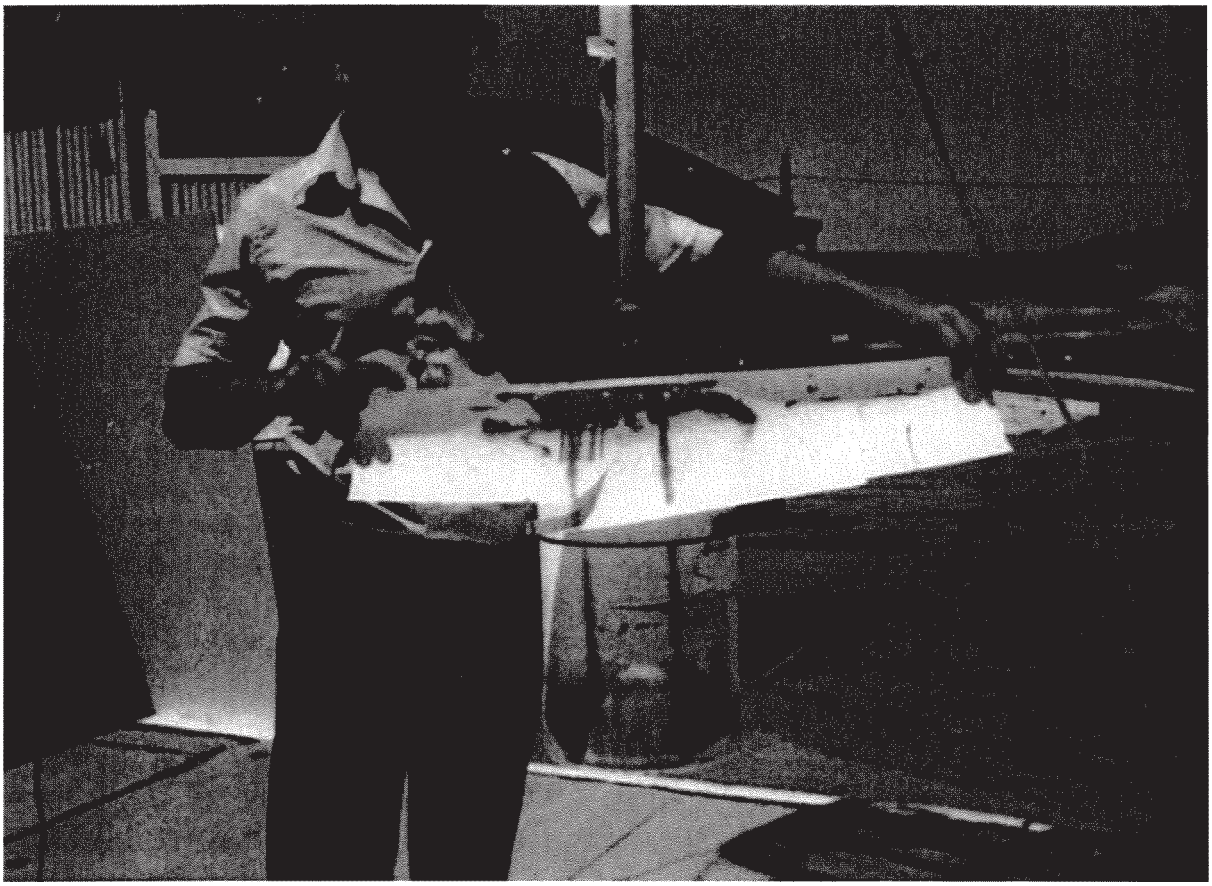

Figure 25. Pressure-sensing film from side drop

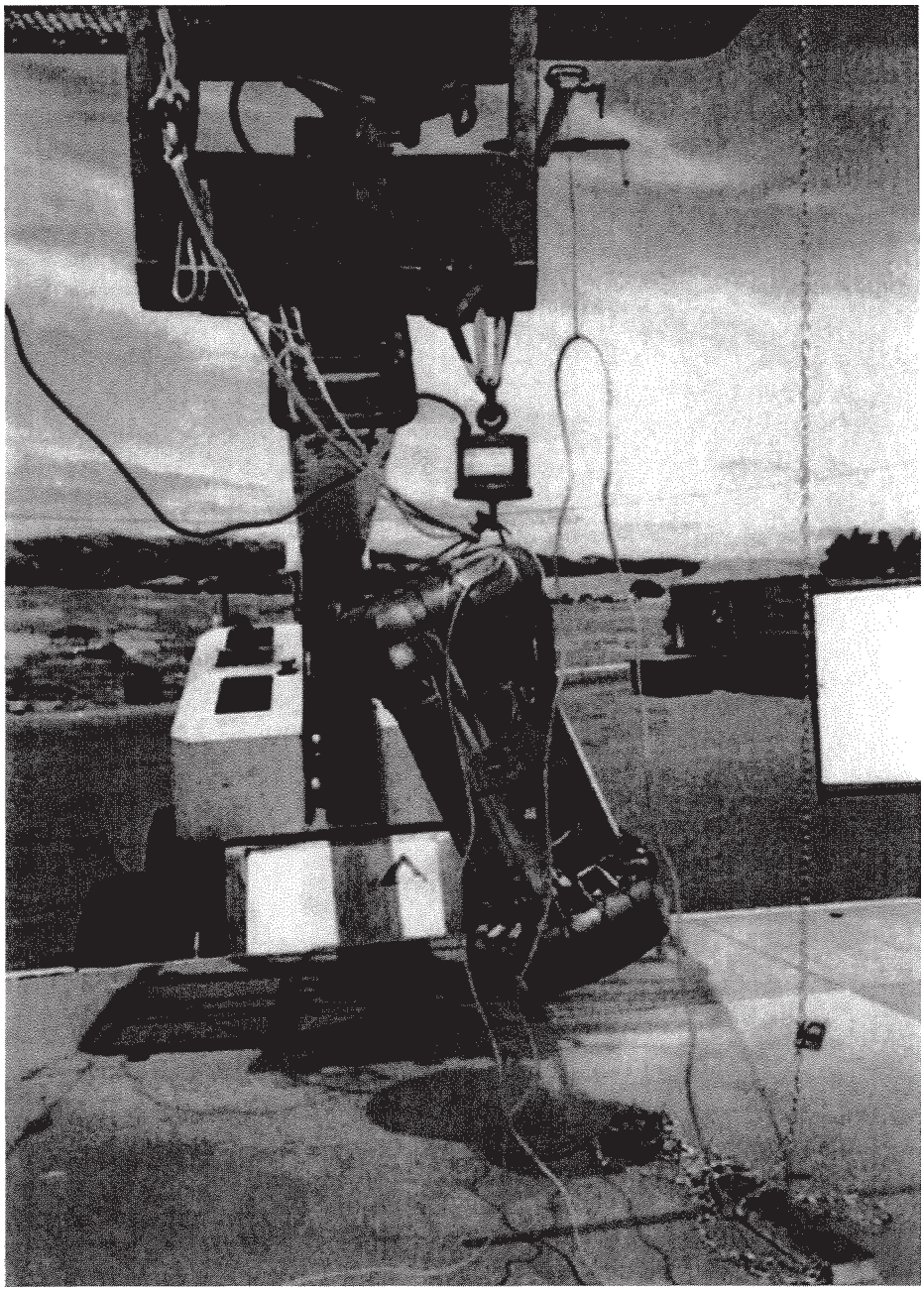

Figure 26. Rigging for CG-over-corner drop

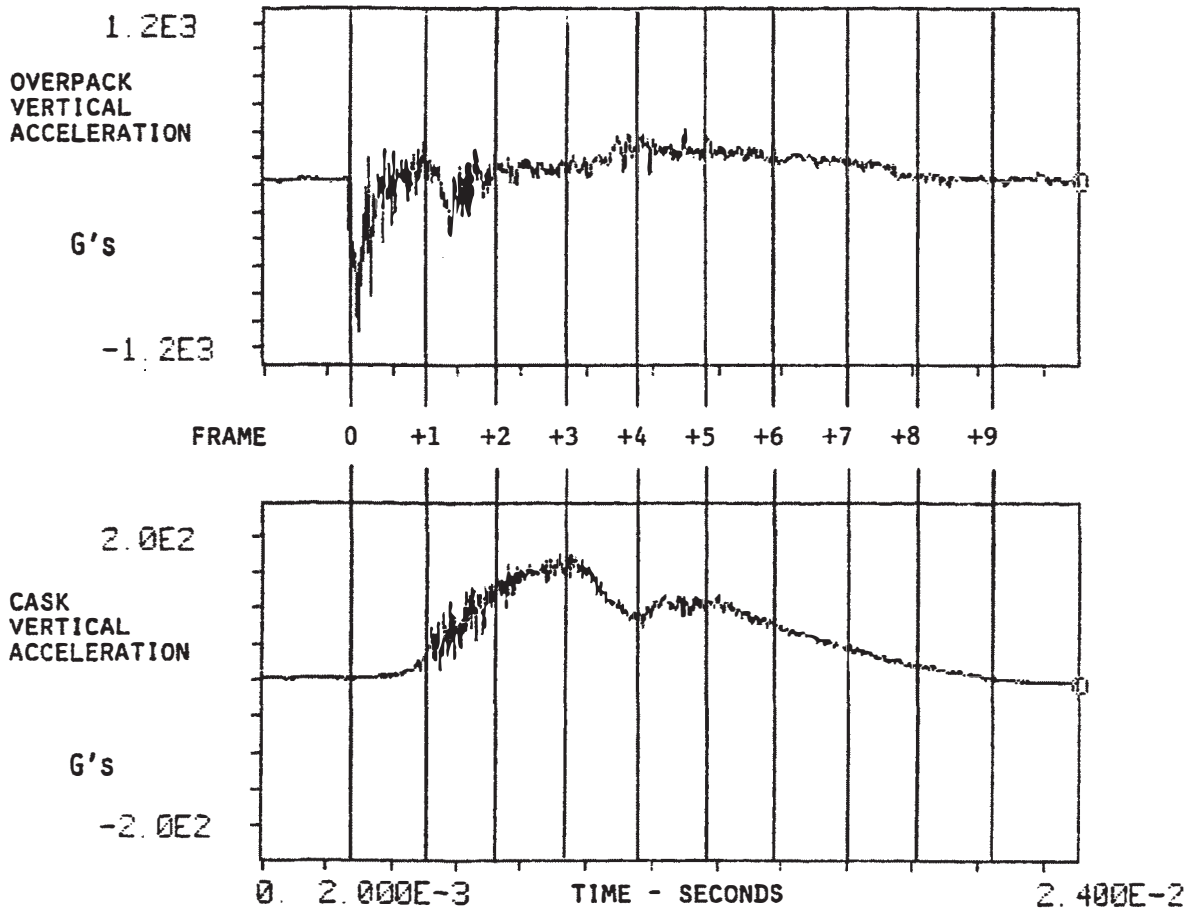

Figure 27. CG-over-corner drop, vertical acceleration

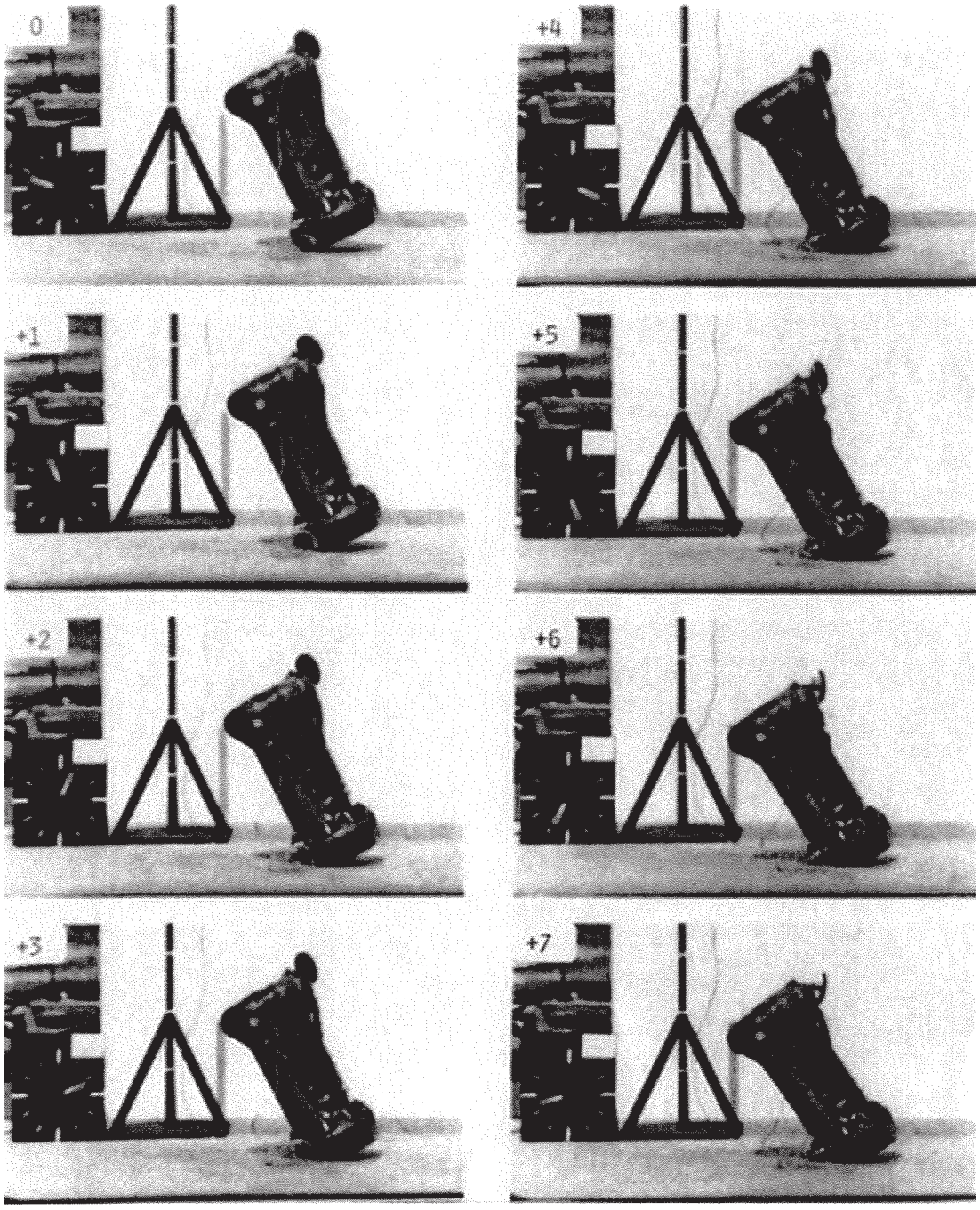

Figure 28. CG-over-corner drop, frames taken at 2.16 millisecond intervals

midair through about 250 degrees before coming to rest. The maximum rebound height and rotational velocity, determined from the high-speed films, were 4.7 inches and 15.1 radians/second. The rotational velocity produced by the impact does not mean that the CG was not aligned over the impact point. Rather, it simply implies that the deformation pattern of the toroid produced a force whose resultant did not pass through the CG. Figure 29 shows the deformation of the top toroid.

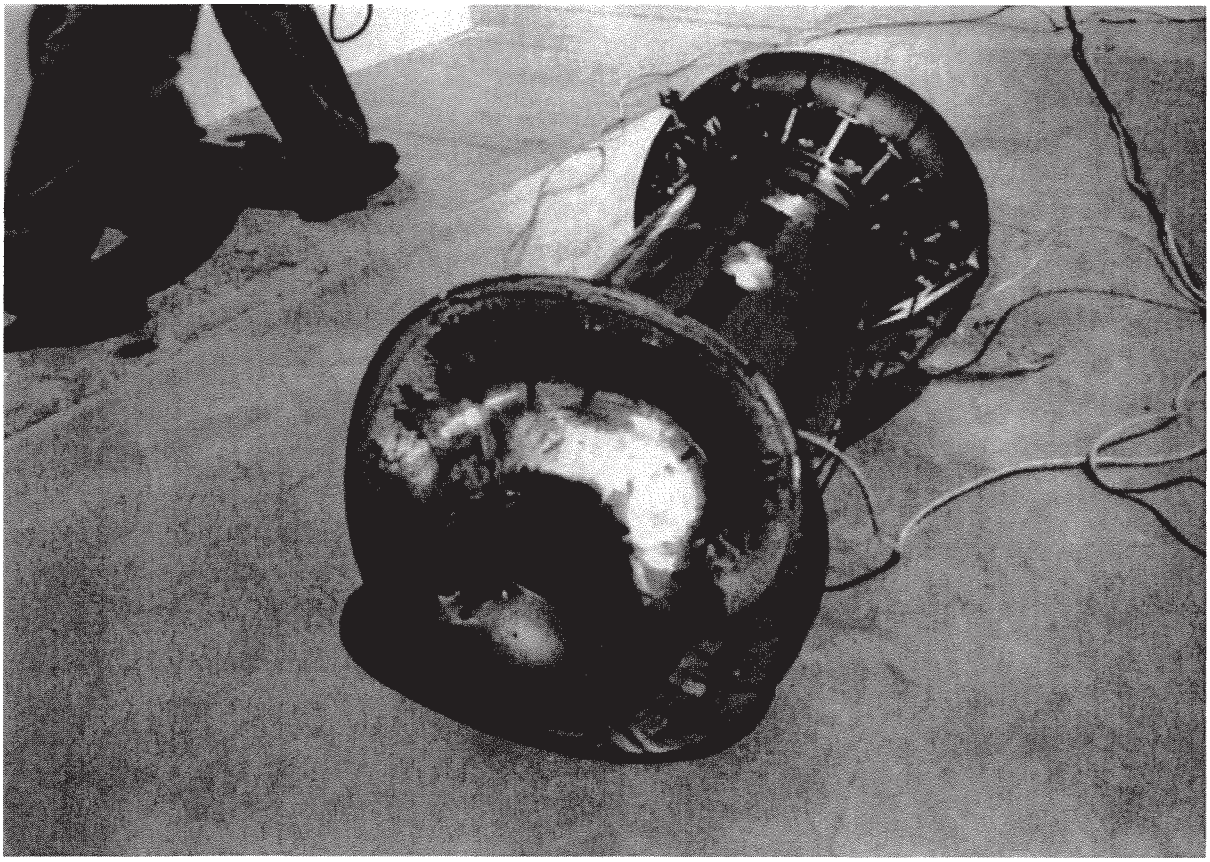

Figure 29. Deformation of overpack produced by CG-over-corner drop

The cask acceleration transient, lasting about 18 milliseconds, was substantially longer than for either the head-on or side drop. This is related to the fact that a toroid struck on a corner produces a softer "cushion" than when struck head-on or from the side. The greater compliance produces a longer acceleration transient with a lower peak value; maximum cask acceleration was the lowest of the three tests at 156 G's. The transient showed the characteristic double peak.

Determination of the net velocity change was straightforward and is shown in Figure 30. The value of 548 inches/second, slightly greater than the impact velocity, is reasonable based on the small value of the rebound height.

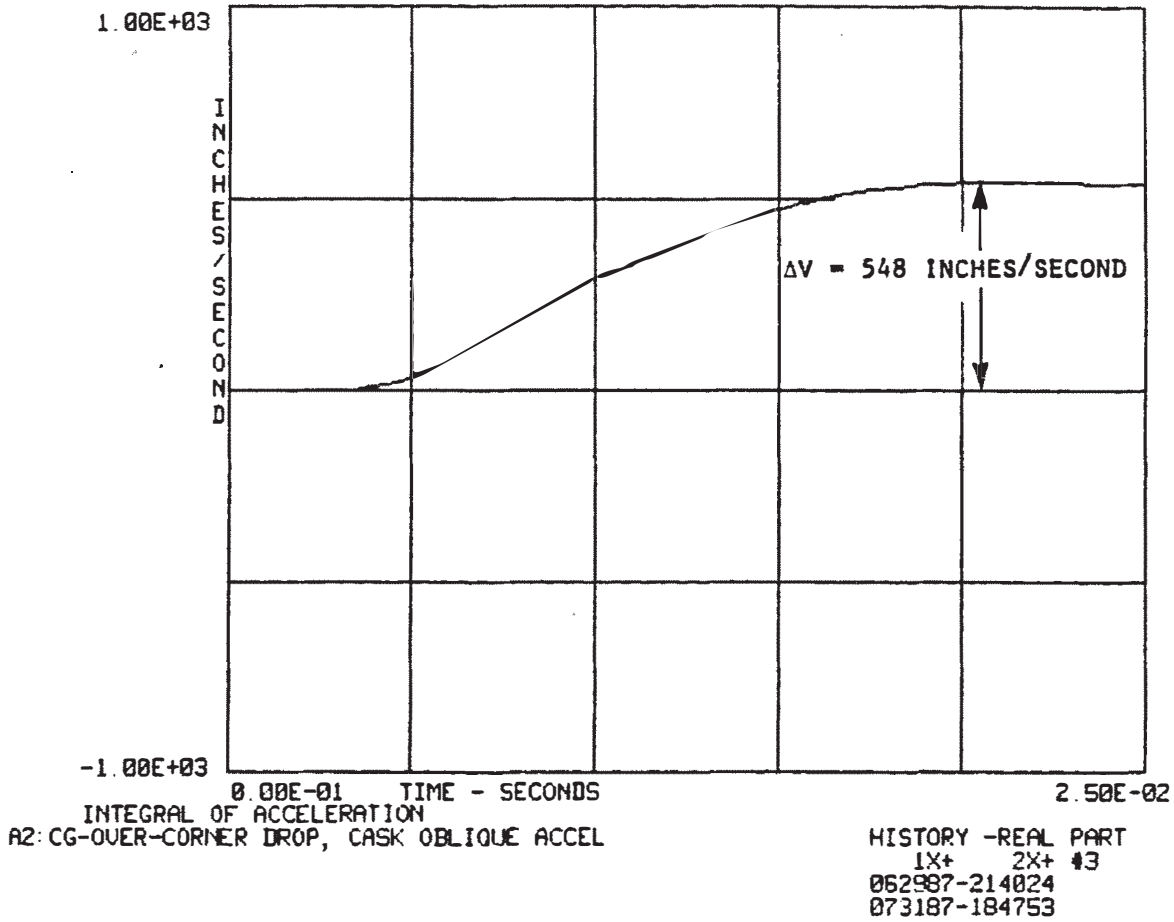

Figure 30. Time integral of cask vertical acceleration, CG-over-corner drop

6.3.2 Pressure-Sensing Film

Figure 31 shows the pressure sensitive film, still on the cask, following the CG-over-corner drop. The pressure over the end cover plate was fairly uniform, consistent with the fact that the honeycomb cushion did not bottom. Pressure on the lateral sides of the cask was confined to circumferential bands near the ends, particularly the lid end which was oriented downwards at impact. The pressure band extends essentially all the way around the cask although the highest pressure was seen on the downward side, as would be expected. Loading of the other side probably occurred on the second impact.

6.3.3 Cask and Overpack Deformation Measurements

Micrometer measurements were made of the cask diameter at a number of axial and azimuthal stations before and after the side drop. No change was found; no measurable plastic deformation of the cask had occurred.

Extensive measurements of the overpack before and after the CG-over-corner drop are given in General Electric Inspection Report No. 6432, dated June 18, 1987. Deformation, as shown in Figure 29, was significant, but was confined to the region around the impact. Maximum depth of the indenting, measured parallel to the package axis along a minor diameter of the toroid, was approximately 5.3 inches.

Figure 31. Pressure-sensing film from CG-over-corner drop

7. Summary and Conclusions

Drop tests in three orientations were performed with no measurable deformation or other damage to the cask. The head-on and CG-over-corner drops were successfully completed with no unexpected results. Complete acceleration and internal load distribution data were obtained for use in design verification.

An unexpected failure of the overpack bolted joint occurred during the side drop. The causes of the failure and the requalification of the joint will be covered in a separate report. The structural failure also caused the loss of some acceleration data. Nonetheless, a valid trace was obtained for the most important part of the impact event, including the portion during which plastic deformation of the overpack occurred and, probably containing the point of maximum acceleration.

Subject to the above uncertainty in the side drop test, the maximum vertical accelerations recorded by the sensors inside the cask for the head-on, side, and CG-over-corner drops were 408, 185, and 156 G's respectively.

2.12.6. Fabrication Stresses

The following sections provide a detailed evaluation of the stresses that occur during the fabrication process of lead pour and also service at extreme cold temperatures between the inner stainless steel shell, lead shell, and outer stainless steel shell of the Model 2000 cask body.

2.12.6.1. Fabrication Stresses Due to Lead Pour

During the fabrication process, liquid lead is poured into the annulus between the inner and outer stainless steel shells of the Model 2000 cask at a temperature of ~620°F with the ambient temperature at ~70°F. Before coming into contact with the liquid lead, the stainless steel shells are at the ambient temperature. Once the liquid lead comes into contact with the stainless steel shells, the temperature difference between the two materials increases the energy in the stainless steel causing the material to expand. The dimensions of the inner and outer shells at 70°F are as follows in Table 2.12.6-1.

Table 2.12.6-1. Dimensions of Stainless Steel Shells

Parameter	Variable	Input	Units
Outer Diameter of Inner Shell	d_o	28.5	in
Inner Diameter of Inner Shell	d_i	26.5	in
Mean Radius Inner Shell	R_i	13.75	in
Outer Diameter of Outer Shell	D_o	38.5	in
Inner Diameter of Outer Shell	D_i	36.5	in
Mean Radius Outer Shell	R_o	18.75	in
Thickness of Inner Shell	t_i	1	in
Thickness of Outer Shell	t_o	1	in

2.12.6.1.1. Thermal Expansion of Stainless Steel Shells

When the inner and outer shells are subjected to the lead temperature of 620°F, the mean radius and thickness of each shell increases and is calculated with the following equations:

$$R' = R(1+\alpha\Delta T)$$

where

R = Mean Radius of Shell

α = Coefficient of Thermal Expansion For 304 Stainless Steel at 620°F (9.92E-06 in/in/°F)

ΔT = Temperature difference (620°F – 70°F = 550°F)

and

$$t' = t(1+\alpha\Delta T)$$

where

t = Thickness of Shell

Using the above equations, the shell growth of the inner shell is:

$R_i' = 13.75[1+ 9.92E\text{-}06\times550]$

$= 13.825$ in

$t_i' = 1[1+ 9.92E\text{-}06\times550]$

$= 1.005$ in

Further, the shell growth of the outer shell is:

$R_o' = 18.75[1+ 9.92E\text{-}06\times550]$

$= 18.852$ in

$t_o' = 1[1+ 9.92E\text{-}06\times550]$

$= 1.005$ in

Accordingly, the dimensions at 620°F for the inner and outer radius of each shell can be calculated using the equations below. For the inner stainless steel shell:

$r_{ii}' = r_{ii}(1+ \alpha\Delta T)$

$= 13.25[1+9.92E\text{-}06\times550]$

$= 13.322$ in

where

r_{ii}' = Inside radius of inner shell at 620°F

r_{ii} = Inside radius of inner shell at 70°F

and

$r_{oi}' = r_{oi}(1+ \alpha\Delta T)$

$= 14.25[1+9.92E\text{-}06\times550]$

$= 14.328$ in

where

r_{oi}' = Outside radius of inner shell at 620°F

r_{oi} = Outside radius of inner shell at 70°F

For the outer stainless steel shell:

$r_{io}' = r_{io}(1+ \alpha\Delta T)$

$= 18.251[1+9.92E\text{-}06\times550]$

$= 18.350$ in

where

r_{io}' = Inside radius of outer shell at 620°F

r_{io} = Inside radius of outer shell at 70°F

and

$r_{oo}' = r_{oo}(1+\alpha\Delta T)$

$= 19.25[1+9.92E\text{-}06\times550]$

$= 19.355$ in

where

r_{oo}' = Outside radius of outer shell at 620°F

r_{oo} = Outside radius of outer shell at 70°F

2.12.6.1.2. Hydrostatic Pressure

In order to determine the stresses that develop in the stainless steel shells, the static pressure that develops due to the column of lead is first calculated as follows,

$q = \rho_{lead} \times h_{lead}$

where

q = Static Pressure

ρ_{lead} = Density of lead (0.4097 lbf/in^3)

h_{lead} = Height of lead column (56 in)

NOTE: Value for the density of lead is interpolated to just below the melting point (620°F). The solid lead value is conservative because the density for liquid lead at 620°F is less and would result in a lower hydrostatic pressure and therefore lower membrane stresses.

Therefore, the hydrostatic pressure is:

$q = 0.4097 \times 56$

$q = 22.943$ psi

This hydrostatic pressure increases the outer shell radius and decreases the inner shell radius as is determined with the following equations. Decrease in inner shell mean radius due to static pressure (Reference 2-19, Table 13.8, Page 608):

$$\Delta R_i' = \frac{-q\times(R_i')^2}{E\times t_i'}$$

$$= \frac{-22.943\times(13.825)^2}{25.2E06\times1.005}$$

$= -0.000173$ in

where

E = Modulus of Elasticity of 304 Stainless Steel at 620°F (25.2E06 psi)

Increase in outer shell mean radius due to static pressure (Reference 2-19, Table 13.8, Page 608):

$$\Delta R_o' = \frac{q\times(R_o')^2}{E\times t_i'}$$

$$= \frac{22.943\times(18.852)^2}{25.2E06\times1.005}$$

$= 0.000322$ in

2.12.6.1.3. Membrane Stresses

The lead column creates a radial pressure on the inner and outer shells. The stresses due to the maximum external pressure on the inner shell are (Reference 2-19, Table 13.8, Page 608):

$$\sigma_1 = 0 \text{ psi}$$

where

σ_1 = Meridional Stress

$$\sigma_2 = \frac{-q \times r'_{oi}}{t'_i} = \frac{-22.943 \times 14.328}{1.005} = -326.941 \text{ psi}$$

where

σ_2 = Hoop Stress

σ_3 = -22.943 psi

where

σ_3 = Radial Stress

It should be noticed that the sign for the hoop stress and radial stress is negative. This is because the direction of the static pressure is acting inward instead of outward. The stresses due to the maximum internal pressure on the outer shell are (Reference 2-19, Table 13.8, Page 608):

σ_1 = 0 psi

$$\sigma_2 = \frac{q \times r'_{io}}{t'_0} = \frac{22.943 \times 18.350}{1.005} = 418.713 \text{ psi}$$

σ_3 = 22.943 psi

The allowable stress is the yield stress for the stainless steel, which is equal to 18,240 psi at 620°F. Comparing this allowable stress with the meridional, hoop and radial stresses for the inner and outer shells shows that they are all below the allowable stress and thus acceptable.

2.12.6.1.4. Buckling

Additional analysis is performed to see if the inner shell will buckle due to the external pressure (Reference 2-33, Equation 188, Page 220):

$$P_{cr} = \frac{(h/R'_i) \times \sigma_{y.p.}}{1+4(\sigma_{y.p.}/E) \times (R'^2_i/h^2)} = \frac{(1.005/13.825) \times 18240}{1+4(18240/25.2E06) \times (13.825^2/1.005^2)} = 857.28 \text{ psi}$$

where

E = Modulus of Elasticity of 304 Stainless Steel at 620°F (25.2E06 psi)

P_c = Critical Pressure

h = Thickness of Wall of [[ ]]

$\sigma_{y.p.}$ = Yield Point in Compression at 620°F

As the analysis shows, the critical pressure is larger than the pressure on the inner shell. Therefore, the liquid lead has a negligible effect on the inner and outer stainless steel shells.

2.12.6.2. Stresses Due to Lead Solidification and Lead Shrinkage

For this analysis, the dimensions of the unloaded solid lead shell are used as a reference point for interference fits. To do this, the loads due to the hydrostatic pressure are removed. The dimension of the inner and outer shells at 620°F are given in Table 2.12.6-2.

Table 2.12.6-2. Dimensions of Inner and Outer Shell at 620°F

Input Parameter	Variable	Input	Units
Inner Radius of Inner Shell at 620°F	r_{ii}'	13.322	in
Outer Radius of Inner Shell at 620°F	r_{oi}'	14.328	in
Inner Radius of Outer Shell at 620°F	r_{io}'	18.350	in
Outer Radius of Outer Shell at 620°F	r_{oo}'	19.355	in

The dimensions given in Table 2.12.6-2 are used to obtain the loaded lead dimensions of the lead shell. The inside radius of the lead shell is set equal to the outside radius of the inner steel shell and the outer radius of the lead shell is set equal to the inside radius of the outer steel shell as follows:

$R_{i\text{-}lead}$ = 14.328 in

$R_{o\text{-}lead}$ = 18.350 in

2.12.6.2.1. Unloaded Lead Dimensions

To obtain the unloaded lead dimensions, a negative load is applied to the loaded dimensions. To do this, the internal and external pressures that are acting on the lead shell are first determined. For the internal pressure acting on the inner surface of the lead shell, the change in the outer radius of the lead (Δa) is (Reference 2-19, Table 13.5, Page 696):

$$\Delta a = \frac{qab^2(2-\nu)}{E(a^2-b^2)}$$

$$= \frac{22.943\times18.350\times14.328^2(2-0.4)}{1.49E06\times(18.350^2-14.328^2)}$$

$$= 0.000706 \text{ in}$$

where

a = Outside Radius of Lead Shell

b	=	Inside Radius of Lead Shell
ν	=	Poisson's Ratio for lead at 620°F (0.4)
E	=	Modulus of Elasticity for Lead at 620°F (1.49E06 psi)

NOTE: Value for poison's ratio and modulus of elasticity are that of solid lead at just below the melting point of 620°F.

The change in the inside radius of the lead (Δb) is (Reference 2-19, Table 13.5, Page 696):

$$\Delta b = qb\frac{a^2(1+\nu)+b^2(1-2\nu)}{E(a^2-b^2)}$$

$$= 22.943\times14.328\frac{18.350^2(1+0.4)+14.328^2(1-2\times0.4)}{1.49E06\times(18.350^2-14.328^2)}$$

$$= 0.000860 \text{ in}$$

For the external pressure acting on the outer surface of the lead shell, the change in outer radius of the lead is:

$$\Delta a = -qa\frac{a^2(1-2\times\nu)+b^2(1+\nu)}{E(a^2-b^2)}$$

$$= -22.943\times18.350\frac{18.350^2(1-2\times0.4)+14.328^2(1+0.4)}{1.49E06\times(18.350^2-14.328^2)}$$

$$= -0.000763 \text{ in}$$

The change in the inside radius of the lead due to the external pressure is:

$$\Delta b = \frac{-qba^2(2-\nu)}{E(a^2-b^2)}$$

$$= \frac{-22.943\times14.328\times18.350^2(2-0.4)}{1.49E06\times(18.350^2-14.328^2)}$$

$$= -0.000904 \text{ in}$$

Now that the loaded dimensions have been determined, the unloaded dimensions are determined by removing the loads. Removing the internal pressure first:

Δa	=	-0.000706 in
Δb	=	-0.000860 in

Followed by removing the external pressure:

Δa	=	0.000763 in
Δb	=	0.000904 in

Therefore the total change in the outer and inner radius of the lead with no load is:

Δa_{total}	=	0.000763 – 0.000706
	=	0.000057 in
Δb_{total}	=	0.000904 – 0.000860
	=	0.000044 in

The dimensions of the lead at 620°F with no load is:

$R_{i\text{-}lead}$ = 14.3277480 + 0.000044

= 14.327792 in

$R_{o\text{-}lead}$ = 18.3495720 + 0.000057

= 18.3496285 in

The results show that the difference between the loaded and unloaded dimensions is negligible. Using the unloaded dimensions, a check for interference is completed.

2.12.6.2.2. Interference

At 70°F, stresses will accumulate between the lead and the inner stainless steel shell due to shrinkage of the materials as they cool down from the lead pour. To determine these stresses, the lead dimensions are calculated at 70°F. It is known that at 620°F the lead outer radius is 18.35 inches. Therefore, the equation shown below is used to determine the outer radius of the lead at 70°F.

$$R_{o70} = \frac{R_{o620}}{(1+\alpha\Delta T)} = \frac{18.350}{1+24.6E-06\times550}$$

= 18.105 in

where

R_{o620} = Outer Radius of Lead at 620°F

R_{o70} = Outer Radius of Lead at 70°F

α = Coefficient of Thermal Expansion for Lead at 620°F (24.6E-06 in/in/°F)

Accordingly, the inner radius of the lead shell at 620°F is 14.328 in and

$$R_{i70} = \frac{R_{i620}}{1+\alpha\Delta T} = \frac{14.358}{1+24.6E-06\times550}$$

= 14.137 in

The no-load dimensions at 70°F for all shells are displayed in Table 2.12.6-3.

Table 2.12.6-3. Dimensions of Shells at 70°F

	Parameter	Variable	Input	Units
1	Inner Radius Inner Shell at 70°F	r_{ii}	13.25	in
2	Outer Radius Inner Shell at 70°F	r_{oi}	14.25	in
3	Inner Radius Outer Shell at70°F	r_{io}	18.25	in
4	Outer Radius Outer Shell at 70°F	r_{oo}	19.25	in
5	Inner Radius of Lead at 70°F	R_{i70}	14.137	in
6	Outer Radius of Lead at 70°F	R_{i70}	18.105	in

The air gap between the outer shell and lead is 18.25 inches – 18.105 inches = 0.145 inches. Additionally, the interference between the inner shell and the lead is:

$$\delta = 14.25 \text{ in} - 14.137 \text{ in} = 0.113 \text{ in}$$

2.12.6.2.3. Interference Contact Pressure

Because there is interference between the inner shell and the lead, an interference contact pressure p arises between the two shells and is calculated with the following press fit equation (Reference 2-34, Equation 3-56, Page 110):

$$\delta = \frac{b_L p\left(\frac{C^2+b_L^2}{C^2-b_L^2}+\nu_L\right)}{E_L} + \frac{b_S p\left(\frac{b_S^2+a^2}{b_S^2-a^2}-\nu_S\right)}{E_S}$$

solving,

$$p = \frac{\delta}{\frac{b_L\left(\frac{C^2+b_L^2}{C^2-b_L^2}+\nu_L\right)}{E_L}+\frac{b_S\left(\frac{b_S^2+a^2}{b_S^2-a^2}-\nu_S\right)}{E_S}}$$

where

δ = Interference between contact surfaces

b_L = Inner radius of lead shell

C = Outer radius of lead shell

ν_L = Poisson's Ratio for lead at 70°F (0.4)

E_L = Modulus of Elasticity for lead at 70°F (2.42E06)

b_s = Outer radius of inner shell

ν_s = Poisson's Ratio for 304 stainless steel at 70°F (0.31)

a = Inner radius of inner shell

E_s = Modulus of Elasticity for 304 stainless steel at 70°F

Substituting values:

$$p = \frac{0.113}{\frac{14.137\left(\frac{18.105^2+14.137^2}{18.105^2-14.137^2}+0.4\right)}{2.42E06}+\frac{14.25\left(\frac{14.25^2+13.25^2}{14.25^2-13.25^2}-0.31\right)}{2.83E07}}$$

$$= 3417.512 \text{ psi}$$

An interface pressure of this magnitude will cause the lead to yield.

2.12.6.2.4. Internal and External Loads on Lead Shell and Inner Shell

To determine a more accurate interface pressure, the maximum pressure is set equal to the pressure that corresponds to the hoop stress at which the lead yields.

Loads at 70°F

The yield strength of lead at 70°F is 620 psi and is set to the hoop stress to obtain the maximum pressure. For a thick-walled shell (Reference 2-19, Table 13.5, Page 696):

$$p = \frac{\sigma_2(C^2-b_L^2)}{C^2+b_L^2}$$

$$= \frac{620(18.105^2-14.137^2)}{18.105^2+14.137^2}$$

$$p = 150.338 \text{ psi}$$

This pressure will translate to the inner shell causing a hoop stress of (Reference 2-19, Table 13.5, Page 696):

$$\sigma_2 = -\frac{p(b_s^2+a^2)}{b_s^2-a^2}$$

$$= -\frac{150.338(14.25^2+13.25^2)}{14.25^2-13.25^2}$$

$$= -2069.882 \text{ psi}$$

It should be noted that any relaxation due to creep can be conservatively neglected.

Loads at -20°F

Now consider the HAC temperature of -20°F for the worst hoop stress on the inner shell. The coefficient of thermal expansion for the lead and stainless steel at the HAC -20°F temperature is:

$\alpha_{ss\text{-}20}$ = 8.17E-06 (in/in/°F)

$\alpha_{L\text{-}20}$ = 1.57E-05 (in/in/°F)

Then the steel and lead shell dimensions at -20°F are as follows

a	=	13.25[1 + 8.17E-06 ×-90]	=	13.240 in
b_s	=	14.25[1 + 8.17E-06 ×-90]	=	14.240 in
b_L	=	14.1365[1 + 1.57E-05 ×-90]	=	14.117 in
C	=	18.105[1 + 1.57E-05 ×-90]	=	18.079 in

This gives an interference of 0.123 in between the inner shell and the lead at -20°F. This interference will cause the lead to yield. Once again, to achieve a more accurate interface pressure, set the maximum pressure to be equal to the pressure that corresponds to the hoop stress at which the lead yields. The yield strength of lead at -20°F is 763 psi, which gives an interface pressure of (Reference 2-19, Table 13.5, Page 696):

$$p = \frac{\sigma_2(C^2-b_L^2)}{C^2+b_L^2}$$

$$= \frac{763(18.079^2-14.117^2)}{18.079^2+14.117^2}$$

$$= 185.013 \text{ psi}$$

This pressure will translate to the inner shell causing a hoop stress of (Reference 2-19, Table 13.5, Page 696):

$$\sigma_2 = -\frac{p(b_s^2+a^2)}{b_s^2-a^2}$$

$$= -\frac{185.013\left(14.24^2+13.24^2\right)}{14.24^2-13.24^2}$$

$$= \text{-2547.290 psi}$$

Loads at -40°F

Now consider the normal conditions of transport extreme cold temperature of -40°F for the worst hoop stress on the inner steel shell. The coefficient of thermal expansion for the lead and stainless steel at the HAC -40°F temperature is:

$\alpha_{ss\text{-}40}$ = 8.09E-06 (in/in/°F)

$\alpha_{L\text{-}40}$ = 1.56E-05 (in/in/°F)

Calculating the lead and steel shell dimensions at -40°F, the following results:

a	=	13.25[1 + 8.09E-06 ×-110]	=	13.238 in
b_s	=	14.25[1 + 8.09E-06 ×-110]	=	14.237 in
b_L	=	14.1365[1 + 1.56E-05 × -110]	=	14.112 in
C	=	18.105[1 + 1.56E-05 × -110]	=	18.074 in

This results in an interference fit of 0.125 in between the inner shell and lead. Accordingly, the yield strength of lead at -40°F is 795 psi, which is set to the hoop stress to obtain maximum pressure as follows (Reference 2-19, Table 13.5, Page 696):

$$p = \frac{\sigma_2\left(C^2-b_L^2\right)}{C^2+b_L^2}$$

$$= \frac{795\left(18.074^2-14.112^2\right)}{18.074^2-14.112^2}$$

$$= 192.77 \text{ psi}$$

Calculating the hoop stress in the inner shell (Reference 2-19, Table 13.5, Page 696):

$$\sigma_2 = -\frac{p\left(b_s^2+a^2\right)}{b_s^2-a^2}$$

$$= \frac{192.77\left(14.237^2+13.238^2\right)}{14.237^2-13.238^2}$$

$$= \text{-2654.123 psi}$$

2.12.6.2.5. Axial Stresses and Strains

The previous calculations only deal with hoop stresses. Axial shrinkage of the lead will cause axial stresses to develop in the inner stainless steel and lead shells.

Cooling From 620°F to -20°F

Axial stresses and strains will occur in the inner shell from cooling down from 620°F to -20°F. The axial strain that results between the lead and stainless steel from the cooling to the extreme cold temperature of -20°F is:

Σ_{strain} = $(\alpha_{L620}- \alpha_{SS620})\,\Delta T + (\alpha_{L\text{-}20}- \alpha_{SS\text{-}20})\,\Delta T$

= (24.6E-06 – 9.92E-06)(550)+(15.7E-06 – 8.18E-06)(-90)

$$= 0.0074$$

$$= 0.74\%$$

As a result of this tensile strain, the lead will yield. The yield strength for lead at -20°F is 763 psi, which will produce an effective force of:

$$P_{axial} = S_y A$$
$$= 763(\pi)(18.079^2 - 14.117^2)$$
$$= 305{,}805 \text{ lb}$$

The same force can develop a compressive axial stress in the inner steel shell from equilibrium as follows:

$$\sigma = -\frac{P_{axial}}{A}$$
$$= -\frac{305{,}805}{\pi(14.240^2 - 13.240^2)}$$
$$= -3544.88 \text{ psi}$$

Cooling From 620°F to -40°F

The axial strain that results between the lead and stainless steel from the cooling to the extreme cold temperature of -40°F is:

$$\Sigma_{strain} = (\alpha_{L620} - \alpha_{SS620})\,\Delta T + (\alpha_{L-40} - \alpha_{SS-40})\,\Delta T$$
$$= (24.6\text{E-}06 - 9.92\text{E-}06)(550) + (15.6\text{E-}06 - 8.09\text{E-}06)(-110)$$
$$= 0.00725$$
$$= 0.725\%$$

Once again, as a result of this tensile strain, the lead will yield. The yield strength for lead at -40°F is 795 psi, which will produce an effective force of

$$P_{axial} = S_y A$$
$$= 795(\pi)(18.074^2 - 14.112^2)$$
$$= 318{,}437 \text{ lb}$$

From equilibrium, the same force can develop a compressive axial stress in the inner steel shell as calculated below:

$$\sigma = -\frac{P_{axial}}{A}$$
$$= -\frac{318{,}437}{\pi(14.237^2 - 13.238^2)}$$
$$= -3692.45 \text{ psi}$$

2.12.6.3. Summary of Results

The stresses on the inner shell of the Model 2000 cask produce an axial stress of -3692.45 psi and a hoop stress of -2654.12 psi when at the low temperature of -40°F. In the case of the -20°F low temperature, an axial stress of -3544.88 psi and a hoop stress of -2547.29 psi is produced on the inner shell.

In the 620°F case, a hoop stress of -326.94 psi is produced on the inner shell and a hoop stress of 418.71 psi is produced on the outer shell. Table 2.12.6-4 below is a summary of stresses that occur in the inner and outer stainless steel shells due to lead pouring, solidification, and shrinkage.

Table 2.12.6-4. Summary of Stresses Due to Lead Pouring, Solidification, and Shrinkage

Temperature (°F)	Inner Shell Stress (psi)			Outer Shell Stress (psi)			Lead Yield Stress (psi)
	σ_1	σ_2	σ_3	σ_1	σ_2	σ_3	S_y
620	0	-326.94	-22.94	0	418.71	22.94	Liquid
70	0	-2069.88	-150.34	0	0	0	620
-20	-3544.88	-2547.29	-185.01	0	0	0	763
-40	-3692.45	-2654.12	-192.29	0	0	0	795

The results of the analysis indicate that the Model 2000 cask meets the general requirements of 10 CFR 71.43 and also the requirements of the standard review plan NUREG-1609.

2.13 References

2-1 U.S. NRC, 10 CFR 71, "Packaging and Transportation of Radioactive Material," Washington D.C.

2-2 U.S. NRC, Regulatory Guide 7.8, “Load Combinations for the Structural Analysis of Shipping Casks for Radioactive Material," March 1989.

2-3 ASME, "Boiler & Pressure Vessel Code, Section III—Subsection NF, Supports," 2010.

2-4 U.S. NRC, Regulatory Guide 7.11, “Fracture Toughness Criteria of Base Material for Ferritic Steel Shipping Cask Containment Vessels with a Maximum Wall Thickness of 4 Inches (0.1 m)," 7.11, June 1991.

2-5 U.S. NRC, "Fabrication Criteria for Shipping Containers," NUREG/CR-3854, 1985.

2-6 U.S. NRC, "Classification of Transportation Packaging and Dry Spent Fuel Storage System Components According to Importance to Safety," NUREG/CR-6407, February 1996.

2-7 ASME, "Boiler & Pressure Vessel Code (BPVC), Section II, Part D, Properties Materials," 2010.

2-8 American Society for Metals (ASM), "Metals Handbook Tenth Edition, Volume 2, Properties and Selection: Nonferrous Alloys and Special Purpose Materials, Uranium and Uranium Alloys," Metals Park, OH, 1990.

2-9 Battelle Columbus Laboratories, "The Mechanical Properties of Depleted Uranium - 2 w/o Molybdenum Alloy," BMI-2032, 1979.

2-10 Henry J. Rack and Gerald A. Knorovsky, "An Assessment of Stress-Strain Data Suitable for Finite-Element Elastic-Plastic Analysis of Shipping Containers," Sandia Laboratories, NUREG/CR-0481, 1978.

2-11 W. Hoffman, Lead and Lead Alloys, English Translation of the Second Revised German Edition ed. New York: Springer-Verlag, 1970.

2-12 Thomas E. Tietz, "Determination of the Mechanical Properties of a High Purity Lead and a 0.058 % Copper-Lead Alloy," Stanford Research Institute, WADC 57-695, 1958.

2-13 Eugene A. Avallone, Theodore Baumeister III, and Ali M. Sadegh, "Marks' Standard Handbook for Mechanical Engineers," Eleventh Edition, 2007.

2-14 Parker-Hannifin Corporation, "Gask-O-Seal and Integral Seal Design Handbook," 2010.

2-15 G. C. Mok, L. E. Fischer, and S. T. Hsu, "Stress Analysis of Closure Bolts for Shipping Casks," LLNL, NUREG/CR-6007, 1993.

2-16 ANSYS®, "Mechanical, Revision 14.0," November 2011.

2-17 U.S. NRC, "Regulatory Guide 7.6, Stress Allowables for the Design of Shipping Cask Containment Vessels," February 1977.

2-18 ASME, "Boiler and Pressure Vessel Code (BPVC), Section III, Division 1 - Appendices," 2010.

2-19 Warren C. Young, "Roark's Formulas for Stress & Strain," Seventh Edition ed. New York: McGraw Hill, 2002.

2-20 Livermore Software Technology Corporation, "LS-DYNA, A Program for Nonlinear Dynamic Analysis of Structure in Three Dimensions," Version 971, Ed. Livermore, CA, 03/23/2011.

2-21 ASME, "Boiler and Pressure Vessel Code (BPVC), Section VIII, Division 2, Alternative Rules, Annex 3.D – Strength Parameters," New York, 2008.

2-22 R. K. Blandford and D. K. Morton, Impact Tensile Testing of Stainless Steels at Various Temperatures, INL/EXT-08-14082. Idaho Falls, Idaho 83415: Idaho National Laboratory, March 2008.

2-23 Hexcel Corporation, HexWeb Honeycomb Energy Absorption System - Design Data. Southbury, CT, March 2005.

2-24 Oak Ridge National Laboratory, "A Guide to the Design of Shipping Casks for the Transportation or Radioactive Material, ORNL-TM-681," Oak Ridge, TN, April 1965.

2-25 Richard G. Budynas and J. Keith Nisbett, Shigley's Mechanical Engineering Design, 9th ed., 2011.

2-26 E. Oberg, F. D. Jones, H. L. Horton, and H. H. Ryffel, Machineries Handbook, 26th ed., Christopher J. McCauley, Ed. New York, United States: Industrial Press INC., 2000.

2-27 J. E. Shigley and L. Mitchell, Mechanical Engineering Design, 4th ed. New York, United States: McGraw-Hill, 1965.

2-28 ASME, "Rules for Construction of Nuclear Facility Components," in 2010 ASME Boiler and Pressure Vessel Code, Section VIII, Division 1, ASME, Ed. New York, United States: The American Society of Mechanical Engineers, 2010.

2-29 R.J. Roark, Formulas for Stress and Strain, 4th ed. New York, United States: McGraw-Hill INC., 1965.

2-30 Erik Oberg and Franklin D. Jones, Machinery's Handbook, 29th ed. New York: Industrial press, 2012.

2-31 American Society of Mechanical Engineers (ASME), "Rules for Construction of Nuclear Facility Components," Article E-1000, Section III, Division I, Appendices, 2010.

2-32 American Society of Mechanical Engineers (ASME), "Article NB-3000," Section III, Division I, 1998.

2-33 Stephen P. Timoshenko, Strength of Materials, 2nd ed. New York: Van Nostrand, 1948.

2-34 Richard G. Budynas and J. Keith Nisbett, Shigley's Mechanical Engineering Design, 8th ed. Boston: McGraw-Hill, 2008.

3 THERMAL EVALUATION

This section presents the thermal evaluation of the Model 2000 Transport Package and high performance insert (HPI) with a contents thermal loading of 1500 W and a contents thermal loading of 3000 W, both under Normal Conditions of Transport (NCT) and Hypothetical Accident Conditions (HAC) as prescribed by 10 CFR 71 (Reference 3-1). The 3000 W results are presented in Sections 3.3 and 3.4, and the 1500 W results are presented in Section 3.5.1.

The decay heat limit for shipping all contents shall be conservatively limited to 1500 W. However, a decay heat of 3000 W is evaluated as the basis for the Model 2000 Transport Package in Chapter 2.

Specifically, the following requirements of 10 CFR 71 are addressed:

1) General standards for all packages, 10 CFR 71.43(g)

A package must be designed, constructed, and prepared for transport so that in still air at 100°F and in the shade, no accessible surface of a package would have a temperature exceeding 122°F in a nonexclusive use shipment, or 185°F in an exclusive use shipment.

2) Normal Conditions of Transport—heat, 10 CFR 71.71(c)(1)

Evaluation of the package design for exposure to an ambient temperature in still air and insolation according to Table 3-1.

Table 3-1. Insolation Data per 10 CFR 71.71

Form and Location of Surface	Total Insolation for a 12-Hour Period (g cal/cm²)
Flat surfaces transported horizontally;	
Base	None
Other surface	800
Flat surfaces not transported horizontally	200
Curved surfaces	400

3) Hypothetical Accident Conditions—thermal, 10 CFR 71.73(c)(4)

Exposure of the package fully engulfed in a hydrocarbon fuel/air fire of sufficient extent, and in sufficiently quiescent ambient conditions, to provide an average emissivity coefficient of at least 0.9, with an average flame temperature of at least 1475°F for a period of 30 minutes, or any other thermal test that provides the equivalent total heat input to the package and which provides a time averaged environmental temperature of 1475°F.

For purposes of calculation, the surface absorptivity coefficient must be either that value which the package may be expected to possess if exposed to the fire specified or 0.8, whichever is greater; and the convective coefficient must be that value which may be demonstrated to exist if the package were exposed to the fire specified. Artificial cooling may not be applied after cessation of external heat input, and any combustion of materials of construction, must be allowed to proceed until it terminates naturally.

§71.73(b) With respect to the initial test conditions, the ambient air temperature before and after the test must remain constant at that value between -20°F and 100°F which is most unfavorable for the feature under consideration.

To demonstrate that the Model 2000 Transport Package, shown in Figure 3-1, meets these requirements, a three-dimensional finite element model of the package was developed and analyzed using the general-purpose finite element analysis (FEA) code ANSYS, Release 14.0 (Reference 3-2). Multiple ANSYS thermal calculations were performed simulating NCT and HAC using the finite element representation of the Model 2000 Transport Package with HPI.

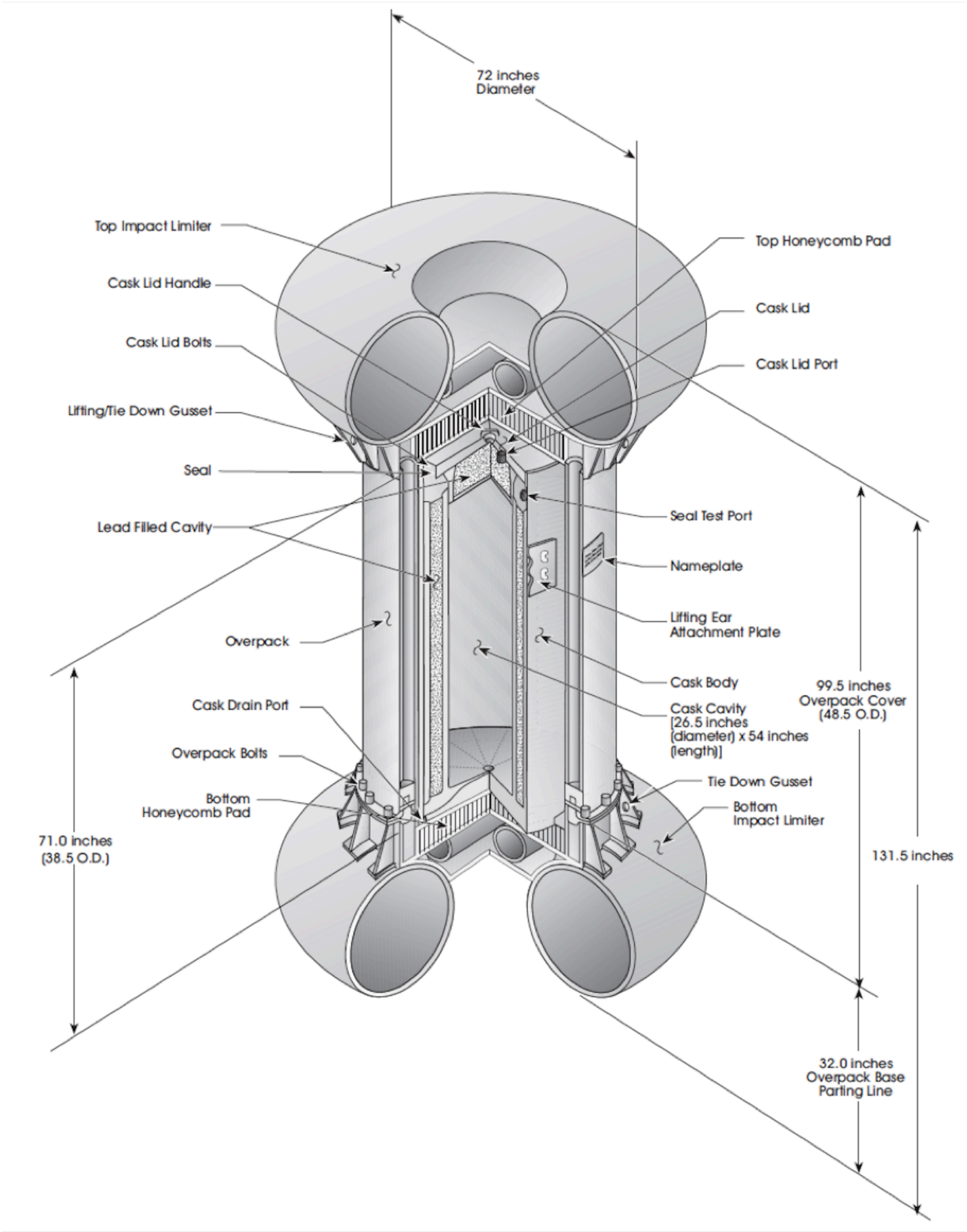

Figure 3-1. Model 2000 Transport Package
(High Performance Insert and Material Basket Not Shown)

3.1 Description of Thermal Design

3.1.1. Design Features

The Model 2000 Transport Package, described in Section 1.2, is designed with a thermally passive system. The cask is enclosed in an overpack that serves as a fire shield. The overpack is designed to reduce heat flow from the fire environment into the cask structure by the use of enclosed air spaces. It is composed of two concentric cylindrical SS304 shells approximately 83 inches long with an OD of 48.5 inches and an ID of 40.5 inches. The shells are separated radially by eight equally spaced [[ ]] along the length of the shells, and horizontally by two [[ ]] sections to provide closed air spaces. A 24-inch diameter toroidal shell is attached at both ends of the outer shell with a circular plate enclosing the inner regions of the torus. The internal shell is also closed at each end by a circular plate. All materials are SS304. The [[

]]

Attached at both ends of the overpack inner surface are aluminum honeycomb pads.

The cask is designed with lead shielding on three sides and a 6-inch thick stainless steel forging at the base that functions as a heat sink that allows the heat to flow through the bottom of the package. When the cask is placed in the overpack during assembly, air gaps of 1.0-inch radially and 1.0-inch at the top separate the cask from the overpack inner surfaces.

The cask lid seal design, which includes an [[ ]] and metal retainer component, is based on a 1500 W content decay heat. The cask lid seal is a [[ ]] retainer with four Parker Compound No. [[ ]] rings, two concentric [[ ]] seals on the top and two [[ ]] seals on the bottom. See Chapter 4 for further discussion. The cask lid is secured to the cask body by fifteen (15) 1¼-inch diameter socket head screws.

The HPI is described in Section 1.2.2.1.

3.1.2. Content's Decay Heat

The derivations of the decay heats for the different contents of the Model 2000 Transport Package are presented in Chapter 5. The decay heat for irradiated hardware and by-product, and cobalt-60 isotope rod contents is determined using watt-per-Curie conversion factors listed in Section 5.5.4 and the radionuclide inventory of the contents.

3.1.3. Summary Tables of Temperatures

Thermal design criteria are specified for regions throughout the cask, cask cavity, and the outside overpack wall. The cask lid seal and port O-ring is limited to the temperature listed in Table 3.1.3-1, and this serves as the thermal criteria for the region associated with the seal area. The maximum allowable internal pressure is 30 psia, which corresponds to air of 100% humidity heated to 600°F at constant volume.

Table 3.1.3-1 presents the maximum design temperatures of the components or materials that affect structural integrity, containment, and shielding under both NCT and HAC for 3000 W of decay heat. Where available, temperature limits for the Model 2000 Transport Package

components are obtained from manufacturers' literature. Otherwise, component temperature limits are defined as the melting temperature of the material of construction.

Table 3.1.3-1. Temperature Limits

Component or Material	Temperature Limit (°F)
Stainless Steel Components	2546
Lead Shielding[a]	622
Depleted Uranium Shielding[a]	2071
Aluminum Honeycomb[b]	350
Cask Lid Seal	5 to 508[c]
Cask Ports	-40 to 612[c]
Accessible Surfaces Of Package	< 185[d]

Notes:
a. Temperature limit is melting temperature (Reference 3-3).
b. Maximum operating temperature (Reference 3-4).
c. See Chapter 4 for additional discussion.
d. Exclusive use requirement per 10 CFR 71.43(g).

3.1.3.1. NCT Temperature Summary

Per the requirements of 10 CFR 71.71(c)(1) (Reference 3-1), the 3000 W case is evaluated for NCT. Specifically, a steady-state thermal analysis is performed simulating exposure of the package to a 100°F ambient temperature in still air and insolation as specified in Table 3-1. The results of the analysis are presented in Section 3.3. The temperatures of several key package components are summarized and compared with their allowable temperatures in Table 3.1.3-2.

Table 3.1.3-2. NCT Temperature Summary and Comparison with Allowable Temperatures

Item	NCT Temperatures (°F)	Allowable Temperature (°F)
Material Basket	1,001 (max)	2,546
HPI Shielding (Depleted Uranium)	601 (max)	2,071
Cask Lid Seal	432 (max)	508[c]
Cask Shielding (Lead)	449 (max)	622
Honeycomb Impact Limiters	359 (max)[a] / 334 (avg)	350
Cask Drain Port (Bottom)	370	612[c]
Cask Test Port (Top)	426	
Cask Vent Port (Lid)	442	
Overpack Outer Surface	215	185[b]

Notes:
a. The maximum honeycomb impact limiter temperature of 359°F exceeds the allowable temperature of 350°F. However, this maximum temperature occurs in a very limited area of the impact limiter and is based on steady-state boundary conditions for the hot case, which ignores the removal of solar insolation during the night cycle. The majority of the impact limiter temperatures are below 350°F. Therefore, the average temperature of 334°F is appropriate to compare to the allowable temperature.
b. Limit specified in 10 CFR 71.43(g), which requires the addition of a personnel barrier to satisfy this requirement. Refer to Section 7.1.4, Preparation for Transport.
c. See Chapter 4 for additional discussion.

The Model 2000 Transport Package components remain below their allowable temperatures for NCT with insolation. Therefore, when exposed to NCT with insolation, and 1500 W decay heat, the Model 2000 Transport Package maintains containment of the contents, as neither the shielding nor the impact limiting materials exceed temperatures that would adversely affect their performance. See Chapter 4 for further details.

3.1.3.2. HAC Temperature Summary

When exposed to the HAC fire prescribed in the regulations, the Model 2000 Transport Package must maintain containment of its contents and maintain its shielding capabilities. The results of the HAC thermal evaluation are presented in Section 3.4. As shown in Table 3.1.3-3, the maximum temperatures of the different package components are below the allowable temperatures. Therefore, the HAC fire does not adversely affect the package's ability to provide containment and shielding for its contents. Note, that the maximum average fill gas temperatures in the HPI and cask are 740°F and 571°F, respectively. The maximum average combined fill gas temperature (HPI + cask) is 585°F.

Table 3.1.3-3. HAC Maximum Temperature Summary and Comparison with Allowable Temperatures

Item	HAC Maximum Temperature (°F)	Allowable Temperature (°F)
Material Basket	1,045	2,546
HPI Shielding (Side)	670	2,071
HPI Shielding (Top)	599	2,071
HPI Shielding (Bottom)	618	2,071
Cask Lid Seal	508	508[b]
Cask Shielding (Side)	570	622
Cask Shielding (Top)	529	622
Cask Shell (Puncture Location)	782	-
Cask Shell (Opposite side to Puncture Location)	512	-
Overpack Outer Shell (Puncture Location)	1,103	-
Overpack Outer Shell (Opposite Side to Puncture Location)	1,337	-
Cask Drain Port (bottom)	612[a]	612[b]
Cask Test Port (top)	608[a]	612[b]
Cask Vent Port (lid)	520	612[b]
HPI Fill Gas (Average)	740	-
Cask Fill Gas (Average)	571	-
Combined HPI and Cask Fill Gas (Average)	585	-

Notes:
a. Temperatures for Drain Port and Test Port exceed 600°F for 21 minutes and 11 minutes, respectively. Seal acceptance testing conditions for cask lid seal and port containment components are specified in Reference 3-5.
b. See Chapter 4 for additional discussion.

3.1.4. Summary Tables of Maximum Pressures

Table 3.1.4-1 shows the maximum normal operating pressure and the maximum pressure under hypothetical accident conditions.

Table 3.1.4-1. Maximum Pressures

Component or Material	Reference	Pressure (psia)
Maximum Design Internal Pressure	Section 2.4.3	30.0
Maximum Normal Operating Pressure	Section 3.3.2	26.8
Maximum Average Pressure under HAC	Section 3.4.3	29.0

3.2 Material Properties and Component Specifications

3.2.1. Material Properties

The thermal properties of the materials of construction used in the analyses for the thermal evaluation are presented in Table 3.2.1-1. When available from the open literature, temperature-dependent properties are used in the analyses. Additionally, the thermal properties of the HPI and cask fill gas (helium) and overpack gas (air) are presented in Table 3.2.1-2 (Reference 3-3).

Table 3.2.1-1. Thermal Properties of Solid Regions in the Model 2000 Finite Element Thermal Model

Material	Temperature (°F)	Density (lbm/in^3)	Thermal Conductivity (Btu/h-in-°F)	Specific Heat (Btu/lbm-°F)	Emissivity
AISI 304 Stainless Steel[a]	-100	---	0.607	0.096	---
	80	0.285	0.717	0.114	0.22
	260	---	0.799	0.123	0.22
	620	---	0.953	0.133	0.24
	980	---	1.088	0.139	0.28
	1340	---	1.223	0.146	0.35
	1700	---	1.348	0.153	---
	2240	---	1.526	0.163	---
Lead[a]	-100	---	1.767	0.030	---
	80	0.410	1.700	0.031	---
	260	---	1.637	0.032	---
	620	---	1.512	0.034	---
Depleted Uranium[a]	-100	---	1.209	0.026	---
	80	0.689	1.329	0.028	---
	260	---	1.425	0.030	---
	620	---	1.637	0.035	---
	980	---	1.858	0.042	---
	1340	---	2.114	0.043	---
	1700	---	2.359	0.038	---
AISI 316 Stainless Steel[a]	80	0.298	0.645	0.112	0.22
	260	---	0.732	0.120	0.22
	620	---	0.881	0.131	0.24
	980	---	1.026	0.138	0.28
	1340	---	1.165	0.144	0.35
[[ ]][b]	---	Same as AISI 304 or AISI 316	Same as AISI 304 or AISI 316	Same as AISI 304 or AISI 316	0.44
Aluminum Honeycomb[c]	-100	---	0.465	---	---
	0	---	0.608	---	---
	75	0.0046	0.715	0.208	0.20
	100	---	0.751	---	---
	200	---	0.894	---	---
	300	---	1.073	---	---

Notes:
a. Reference 3-3, Table A.1 (density, thermal conductivity, and specific heat) and Table A.11 (emissivity).
b. Reference 3-6.
c. Density and thermal conductivity – Reference 3-4. Specific heat of Aluminum 2024-T6– Reference 3-3, Table A.1. Emissivity of heavily oxidized aluminum– Reference 3-7, Appendix D.

Table 3.2.1-2. Thermal Properties of Gaseous Regions in the Finite Element Thermal Model

Material	Temperature (°F)	Density (lbm/in^3)	Thermal Conductivity (Btu/h-in-°F)	Specific Heat (Btu/lbm-°F)	Emissivity
Helium	-64	---	5.93E-3	---	---
	-28	---	6.26E-3	---	---
	8	---	6.60E-3	---	---
	44	---	6.98E-3	---	---
	80	5.871E-6	7.32E-3	1.24	---
	170	---	8.19E-3	---	---
	260	---	9.00E-3	---	---
	350	---	9.82E-3	---	---
	440	---	1.06E-2	---	---
	620	---	1.21E-2	---	---
	710	---	1.27E-2	---	---
	800	---	1.34E-2	---	---
	890	---	1.40E-2	---	---
	980	---	1.46E-2	---	---
	1160	---	1.59E-2	---	---
	1340	---	1.70E-2	---	---
Air	-100	---	8.72E-4	0.241	---
	-10	---	1.07E-3	0.240	---
	80	4.196E-5	1.27E-3	0.241	---
	170	---	1.44E-3	0.241	---
	260	---	1.63E-3	0.242	---
	350	---	1.80E-3	0.244	---
	440	---	1.96E-3	0.246	---
	530	---	2.11E-3	0.248	---
	620	---	2.26E-3	0.251	---
	710	---	2.39E-3	0.254	---
	800	---	2.52E-3	0.257	---
	890	---	2.64E-3	0.260	---
	980	---	2.76E-3	0.263	---
	1070	---	2.87E-3	0.263	---
	1160	---	2.99E-3	0.268	---
	1250	---	3.10E-3	0.270	---
	1340	---	3.21E-3	0.273	---
	1520	---	3.44E-3	0.277	---
	1700	---	3.67E-3	0.281	---

3.2.2. Component Specifications

The Model 2000 Transport Package component materials are primarily stainless steel, lead, and aluminum. The maximum allowable temperatures of these materials are given in Table 3.1.3-1. The temperatures resulting from normal and accident thermal conditions fall within these temperatures.

The only component material that is temperature sensitive is the [[ ]] material in the cask lid seal and port plug O-rings. The material used is [[ ]] that offers an operating temperature range adequate for 1500 W decay heat (Reference 3-8). The cask lid seal design includes an aluminum [[ ]]; temperatures resulting from normal and accident thermal conditions fall within the material limits. See Chapter 4 for additional discussion.

3.3 Thermal Evaluation under Normal Conditions of Transport

Thermal performance for 3000 W decay heat is analyzed for NCT (with and without insolation) by performing steady-state heat transfer analyses on a finite element representation of the package. Specifically, the general-purpose finite element code ANSYS, Release 14.0 (Reference 3-2), is used to model and analyze the Model 2000 Transport Package with a content heat load of 3000 W for NCT. Several ANSYS macros are created in order to build the model, apply boundary conditions, and perform the steady-state analyses.

Assumptions made for this evaluation are:

- The Model 2000 Transport Package is assumed to be in an upright (vertical) orientation during NCT.
- The cask and HPI are backfilled with Helium at 70°F and 14.7 psia.
- Natural convection within the package cavities is neglected.
- The contents of the HPI are assumed to generate a maximum of 3000 W that is uniformly distributed among the [[ ]].
- During NCT, the package is assumed to have an emissivity consistent with the material of construction at temperature.

As mentioned above, for the NCT analysis, a steady-state thermal analysis was performed simulating exposure of the package to a 100°F ambient temperature in still air and insolation as specified in Table 3-1. The results of the analysis are presented below. The temperatures of the key package components are summarized and compared with their allowable temperatures in Table 3.1.3-2.

NCT sensitivity studies were also performed to evaluate the thermal performance of the package using boundary conditions applied as both steady state and as constant boundary conditions solved as a transient. Because the solutions are radiation-dominated, the transient solution results in better convergence and slightly higher temperatures. To achieve steady-state conditions with the transient solver, a simulated time of 2000 hours was used. The 2000-hour duration of the transient analyses is sufficiently long enough for the temperatures within the package to reach steady-state

values, that is, the temperature of a node within the package model doesn't change from one time step to the next.

Model Description

The general-purpose finite element code ANSYS, Release 14.0 (Reference 3-2), is used to model and analyze the Model 2000 Transport Package with a content heat load of 3000 W for NCT. Several ANSYS macros are created in order to build the model, apply boundary conditions, and perform the steady-state analyses.

The model, shown in Figure 3.3-1 through Figure 3.3-3, represents a half-symmetry of the package. A half-symmetry model is used so that damage from the HAC drop/puncture test may be incorporated using the same model.

In the model, the decay heat of the contents, applied as a heat flux to the material basket [[ ]], is transferred through the solid and gaseous regions via conduction heat transfer, across gaseous regions separating solids via thermal radiation, and then rejected to the surroundings via natural convection and thermal radiation. Heat transfer via convection within the package is not considered. In addition to the decay heat of the contents, other heat sources—insolation (heat flux) and/or fire (convection/thermal radiation)—are also included as boundary conditions where appropriate.

To simulate this heat flow, a finite element model of the Model 2000 Transport Package with HPI is generated with the APDL using a combination of SOLID70, CONTA173, TARGE170, LINK34, SURF152, and SURF252 elements. Each of the element types used to model the Model 2000 Transport Package and the modes of heat transfer modeled by the various element types are discussed in the following paragraphs.

The SOLID70 elements are 3D, 8-node, single degree-of-freedom (DOF) thermal solid elements and are used to model heat flow through the solid and gaseous regions of the package via conduction heat transfer.

The CONTA173/TARGE170 pairs are 3D, 4-node, surface-to-surface contact elements that are overlaid onto area faces of the SOLID70 elements and are used to model heat flow across interfaces between contacting components or across interfaces between dissimilar meshes. The LINK34 elements are uniaxial elements with the ability to convect heat between 2 nodes; however, because thermal contact conductance has the same units as the convection heat transfer coefficient, the LINK34 elements are used to model heat flow between contacting components that either have a line-of-contact or are physically separated in the model and, therefore, do not lend themselves to the use of the CONTA173/TARG170 pairs.

The SURF152 3D thermal surface effect elements are overlaid onto area faces of the SOLID70 elements and are used to apply heat flux (fuel material basket [[ ]] internal surfaces) and convection (overpack external surfaces) boundary conditions. For NCT, insolation (heat flux) is applied directly to area faces of the SOLID70 elements; SURF152 elements are not used to apply this heat load.

Finally, radiation exchange between solid surfaces separated by gaseous regions is modeled using the radiosity solver in conjunction with SURF252 elements. SURF252 are 3D, 4-node, radiosity surface elements that are overlaid onto area faces of the SOLID70 elements that have a radiosity boundary condition using the RSUF command, and then expanded into full 360° in order to properly calculate radiation view factors for models that only model a portion of the actual item due to symmetry.

[[

]]

Figure 3.3-1. Finite Element Model of the Model 2000 Transport Package

[[

]]

Figure 3.3-2. Finite Element Model of the Model 2000 Transport Package - Air and Helium Not Shown

[[

]]

Figure 3.3-3. Finite Element Model of the Model 2000 Transport Package - Exploded View

Thermal Contact Resistance/Conductance

To simulate welded joints (e.g., the cask cavity shell welded to the cask bottom), the nodes of each mating component are merged at the weld joint. This allows heat to flow across these welded interfaces. However, for all other component interfaces, each component in the finite element model is independent and does not share nodes with its neighboring component(s). Therefore, in order to allow heat to flow through the model, each component is connected to its neighboring component using CONTA173/TARGE170 thermal contact/target elements. For components that have only a line of contact (e.g., Hertzian contact), or if the elements of contacting components are not physically modeled as being in contact, LINK34 convection 2-node elements are used to model the contact resistance.

Thermal contact resistance, R_{tc}, between mating parts results in a temperature drop across the interface between these parts (see Figure 3.3-4). Note that the surface roughness is exaggerated in the figure. The existence of a finite contact resistance is due primarily to the surface roughness of the mating parts. Other factors that affect the contact resistance are the mating materials, interfacial fluid/gas, and pressure. Theoretical methods to calculate this resistance have been developed; however, empirically derived resistances have provided better correlation with actual measured temperature drops across contact interfaces (Reference 3-3).

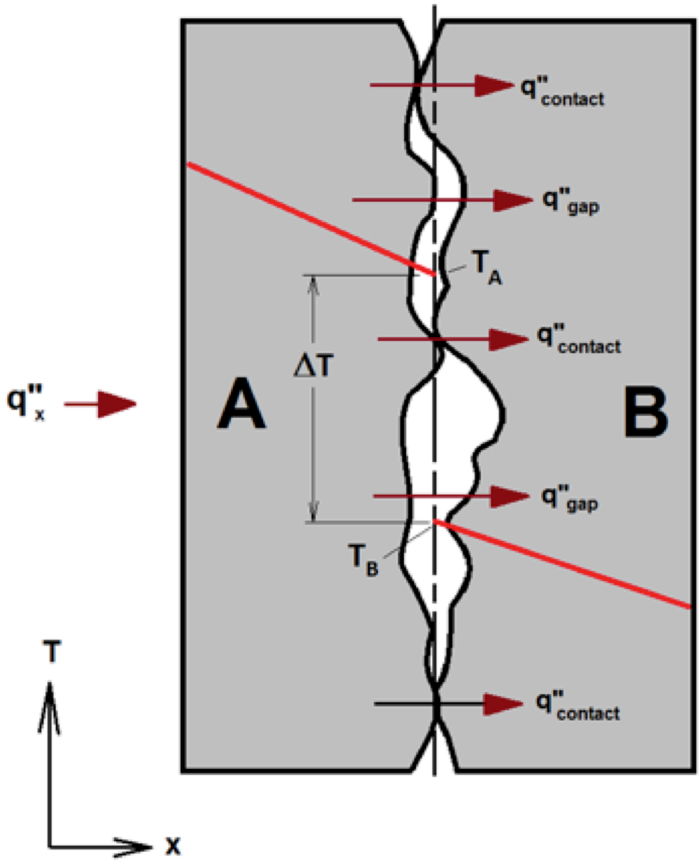

Figure 3.3-4. Heat Transfer Through the Contact Plane Between Two Solid Surfaces

The thermal resistance effect shown in Figure 3.3-4 is described by the following equation from Reference 3-3, Equation 3.20, for a unit area of interface:

$$R''_{tc} = \frac{T_A - T_B}{q''_x}$$

where R''_{tc} = thermal resistance per unit area,

T_A = temperature of material A,

T_B = temperature of material B, and

q''_x = heat flux.

Thermal contact is modeled in ANSYS by specifying the thermal contact conductance (TCC) of the interface either as a real constant (for the CONTA173/TARGE170 pairs) or as a material property (LINK34). The TCC is defined as the reciprocal of the thermal contact resistance; therefore, a high TCC value implies low thermal contact resistance, and a low TCC value implies high thermal contact resistance.

While the LINK34 is a 2-node convection element, the natural convection coefficient has the same units as that of thermal contact conductance. Therefore, the LINK34 element can be used to simulate thermal contact between two nodes by substituting the TCC value for the convection coefficient.

Experimentally determined TCC values for various mating materials, surface finishes, interfacial gases, and interface pressures are shown in Table 3.3-1.

Because there are a large number of thermal contact interfaces to manage in the Model 2000 Transport Package thermal model, and because exact conditions (such as surface finish and pressure) at the interfaces are unknown, a subjective approach is taken when assigning TCC values to these interfaces in the FEA model. To this end, five contact resistance levels ranging from low to high resistance are established with an assigned TCC value based on the typical values obtained from the open literature as presented in Table 3.3-1. The five TCC values used in the analyses presented in this report are presented in Table 3.3-2. Then, each thermal contact interface in the model is assigned one of these five resistance levels (see Table 3.3-3 and Figure 3.3-5). The approach to assigning the five contact resistance levels is:

- The interfaces (when dissimilar meshes exist) between elements representing fill gases and their adjacent solid meshes are assigned “Low” resistance levels.
- Interfaces between bolted junctures are assigned “Low” or “Low/Moderate” resistance levels.
- Interfaces between shielding materials and the shells that contain them are assigned “Low/Moderate” resistance levels.
- Interfaces between loosely fitted components (e.g., the cask lid cylindrical sides and the cask top flange) are assigned “High” resistance levels.

- Interfaces between heavy objects and the component on which they rest are assigned "Low/Moderate", "Moderate", or "Moderate/High" resistance levels depending on how heavy the object is and how much the component on which they rest may flex under the weight.

During normal transport, the Model 2000 Transport Package is in an upright orientation with the material basket bottom contacting the HPI bottom [[ ]], the HPI bottom [[ ]] contacting the cask bottom, and the cask bottom contacting the cask support plate of the overpack. Because the inner surface of the cask bottom is dished to allow for water drainage, the entire surface of the HPI bottom [[ ]] will not be in contact with the cask bottom. Additionally, in order to maintain well-shaped elements, the outer, bottom corner of the HPI is modeled with a small offset from the cask bottom. Therefore, LINK34 elements are used to model a line of contact between the outer edge of the HPI bottom [[ ]] and cask bottom. The LINK34 elements are assigned a thermal conductance value of 15.0 Btu/h-in²-°F, and the contact area is modeled as a 2.5-inch wide annular band with an outer diameter equivalent to the outer diameter of the HPI bottom [[ ]].

Table 3.3-1. Typical Thermal Contact Conductance Values from Open Literature

Material (Both Surfaces)	Surface Roughness (μ in)	Interfacial Gas	Pressure (psi)	TCC (Btu/h-in²-°F)	Source
Stainless Steel	Not Specified	Vacuum	14.5	0.5 – 2.0	Reference 3-3 Table 3.1
Stainless Steel	Not Specified	Vacuum	1450	3.1 – 17.5	Reference 3-3 Table 3.1
Stainless Steel	Normal Finish	Air	14.7 – 1470	2.1 – 4.5	Reference 3-9 Table 2.3
416 Stainless Steel	30	Air	100	13.9	Reference 3-10 Table 1.2
416 Stainless Steel	100	Air	44 – 368	4.6	Reference 3-9 Table 2.3
304 Stainless Steel	45	Air	588 – 1029	2.3	Reference 3-9 Table 2.3
Carbon Steel	1000	Air	100 – 300	0.6 – 0.8	Reference 3-10 Table 1.2
Carbon Steel	63	Air	100 – 300	3.5 – 4.6	Reference 3-10 Table 1.2
Aluminum	Not Specified	Vacuum	14.5	2.4 – 8.2	Reference 3-3 Table 3.1
Aluminum	Not Specified	Vacuum	1450	30.6 – 61.2	Reference 3-3 Table 3.1
Aluminum	397	Air	14500	4.4	Reference 3-3 Table 3.1

Table 3.3-1. Typical Thermal Contact Conductance Values from Open Literature

Material (Both Surfaces)	Surface Roughness (μ in)	Interfacial Gas	Pressure (psi)	TCC (Btu/h-in²-°F)	Source
Aluminum	397	Helium	14500	11.6	Reference 3-3 Table 3.1
Aluminum	Normal Finish	Air	14.7 – 1470	2.7 – 14.7	Reference 3-9 Table 2.3
Aluminum	Rough	Vacuum	Low	0.2	Reference 3-9 Table 2.3
Aluminum	120	Air	100 – 300	6.3 – 11.5	Reference 3-10 Table 1.2
Aluminum	65	Air	100 – 300	9.0 – 14.6	Reference 3-10 Table 1.2
Aluminum	100	Air	176 – 368	13.9	Reference 3-9 Table 2.3
Aluminum	10	Air	176 – 368	69.4	Reference 3-9 Table 2.3

Table 3.3-2. TCC Values Used in the Thermal Analyses

Thermal Contact Resistance ID	Thermal Contact Resistance Level	TCC (Btu/h-in²-°F)
1[a]	Low (Perfect Contact)	1000
2	Low/Moderate	15
3	Moderate	5
4	Moderate/High	1
5	High	0.5

Note:

a. Thermal contact resistance ID #1 is used to connect dissimilar meshes in which perfect contact is desired.

Table 3.3-3. Thermal Contact Resistance Levels Assigned to the Modeled Contact Elements

Contact ID (Real Constant)	Surface 1 (CONTA173)	Surface 2 (TARGE170)	Thermal Contact Resistance ID (See Table 3.3-2)
101	Cask Shield (Side)	Cask Bottom	2
102	Cask Shield (Side)	Cask Shell	2
103	Cask Shield (Side)	Cask Cavity Shell	2
104	Cask Shield (Side)	Cask Top	2
105	Cask Bottom	Cask Shell	4
106	Cask Top	Cask Shell	4
107	Cask Top	Cask Cavity Shell	4
108	Cask Shield (Lid)	Cask Lid	2
109	Cask Lid (At Bolted Interface)	Cask Top	2
110	Cask Lid (Cylindrical Sides)	Cask Top	5
112	Cask Fill Gas	Cask Bottom	1
113	Cask Fill Gas	Cask Cavity Shell	1
114	Cask Fill Gas	Cask Lid	1
115	Overpack Toroidal Stiffener (Bottom)	Overpack Toroidal Shell (Bottom)	4
116	Overpack Gusset Base (Bottom)	Overpack Toroidal Shell (Bottom)	2
117	Overpack Gusset (Bottom)	Overpack Stiffening Ring (Bottom)	2
118	Overpack Gusset & Stiffening Ring (Bottom)	Overpack Bolting Ring (Bottom)	2
119	Overpack Stiffening Ring (Bottom)	Overpack Outer Shell	4
120	Overpack Bolting Ring (Bottom)	Overpack Outer Shell	4
121	Overpack Bolting Ring (Bottom)	Overpack Inner Shell	4
122	Overpack [[ ]] (Bottom)	Overpack Bottom End Plate	5
123	Overpack [[ ]] (Bottom)	Overpack Bottom Plate	2
124	Honeycomb Impact Limiter (Bottom)	Overpack Bottom Plate	5
125	Honeycomb Impact Limiter (Bottom)	Overpack Inner Shell	5
126	Honeycomb Impact Limiter (Bottom)	Overpack Cask Support Plate	5
127	Overpack Gas	Overpack Cask Support Plate	1

Table 3.3-3. Thermal Contact Resistance Levels Assigned to the Modeled Contact Elements

Contact ID (Real Constant)	Surface 1 (CONTA173)	Surface 2 (TARGE170)	Thermal Contact Resistance ID (See Table 3.3-2)
128	Overpack Gas	Overpack Inner Shell	1
129	Overpack Gas	Overpack Bolting Ring (Bottom)	1
130	Overpack Bolting Ring (Bottom)	Overpack Bolting Ring (Top)	4
131	Cask Bottom Or Cask Top*	Overpack Cask Support Plate Outer Radius (OR)	3
132	Overpack Bolting Ring (Top)	Overpack Outer Shell	4
133	Overpack Bolting Ring (Top)	Overpack Inner Shell	4
134	Overpack [[ ]] (Between Shells)	Overpack	4
135 - 139	---Not Used---		
140	Overpack Stiffening Ring (Top)	Overpack Outer Shell	4
141	Overpack Gusset (Top)	Overpack Stiffening Ring (Top)	2
142	Overpack Gusset Base (Top)	Overpack Toroidal Shell (Top)	2
143	Overpack Toroidal Stiffener (Top)	Overpack Toroidal Shell (Top)	4
144	Honeycomb Impact Limiter (Top)	Overpack Top Plate	5
145	Honeycomb Impact Limiter (Top)	Overpack Inner Shell (Top)	5
146	Overpack [[ ]] (Top)	Overpack Top Plate	2
147	Overpack [[ ]] (Top)	Overpack End Plate (Top)	5
148	Overpack Gas	Overpack Bolt Ring (Top)	1
149	Overpack Gas	Overpack Inner Shell (Top)	1
150	Overpack Gas	Honeycomb Impact Limiter (Top)	1
151	Cask Fill Gas	[[ ]]	1
152	Cask Fill Gas	[[ ]]	1
153	Cask Fill Gas	HPI Horizontal Plate	1
154	---Not Used---		
155	[[		5
156			2
157			2
158			3
159		]]	3
160	[[		2

Table 3.3-3. Thermal Contact Resistance Levels Assigned to the Modeled Contact Elements

Contact ID (Real Constant)	Surface 1 (CONTA173)	Surface 2 (TARGE170)	Thermal Contact Resistance ID (See Table 3.3-2)
161			2
162			2
163			2
164			3
165			2
166			2
167		]]	2
168	HPI Fill Gas	[[	1
169	HPI Fill Gas		1
170	HPI Fill Gas	]]	1
171	---Not Used---		
172*	Material Basket [[ ]]	[[ ]]	3
173*	[[ ]]	Cask Lid or Cask Bottom	2

Note: * Used only if the material basket, HPI, and/or cask are not centered axially in the cavities (NCT).

[[

]]

Figure 3.3-5. Thermal Contact Pair Locations in the Finite Element Model

Boundary Conditions

The following boundary conditions are applied to the model to simulate NCT (steady-state analysis with the package modeled in an upright orientation):

1) Natural convection from the package external surfaces to the 100°F environment
2) Thermal radiation (emissivity, ε, of package surfaces approximately 0.22 (see Table 3.2.1-1))
3) Solar heat flux per 10 CFR 71.71 (additional case is run without solar heat flux to address the requirements of 10 CFR 71.43(g))
4) Heat flux to material basket [[ ]] to simulate the content heat generation.

Natural Convection and Thermal Radiation to the Environment

Heat is rejected from the model via natural convection and thermal radiation boundary conditions. In order to simplify the application of boundary conditions, a single convection boundary condition is applied to each external surface of the package that has a convection coefficient (h), combining natural convection (hc) based on the geometry of that surface and thermal radiation (hr) based on the emissivity of that surface. This combined, temperature-dependent convection coefficient (hc + hr) is defined for each external surface and stored in an ANSYS material property definition.

The natural convection coefficient is calculated using the following from Reference 3-3, Equation 9.24:

$$hc = \frac{Nu \times k}{L}$$

where, Nu = Nusselt number,
k = thermal conductivity of air at the film temperature, and
L = characteristic length of the surface.

The Nusselt number (Nu) is a function of surface geometry and the Rayleigh number (Ra). The Rayleigh number is, in turn, a function of surface geometry, temperature, and properties of the surrounding air and is calculated using the following equation from Reference 3-3, Equation 9.25:

$$Ra = \frac{g\,\beta\,(T_s - T_\infty)\,L^3}{\nu\,\alpha}$$

where, g = gravitational constant (386.1 in/s²),
β = 1/(Tf + 459.67),
T_f = film temperature = (Ts + T∞)/2,
T_s = surface temperature,
T_∞ = ambient temperature,
L = characteristic length,
ν = air kinematic viscosity at Tf, and
α = air thermal diffusivity at Tf.

Horizontal Cylinder—natural convection to environment

The characteristic length, L, of a horizontal cylinder is its diameter, D. The Nusselt number for a horizontal cylinder for a wide range of Rayleigh numbers is calculated using the following equation (Reference 3-3, Equation 9.34):

$$\mathrm{Nu} = \left\{0.60 + \frac{0.387\ \mathrm{Ra}^{1/6}}{\left[1+(0.559/\mathrm{Pr})^{9/16}\right]^{8/27}}\right\}^2 \quad (\mathrm{Ra} \le 10^{12})$$

where, Ra = Rayleigh number, and

Pr = Prandtl number.

Horizontal Plate—natural convection environment

The characteristic length, L, of a horizontal plate is the ratio of its surface area to its perimeter (for circular plates, this is equal to D/4, where D = the plate diameter). The Nusselt number for the upper surface of a heated horizontal plate is calculated using one of the following equations (Reference 3-3, Equations 9.30 and 9.31):

$$\mathrm{Nu} = 0.54\ \mathrm{Ra}^{1/4} \qquad (10^4 \le \mathrm{Ra} \le 10^7)$$

$$\mathrm{Nu} = 0.54\ \mathrm{Ra}^{1/3} \qquad (10^4 \le \mathrm{Ra} \le 10^7)$$

The Nusselt number for the lower surface of a heated horizontal plate is calculated using the following equation (Reference 3-3, Equation 9.32):

$$\mathrm{Nu} = 0.27\ \mathrm{Ra}^{1/4}$$

Vertical Flat Plate—natural convection to environment

The characteristic length, L, of a flat plate is its length. The Nusselt number for a vertical plate over the entire range of Rayleigh numbers (laminar and turbulent) is calculated using the following equation (Reference 3-3, Equation 9.26):

$$\mathrm{Nu} = \left\{0.825 + \frac{0.387\ {Ra}^{1/6}}{\left[1+ (0.492/Pr)^{9/16}\right]^{8/27}}\right\}^2$$

For laminar flow (i.e., Ra < 10^9), the Nusselt number for a vertical flat plate is calculated with slightly better accuracy using the following equation (Reference 3-3, Equation 9.27):

$$\mathrm{Nu} = 0.68 + \frac{0.670\ \mathrm{Ra}^{1/4}}{\left[1+ (0.492/\mathrm{Pr})^{9/16}\right]^{4/9}}$$

The thermophysical properties of air used in the calculation of the natural convection coefficients are presented in Table 3.3-4.

Table 3.3-4. Thermophysical Properties of Dry Air (from Reference 3-3)

Temperature (°F)	Density (lbm/in^3)	Thermal Conductivity (Btu/h-in-°F)	Specific Heat (Btu/lbm-°F)	Viscosity (in^2/h)	Thermal Diffusivity (in^2/h)	Prandtl Number
-10	5.039E-5	1.074E-3	2.403E-1	6.384E+1	8.872E+1	0.720
80	4.196E-5	1.266E-3	2.405E-1	8.867E+1	1.255E+2	0.707
170	3.595E-5	1.445E-3	2.410E-1	1.167E+2	1.668E+2	0.700
260	3.147E-5	1.628E-3	2.422E-1	1.474E+2	2.137E+2	0.690
350	2.796E-5	1.796E-3	2.439E-1	1.807E+2	2.634E+2	0.686
440	2.516E-5	1.960E-3	2.460E-1	2.164E+2	3.164E+2	0.684
530	2.286E-5	2.114E-3	2.484E-1	2.543E+2	3.722E+2	0.683
620	2.097E-5	2.258E-3	2.510E-1	2.940E+2	4.291E+2	0.685
710	1.935E-5	2.393E-3	2.539E-1	3.360E+2	4.871E+2	0.690
800	1.797E-5	2.523E-3	2.568E-1	3.800E+2	5.468E+2	0.695
890	1.677E-5	2.644E-3	2.596E-1	4.261E+2	6.082E+2	0.702
980	1.573E-5	2.759E-3	2.625E-1	4.739E+2	6.696E+2	0.709
1070	1.480E-5	2.870E-3	2.651E-1	5.234E+2	7.310E+2	0.716
1160	1.397E-5	2.985E-3	2.678E-1	5.742E+2	7.979E+2	0.720
1250	1.324E-5	3.096E-3	2.702E-1	6.261E+2	8.649E+2	0.723
1340	1.258E-5	3.212E-3	2.725E-1	6.802E+2	9.374E+2	0.726
1520	1.144E-5	3.443E-3	2.768E-1	7.912E+2	1.088E+3	0.728

Forced Convection Correlations

During the HAC 30-minute fire, heat is transferred from the environment to the model via forced convection and thermal radiation boundary conditions. Again, in order to simplify the application of boundary conditions, a single convection boundary condition is applied to each external surface of the package that has a convection coefficient (h) combining forced convection (hc) based on the geometry of that surface and thermal radiation (hr) based on the emissivity of that surface. This combined temperature-dependent convection coefficient (hc + hr) is defined for each external surface and stored in an ANSYS material property definition.

The forced convection coefficient is calculated using the following equation (Reference 3-3, Equation 6.5.7):

$$hc = \frac{Nu \times k}{L}$$

where, Nu = Nusselt number,

k = thermal conductivity of air at the film temperature, and

L = characteristic length of the surface.

The Nusselt number (Nu) is a function the Reynolds number (Re) and the Prandtl number. The Reynolds number is, in turn, a function of surface geometry, temperature, flow velocity, and properties (density and viscosity) of the surrounding air, which is calculated using the following equation (Reference 3-3, Equation 6.45):

$$Re = \frac{VL}{\nu}$$

where, V = air free-stream velocity,

L = characteristic length,

ν = air dynamic viscosity at T_f,

T_f = film temperature = $(T_s + T_\infty)/2$,

T_s = surface temperature, and

T_∞ = ambient temperature.

Cylinder in Cross Flow—forced convection from environment to package

The characteristic length, L, of a cylinder is its diameter, D. The Nusselt number for a cylinder in cross flow is calculated using the following equation (Reference 3-3, Equation 7.55b):

$$Nu = C\, Re_D^{\,m}\, Pr^{1/3}$$

where, Re_D = Reynolds number, and

Pr = Prandtl number.

The constants 'C' and 'm' in the previous equation are functions of the Reynolds number (Re_D) and are listed in Table 3.3-5.

Table 3.3-5. Constants 'C' and 'm' for the Nusselt Number Calculation of a Cylinder in Cross Flow (from Reference 3-3, Table 7.2)

Re_D	C	m
0.4 – 4	0.989	0.330
4 – 40	0.911	0.385
40 – 4,000	0.683	0.466
4,000 – 40,000	0.193	0.618
40,000 – 400,000	0.027	0.805

For mixed parallel flow (laminar and turbulent), the Nusselt number for a flat plate is calculated using the following equation (Reference 3-3, Equation 7.44):

$Nu=0.037\ Re_L^{4/5}\ Pr^{1/3}\ (5\times10^5 < Re_L \leq 10^8)$

where, Re_L = Reynolds number.

For mixed parallel flow (laminar and turbulent), the Nusselt number for a flat plate is calculated using the following equation (Reference 3-3, Equation 7.44):

$Nu=0.037\ Re_L^{4/5}\ Pr^{1/3}\ (5\times10^5 < Re_L \leq 10^8)$

Thermal Radiation to Environment

As previously discussed, the convection boundary conditions applied to the model are a combination of both natural convection and thermal radiation coefficients. The thermal radiation coefficient (hr) is calculated by linearizing the radiation. Assuming a view factor of 1.0 with the surroundings, the heat transfer rate by thermal radiation, Q_{rad}, from a surface can be described as follows:

$$Q_{rad} = \varepsilon\sigma A\left(T_s^{\,4} - T_\infty^{\,4}\right)$$

where, ε = emissivity,

σ = Stefan-Boltzmann constant (1.19 E -11 Btu/h-in²-°F),

A = surface area,

Ts = surface temperature (R), and

T∞ = temperature of surroundings (R).

Due to the temperatures being raised to the 4th power in the previous equation, the heat transfer rate is nonlinear. Instead, treating the thermal radiation as a convection boundary condition and substituting hr (radiation coefficient) for hc (convection coefficient) yields the linear equation:

$$Q_{rad} = hr\ A(T_s - T_\infty)$$

Setting the two equations for Qrad equal to each other yields the following equation:

$$hr\ A(T_s - T_\infty) = \varepsilon\sigma A\left(T_s^4 - T_\infty^4\right)$$

Solving for the thermal radiation coefficient (hr) yields:

$$hr = \varepsilon\,\sigma\left(T_s^2 + T_\infty^2\right)(T_s + T_\infty)$$

Normal Conditions Convection Coefficients

During normal transport, the Model 2000 Transport Package is transported in an upright orientation as depicted in Figure 1.2-3. For the purpose of calculating natural convection coefficients, the overpack top and bottom toroidal shells are approximated as horizontal cylinders (L = D = 24 inches), the overpack top cover is approximated as a heated flat plate facing up (L = D/4 = 48 inches/4 = 12 inches), the overpack bottom end plate is approximated as a heat flat plate facing down (L = D/4 = 24 inches/4 = 6 inches), and the cylindrical sides of the overpack are approximated as a vertical plate (L = 83.5 inches). The convection boundary conditions for NCT are shown on a cross-section of the model in Figure 3.3-6. The calculated natural convection coefficients (hc) and radiation coefficient (hr) for NCT (in shade and with insolation) are presented graphically in Figure 3.3-7.

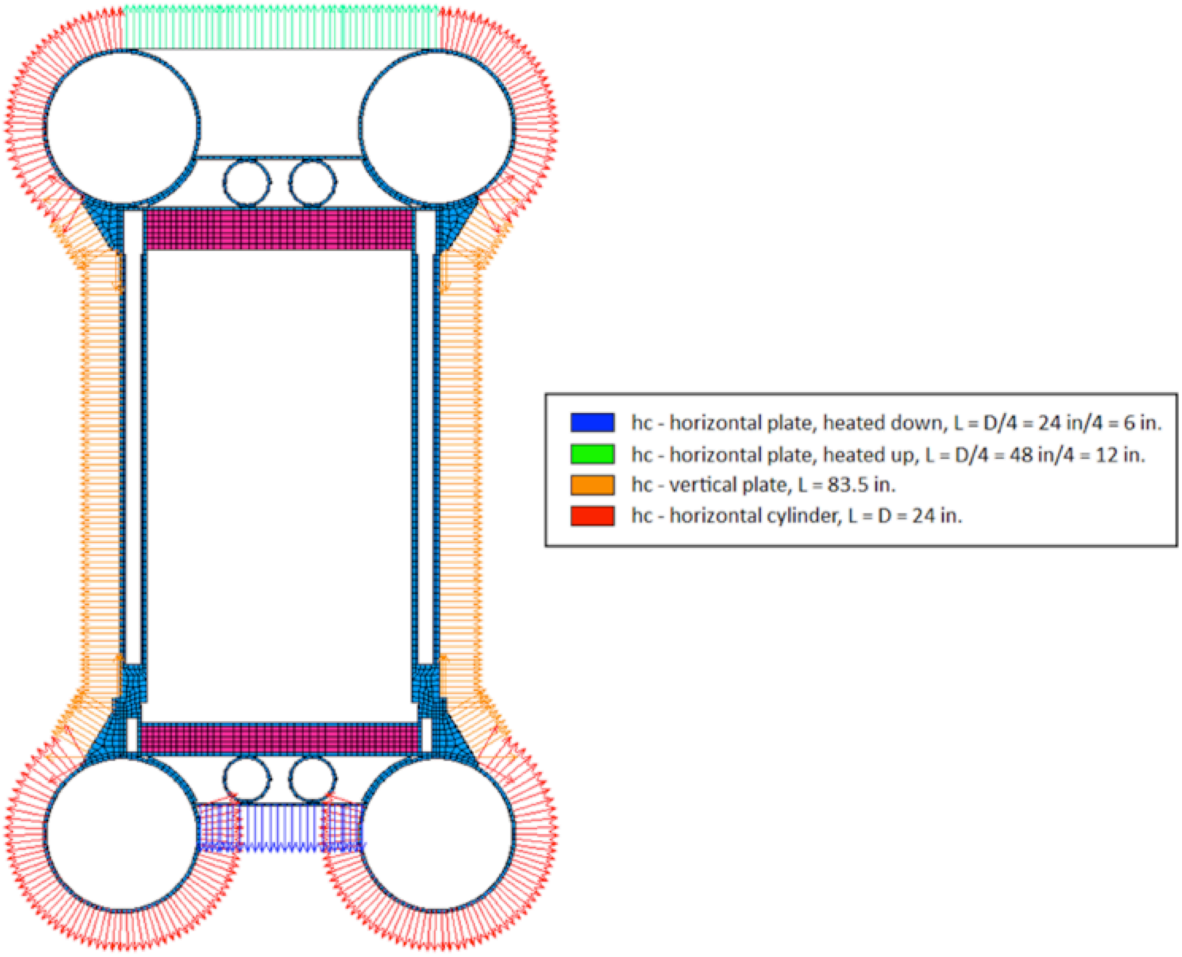

Figure 3.3-6. Natural Convection Boundary Conditions for NCT

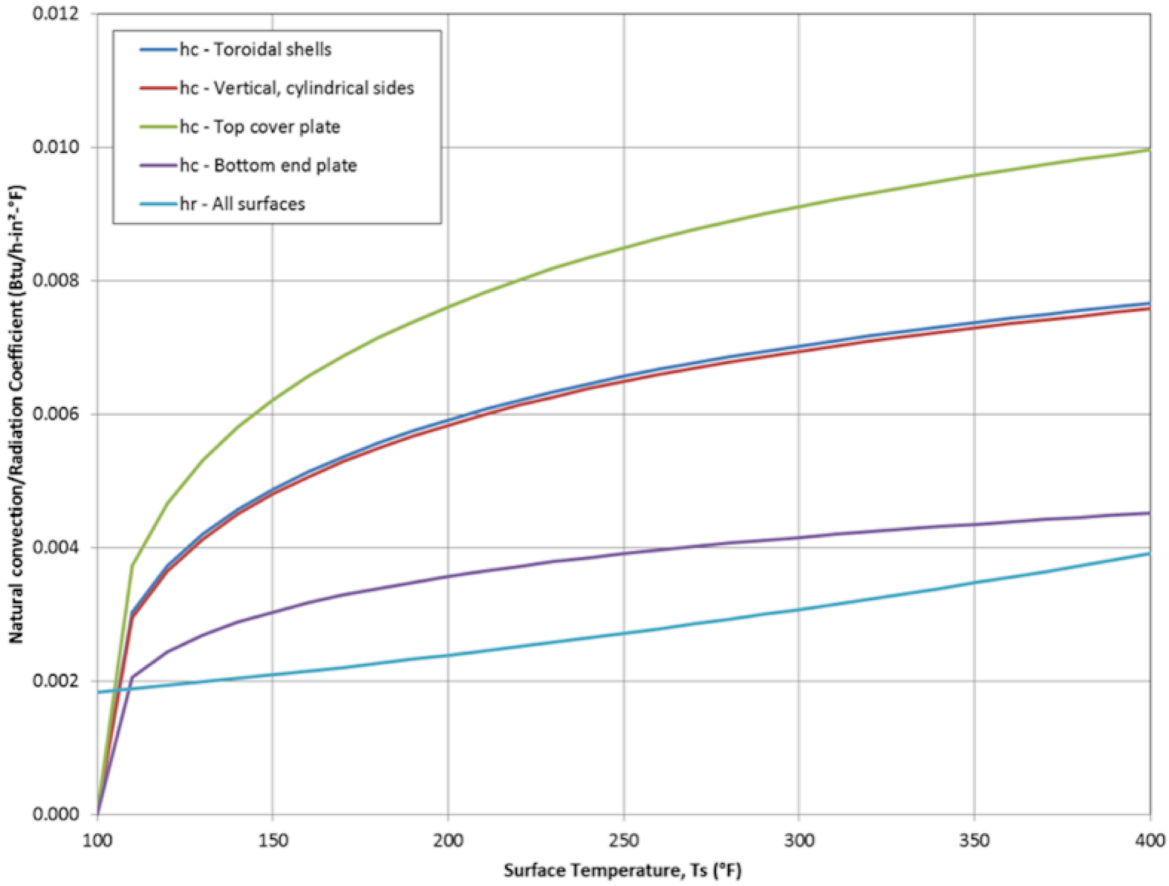

Figure 3.3-7. Natural Convection and Thermal Radiation Coefficients for NCT

(Note data for NCT in shade and with insolation)

Heat Generation by Contents

In order to apply the design basis 3000 W decay heat, the HPI material basket is included in the model. The contents are not specifically modeled in the analyses. Rather, the 3000 W of decay heat is included as a heat flux applied to the material basket [[ ]] contained within the HPI.

As described in Section 1.2.2.2, the material basket has nineteen locations that are formed by twenty [[ ]] The center position does not have a full-length [[ ]], but instead two 2.0-inch long [[ ]], one fastened at either end, form the center area. In the thermal model, the 3000 W of decay heat is assumed to be evenly distributed among the nineteen [[ ]]; therefore, each [[ ]] has approximately 157.9 W applied to its inner surface as a uniformly distributed heat flux over its length [[ ]]. For the center area, the heat load is applied to the inner surface of the two shorter [[ ]] and to the external surfaces of the surrounding [[ ]] where they would contact the center [[ ]] if one existed. This results in a lower heat flux at the center due to the larger area.

SURF152 elements are overlaid onto the SOLID70 thermal solid elements of the material basket [[ ]], and the heat flux is calculated based on the area of these elements. The actual area

of the SURF152 elements (obtained using the *GET command in ANSYS) is used to calculate the applied heat flux rather than using the area calculated from the dimensions of the [[ ]].

The heat flux, q''_{gen}, applied to the [[ ]] is:

[[

]]

where, $A_{SURF152}$ = the area of the SURF152 elements overlaid on the inner surface of the [[ ]] (note: multiplied by 2 to account for the half-symmetry of the model).

Similarly, the heat flux applied to the center [[ ]] around the center region is:

[[

]]

where, $A_{SURF152}$ = the area of the SURF152 elements overlaid on the inner surface of the center [[ ]] (note: multiplied by 2 to account for the half-symmetry of the model).

The actual heat flux applied to the material basket [[ ]] is shown in Figure 3.3-8.

[[

]]

Figure 3.3-8. Contents Heat Flux Applied to Material Basket [[ ]]

3.3.1. Heat and Cold

3.3.1.1. Hot Case

3.3.1.1.1. NCT Solar Heat Flux (Insolation)

Per the requirements of the regulations for NCT, the Model 2000 Transport Package is exposed to an ambient temperature of 100°F and insolation according to Table 3-1. The solar heat fluxes specified to Table 3-1 are per 12-hour period. This 12-hour period represents a 12-hour long "day" in a 24-hour day/night cycle. Because the solar heat flux is constant, the insolation value should be time averaged over 24 hours in order to maintain the proper total heat flux to the package over the full day/night cycle. Therefore, to simulate a day-night cycle, these heat fluxes are time-averaged over a 24-hour period as follows:

Flat surfaces (other than transported horizontally base)

$$q" = \frac{800\ cal/cm^2}{24\ h}\left(\frac{4.1868\ J}{cal}\right)\left(\frac{100\ cm}{m}\right)^2\left(\frac{1\ h}{3600\ s}\right)\left(\frac{1\ W}{1\ J/s}\right)\left(\frac{0.3171\frac{Btu}{h-ft^2}}{1\ W/m^2}\right)\left(\frac{1\ ft^2}{144\ in^2}\right)$$

$$= 0.854\ \frac{Btu}{h - in^2}$$

Curved surfaces

$$q" = \frac{400\ cal/cm^2}{24\ h}\left(\frac{4.1868\ J}{cal}\right)\left(\frac{100\ cm}{m}\right)^2\left(\frac{1\ h}{3600\ s}\right)\left(\frac{1\ W}{1\ J/s}\right)\left(\frac{0.3171\frac{Btu}{h - ft^2}}{1\ W/m^2}\right)\left(\frac{1\ ft^2}{144\ in^2}\right)$$

$$= 0.427\ \frac{Btu}{h - in^2}$$

Flat surfaces not transported horizontally

$$q" = \frac{200\ cal/cm^2}{24\ h}\left(\frac{4.1868\ J}{cal}\right)\left(\frac{100\ cm}{m}\right)^2\left(\frac{1\ h}{3600\ s}\right)\left(\frac{1\ W}{1\ J/s}\right)\left(\frac{0.3171\frac{Btu}{h - ft^2}}{1\ W/m^2}\right)\left(\frac{1\ ft^2}{144\ in^2}\right)$$

$$= 0.214\ \frac{Btu}{h - in^2}$$

During normal transport, the Model 2000 Transport Package is oriented in an upright position. As such, for the case with insolation, a heat flux of 0.854 Btu/h-in² is applied to the top cover plate, and a heat flux of 0.427 Btu/h-in² is applied to the toroidal shells and overpack sides as shown in Figure 3.3.1-1.

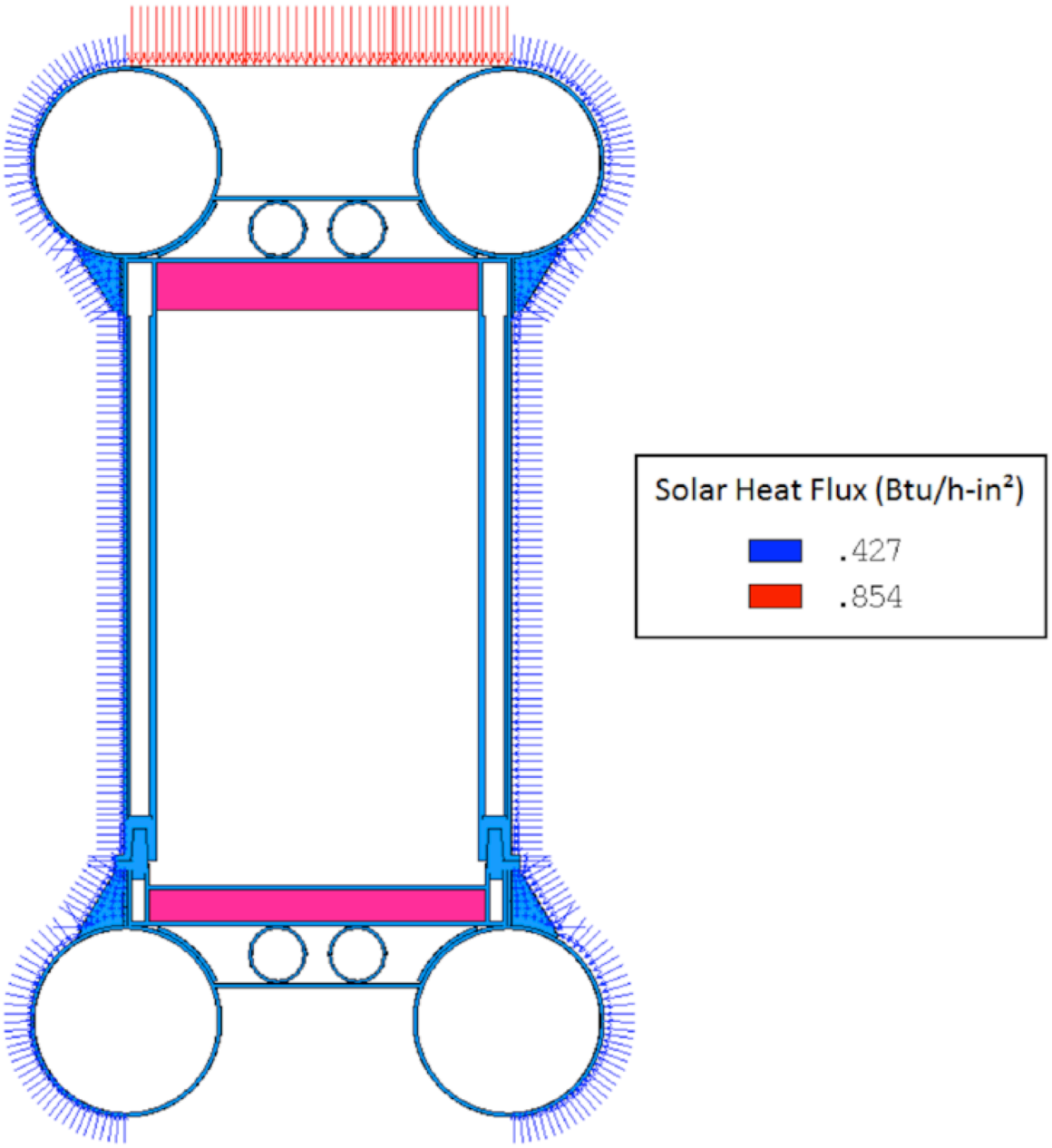

Figure 3.3.1-1. Solar Heat Flux Boundary Conditions for NCT

3.3.1.1.2. Detailed NCT Results

The results of the steady-state thermal analyses are presented in tabular format in Table 3.3.1-1 and graphically (temperature contours) in Figure 3.3.1-2. The 3000 W thermal analysis demonstrates that the Model 2000 Transport Package components remain below their allowable temperatures for NCT with insolation. There is no change in material conditions that would affect structural, shielding, or impact-limiting performance. Further, the package will maintain containment of the contents.

Table 3.3.1-1. Temperature Results, NCT (in Shade and with Insolation)

Component	100°F Ambient Temperature, in Shade, (°F)			100°F Ambient Temperature, with Insolation (°F)		
	Max	Min	Avg	Max	Min	Avg
Material Basket	989	465	801	1,001	490	815
HPI	581	360	---	604	388	---
HPI shielding (top)	517	506	513	539	529	535
HPI shielding (sides)	581	435	544	601	460	565
HPI shielding (bottom)	477	427	451	501	452	475
Cask (bottom, shells, top, lid)	430	309	---	455	338	---
Cask shielding (lid)	424	408	414	449	433	440
Cask shielding (sides)	405	341	385	431	370	412
Cask lid seal	406	383	---	432	409	---
Cask drain port (bottom)	342	309	---	370	338	---
Cask test port (top)	400	383	---	426	409	---
Cask vent port (lid)	416	410	---	442	435	---
Overpack base	335	159	---	364	184	---
Overpack cover	272	108	---	308	174	---
Overpack toroidal shell (top)	159	110	125	207	165	179
Overpack toroidal shell (bottom)	215	114	139	249	136	176
Overpack honeycomb impact limiter (top)	220	205	215	263	249	258
Overpack honeycomb impact limiter (bottom)	330	275	304	359	305	334
HPI fill gas	971	460	672	983	485	689
Cask fill gas	574	346	462	594	374	486
HPI and Cask fill gas, combined	971	346	481	983	374	505

[[

]]

Figure 3.3.1-2. Steady-State Temperature Distribution—NCT

3.3.1.1.3. Maximum Surface Temperature Results

The Model 2000 Transport Package is also evaluated to the requirements of 10 CFR 71.43(g) (Reference 3-1), which requires that no accessible surface of the package exceed 185°F in an exclusive use shipment when exposed to a 100°F ambient temperature in still air and shade. As shown in Figure 3.3.1-3, the overpack in the region of the bolting ring exceeds the allowable temperature of 185°F. Therefore, a personnel barrier not part of the packaging will be used to block access to this region when readied for transport.

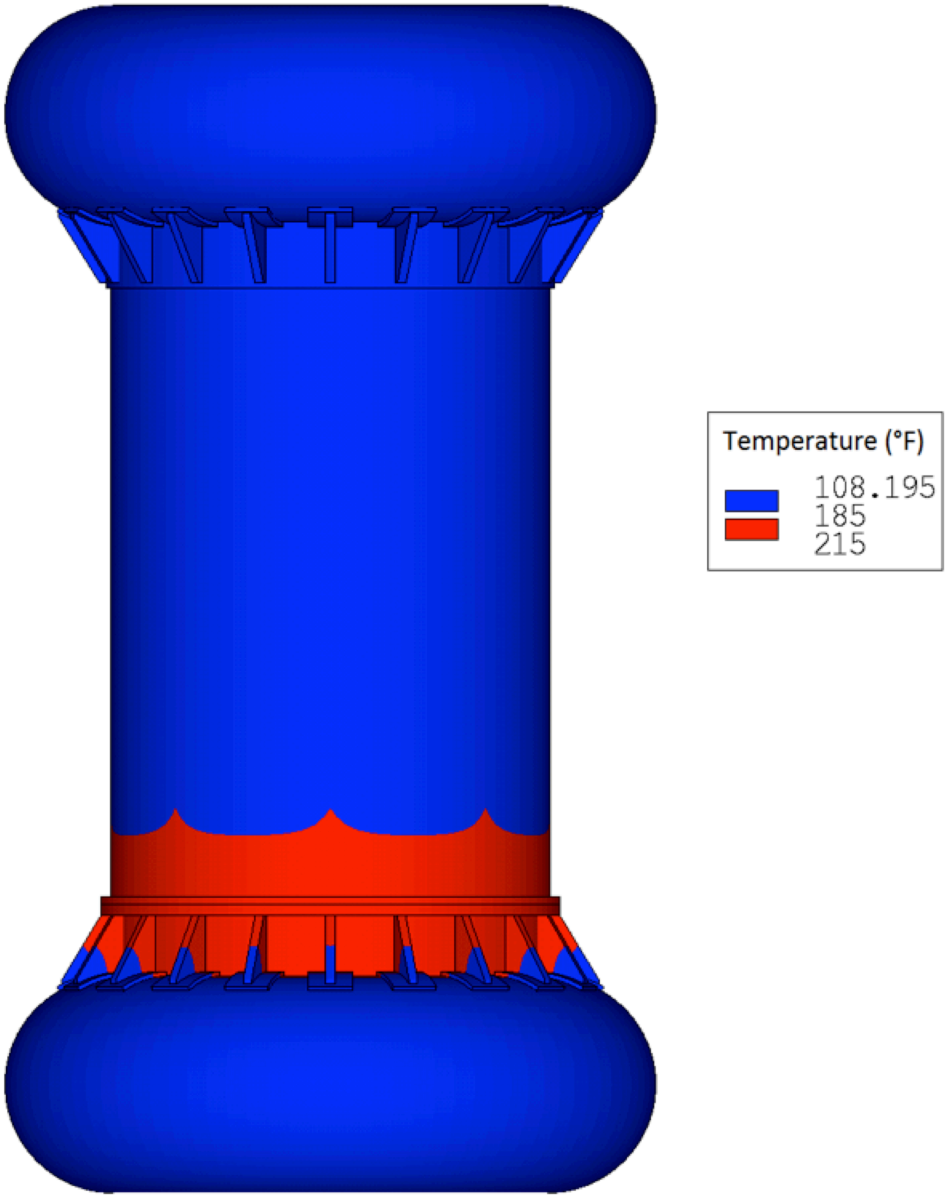

Figure 3.3.1-3. Overpack Steady-State Temperatures, 100°F Ambient Temperature

(Note: Assumes ambient temperature in shade)

3.3.1.1.4. NCT Thermal Contact Resistance Sensitivity Study

The presented thermal analyses have thermal contact resistance modeled between contacting components that have a mixture of low (perfect contact) to high resistance levels as discussed above. In order to assess the effect that using the mixed thermal resistance levels have on package temperatures, the analyses for NCT (with insolation) is repeated with all of the thermal resistance levels set to "low" (i.e., perfect contact). The results of this analysis is compared with the results from Table 3.3.1-1, and presented in Table 3.3.1-2.

Table 3.3.1-2. Comparison of Mixed and Perfect Thermal Contact for NCT with Insolation

Item	100°F Ambient temperature, with insolation, mixed thermal contact resistance[1] (°F)			100°F Ambient temperature, with insolation, perfect contact (°F)		
	Max	Min	Avg	Max	Min	Avg
Material Basket	1,001	490	815	998	482	811
HPI	604	388	---	598	379	---
HPI shielding (top)	539	529	535	534	523	530
HPI shielding (sides)	601	460	565	596	452	559
HPI shielding (bottom)	501	452	475	494	444	468
Cask (bottom, shells, top, lid)	455	338	---	450	327	---
Cask shielding (lid)	449	433	440	443	428	434
Cask shielding (sides)	431	370	412	426	361	407
Cask lid seal	432	409	---	428	405	---
Cask drain port (bottom)	370	338	---	362	327	---
Cask test port (top)	426	409	---	422	405	---
Cask vent port (lid)	442	435	---	436	430	---
Overpack base	364	184	---	356	184	---
Overpack cover	308	174	---	305	174	---
Overpack toroidal shell (top)	207	165	179	206	165	179
Overpack toroidal shell (bottom)	249	136	176	250	136	177
Overpack honeycomb impact limiter (top)	263	249	258	259	243	254
Overpack honeycomb impact limiter (bottom)	359	305	334	355	298	329
HPI fill gas	983	485	689	979	477	684
Cask fill gas	594	374	486	589	366	480
HPI and Cask fill gas, combined	983	374	505	979	366	499

Note:

1. In general, the package temperatures are lower when modeling the thermal contact as perfect as opposed to the mixed thermal contact levels. This is because the mixed thermal contact resistances impede the flow of the heat generated by the contents from getting out of the package where it is rejected to the surroundings.

3.3.1.2. Cold Case

For the cold case, the thermal model is modified to calculate package temperatures for exposure to an ambient temperature of -40°F in the shade. Various content heat loads are considered, and the results are presented in Table 3.3.1-3. The cask lid seal and cask ports maintain temperatures above their minimum allowable temperatures presented in Table 3.1.3-1. It can be noted in this table that the minimum temperature at the cask lid seal and port O-rings is 21°F with an internal wattage of only 500 W.

Table 3.3.1-3. Model 2000 Transport Package Temperatures for Exposure to -40°F in Shade

Item	Temperature (°F)											
	$Q_{contents}$ = 500 W			$Q_{contents}$ = 1,000 W			$Q_{contents}$ = 2,000 W			$Q_{contents}$ = 3,000 W		
	Max	Min	Avg	Max	Min	Avg	Max	Min	Avg	Max	Min	Avg
Material Basket	259	66	195	460	150	357	745	283	588	954	387	756
HPI	104	36	---	216	96	---	391	193	---	523	269	---
HPI shielding (top)	84	81	83	182	176	179	334	325	331	451	439	446
HPI shielding (sides)	103	59	91	214	136	194	388	259	355	520	355	478
HPI shielding (bottom)	69	57	63	155	132	143	291	252	271	400	346	372
Cask (bottom, shells, top, lid)	55	21	---	132	69	---	256	147	---	354	209	---
Cask shielding (lid)	54	51	52	129	123	126	251	239	244	347	330	337
Cask shielding (sides)	49	31	42	120	87	108	235	177	215	325	249	300
Cask lid seal	50	45	---	122	113	---	237	221	---	328	304	---
Cask drain port (bottom)	31	21	---	88	69	---	178	147	---	250	209	---
Cask test port (top)	48	45	---	119	113	---	232	221	---	321	304	---
Cask vent port (lid)	52	51	---	127	124	---	246	241	---	339	332	---
Overpack base	30	-22	---	84	-9	---	171	11	---	240	27	---
Overpack cover	-2	-38	---	32	-37	---	96	-36	---	155	-34	---
Overpack toroid (top)	-28	-37	-34	-17	-36	-30	4	-34	-22	24	-32	-14
Overpack toroid (bottom)	-6	-36	-28	19	-34	-21	60	-31	-8	94	-29	2
Overpack honeycomb (top)	-16	-19	-17	7	0	4	50	38	46	93	75	87
Overpack honeycomb (bottom)	29	10	20	82	49	67	167	113	143	235	165	204
HPI fill gas	255	65	147	453	148	281	732	279	476	935	382	619
Cask fill gas	101	32	66	212	89	150	383	180	283	513	253	387
HPI + Cask fill gas, combined	255	32	74	453	89	162	732	180	301	935	253	408

3.3.2. Maximum Normal Operating Pressure

3.3.2.1. NCT Pressure Evaluation

During NCT, the average temperature of the cask fill gas (including the gas within the HPI) is 505°F. Using the ideal gas law, the cask internal pressure from gas expansion is:

$$\frac{P_1}{T_1} = \frac{P_2}{T_2}$$

$$P_2 = 14.7 \text{ psia} \times \left(\frac{505+460}{70+460}\right) = 26.8 \text{ psia} < 30 \text{ psia}$$

where,

P_1	=	14.7 psia	initial fill gas pressure,
T_1	=	70°F	initial fill gas temperature, and
T_2	=	505°F	average gas volume temperature during NCT.

The cask internal pressure during NCT is less than the design pressure of 30 psia. Therefore, no further evaluation is required.

3.4 Thermal Evaluation under Hypothetical Accident Conditions

The thermal performance of the Model 2000 Transport Package is analyzed for HAC by performing a transient heat transfer analysis on a finite element representation of the package. The model represents the Model 2000 Transport Package with damage consistent with a 30-foot side drop and 40-inch drop onto a 6-inch pin. Again, the general-purpose finite element code ANSYS, Release 14.0, is used to analyze the Model 2000 Transport Package with a content heat load of 3000 W for HAC. Several ANSYS macros are created in order to build the model, modify nodal locations to simulate damage, apply boundary conditions, and perform the transient analysis. Many of the macros used to evaluate the package for NCT are used to evaluate it for HAC.

Assumptions made for this evaluation are:

- The package is assumed to be in a horizontal orientation during the HAC fire because the package is modeled with damage consistent with a side drop.
- The cask and HPI are backfilled with Helium at 70°F and 14.7 psia.
- Natural convection within the package cavities is neglected.
- The contents of the HPI are assumed to generate a maximum of 3000 W that is uniformly distributed among the [[ ]] and is consistent with the isotope rod design where the Co-60 source is uniformly distributed along the length of each [[ ]]
- For HAC, the package is assumed to be exposed to the NCT prior to and following the 30-minute fire.
- During pre-fire/post-fire HAC, the package is assumed to have an emissivity consistent with the material of construction at temperature. However, during the HAC fire, the

package is assumed to have an emissivity value of 0.9. Post-fire, the package is assumed to have an emissivity value of 0.8.

Boundary Conditions

The following boundary conditions are applied to the model to simulate HAC (with the package modeled in a horizontal orientation):

Pre-fire (steady-state analysis)

- Heat flux to material basket [[ ]] to simulate the content heat generation
- Natural convection from the package external surfaces to the 100°F environment
- Thermal radiation (emissivity, ε, of package surfaces approximately 0.22 (see Table 3.2.1-1))
- Solar heat flux per 10 CFR 71.71

Thirty minute fire (transient analysis)

- Heat flux to material basket [[ ]] to simulate the content heat generation
- Forced convection from the 1475°F environment to the package external surfaces
- Thermal radiation exchange between the fire and the package surfaces (ε = 0.9)

Post-fire cool-down (transient analysis)

- Heat flux to material basket [[ ]] to simulate the content heat generation
- Natural convection from the package external surfaces to the 100°F environment
- Thermal radiation (ε = 0.8, which is consistent with a heavily oxidized steel surface)
- Solar heat flux per 10 CFR 71.71

3.4.1. Initial Conditions

When evaluating the package for the HAC 30-minute fire, the package must include damage from a 30-foot drop onto an unyielding surface and a 40-inch drop onto a 6-inch diameter pin (Reference 3-1). The structural evaluation of the Model 2000 Transport Package considers several drop orientations for HAC; however the side-drop orientation is chosen as the worst-case from a thermal standpoint. The reason for this is due primarily to the damage to the overpack side from the 40-inch drop onto the 6-inch diameter pin. The drop onto the pin causes the overpack outer and inner shells to come in contact—thus, creating a path for the heat from the fire to more easily reach the cask (and cask shielding). Although the damage from the drop onto the pin is not modeled in the deformed geometry (Figure 3.4.1-1), its effect is included by using LINK34 elements to model the contact of the two shells.

[[

]]

Figure 3.4.1-1. Three-Dimensional Finite Element Model of the Model 2000 (Half Symmetry)

(Note: damage consistent with that sustained from a 30-foot drop and 40-inch drop onto a 6-inch pin—elements representing air and helium not shown for clarity.)

3.4.1.1. Additional Thermal Contact for the Hypothetical Accident Condition

Because the Model 2000 Transport Package is assumed to be in a horizontal orientation during the HAC fire and cool-down, additional thermal contact modeling is required. The components are not physically shifted to be in contact (e.g., the sides of the cask shell contacting the overpack inner shell). Therefore, the CONTA173/TARGE170 pairs will not be appropriate to use to model the thermal contact that will be present when the package is oriented horizontally. To model the contact present when the package is on its side, LINK34 convection elements are incorporated into the model. Although these are convection elements, they can be used to model thermal contact because the thermal contact conductance has the same units as the convection coefficient used by these elements.

When oriented on its side, the contact between the material basket [[ ]], between the HPI [[ ]] and cask cavity shell, and between the cask shell and overpack [[ ]] are modeled with a "Low/Moderate" thermal contact resistance (thermal contact conductance of 15.0 Btu/h-in²-°F) and 2° of contact as shown in Figure 3.4.1-2. Additionally, the puncture damage is simulated by adding LINK34 elements (20° contact area) between the overpack inner and outer shells as shown in Figure 3.4.1-2. The "Low/Moderate" thermal contact resistance is chosen for these contact elements in order to maximize the heat from the contents and the HAC fire into the cask shield at the puncture location.

3.4.1.2. Hypothetical Accident Conditions Convection Coefficients

For HAC, the Model 2000 is modeled with damage simulating a side drop from 30 feet onto an unyielding surface followed by a drop from 40 inches onto a 6-inch diameter pin. The HAC thermal analysis simulates exposure of the model to a 30-minute fire following this side drop/puncture; therefore, the package is assumed to be on its side when exposed to the fire. For the purpose of calculating natural convection (pre-fire and post-fire) and forced convection (fire)

coefficients, the overpack sides are approximated as a horizontal cylinder (L = D = 48.5 inches), the overpack toroidal shells are approximated as horizontal cylinders (L = D = 24 inches), and the overpack top and bottom end plates are approximated as vertical flat plates (L = D = 24 inches). The convection boundary conditions for HAC are shown on a cross-section of the model in Figure 3.4.1-3. The calculated natural and forced convection coefficients (hc) and radiation coefficients for HAC (pre-fire, fire, and post-fire cool-down) are presented graphically in Figure 3.4.1-4.

[[

]]

Figure 3.4.1-2. LINK34 Incorporated to Simulate HAC Side Contact and Puncture Damage

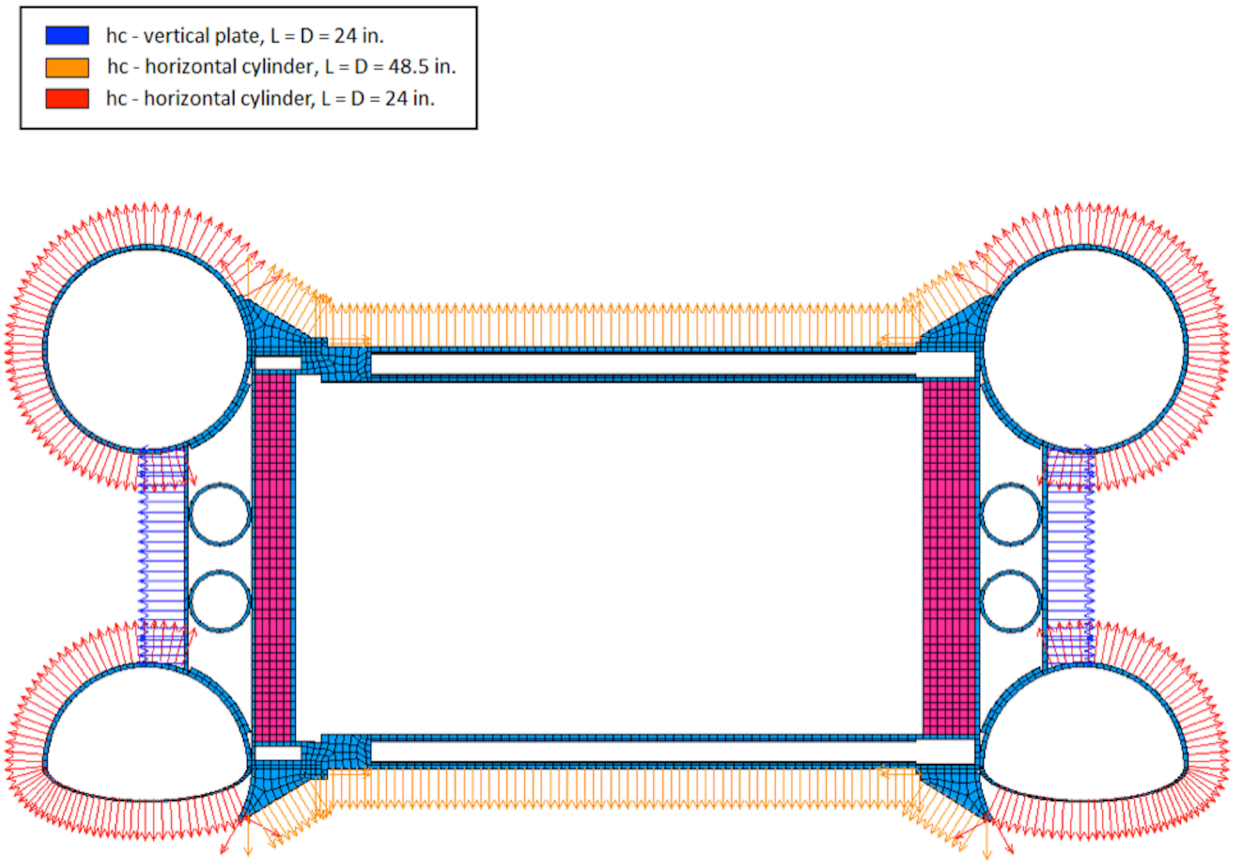

Figure 3.4.1-3. Natural Convection Boundary Conditions for HAC

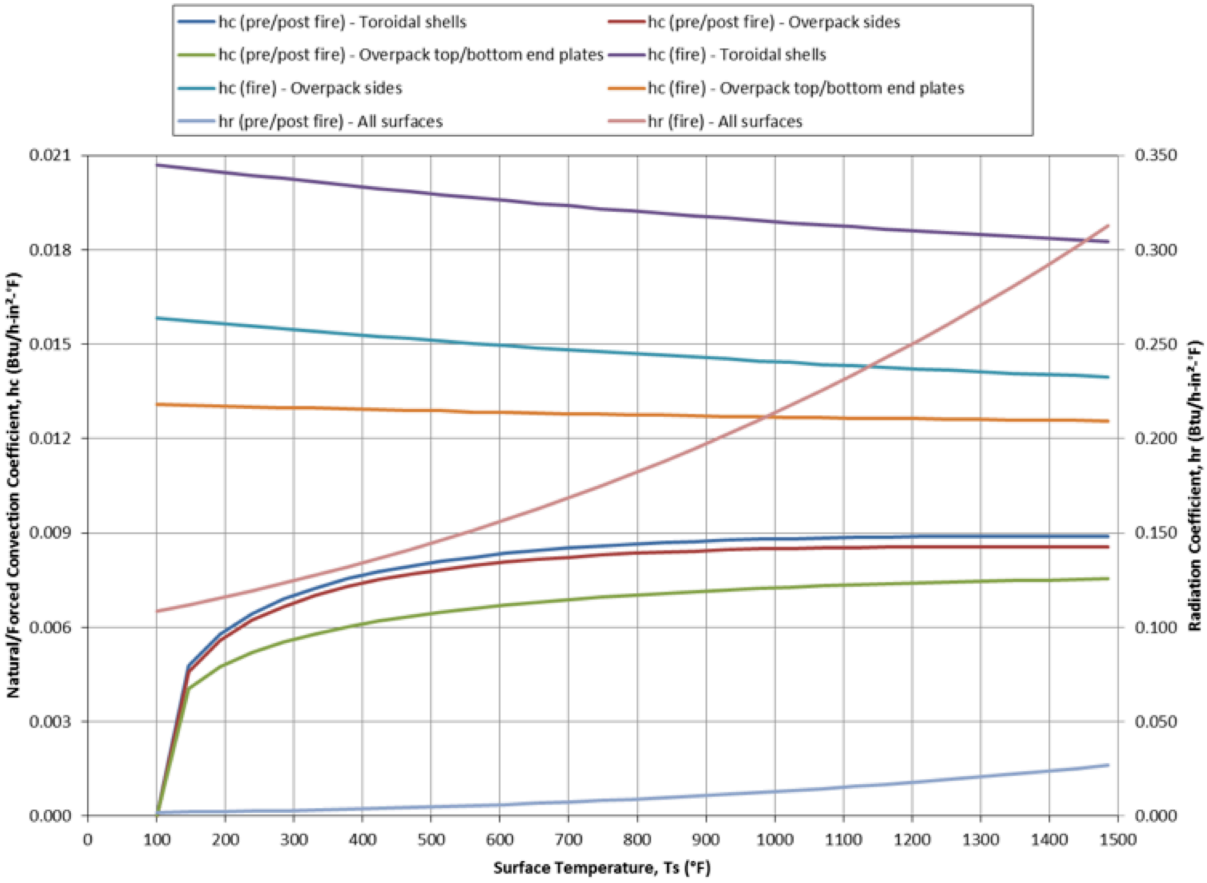

Figure 3.4.1-4. Natural/Forced Convection and Thermal Radiation Coefficients for HAC

(Note: Coefficients are for HAC Pre-Fire, Fire, and Post-Fire)

3.4.2. Fire Test Conditions

3.4.2.1. HAC Solar Heat Flux (Insolation)

Previous versions of 10 CFR 71.73 (i.e., prior to ~1997), stated that insolation need not be considered before, during, or after the 30-minute hypothetical accident fire. However, the current regulations do not specifically address whether insolation should be included prior to, during, or after the HAC fire. The HAC thermal analysis presented in this report does not include insolation during the HAC fire; however, insolation is applied to the package surfaces during steady-state conditions prior to the fire and during the transient post-fire cool-down. Because the side drop and side puncture damage is simulated for the HAC thermal evaluation, the Model 2000 Transport Package is assumed to be in a horizontal orientation. Therefore, prior to the fire and during the post-fire cool-down, a heat flux of 0.427 Btu/h-in² is applied to the toroidal shells and overpack sides, and a heat flux of 0.214 Btu/h-in² is applied to the overpack top and bottom end plates as shown in Figure 3.4.2-1.

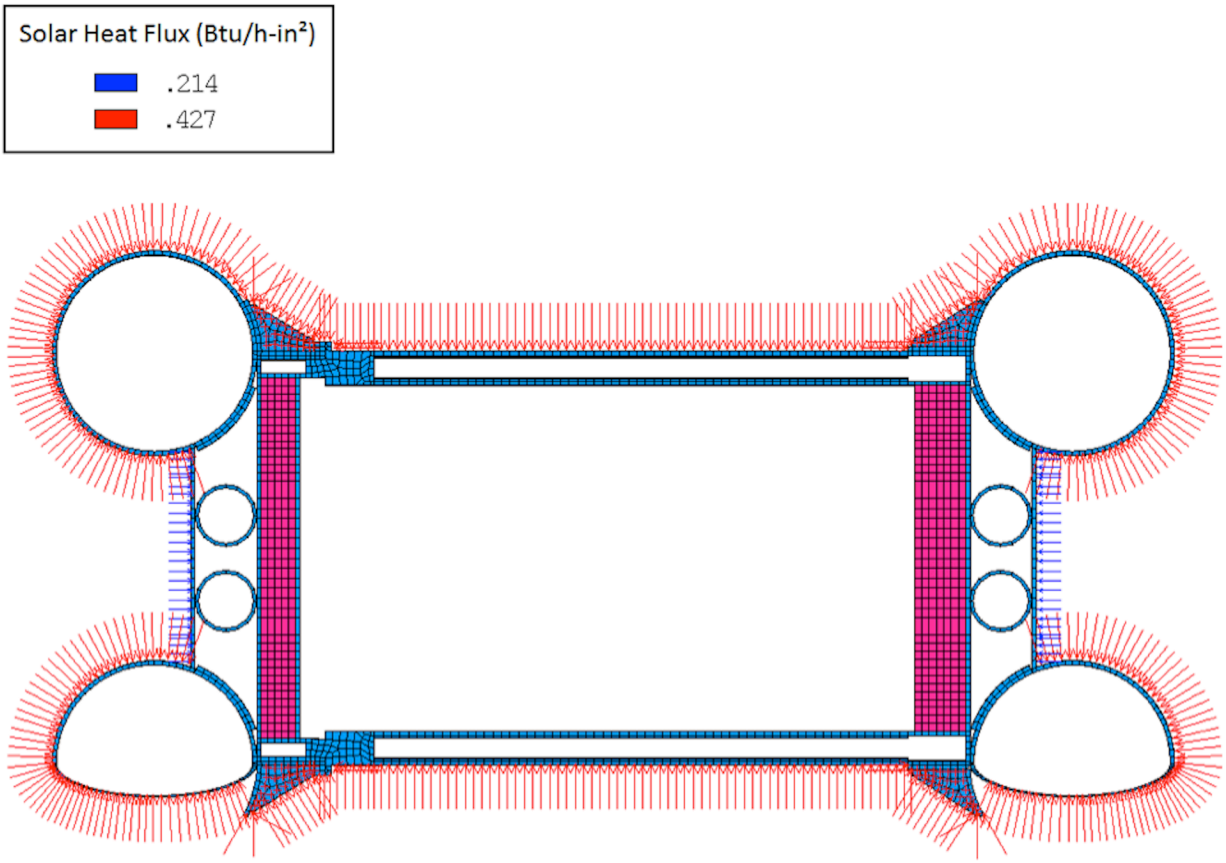

Figure 3.4.2-1. Solar Heat Flux Boundary Conditions for HAC (Post-Fire Cool-Down)

3.4.3. Maximum Temperatures and Pressure

When exposed to the HAC fire prescribed in 10 CFR 71.73(c)(4) (Reference 3-1), the Model 2000 Transport Package must maintain containment of its contents and maintain its shielding capabilities. The results of the HAC thermal evaluation are presented in Table 3.4.3-1. Comparing with Table 3.1.3-1, it can be seen that the maximum temperatures of the different components are below the allowable temperatures. Therefore, the HAC fire will not adversely affect the package's ability to provide containment and shielding for its contents.

3.4.3.1. HAC Temperature Results

A transient thermal analysis was performed on the model. This transient analysis simulates exposure of the Model 2000 Transport Package to a 30-minute hypothetical accident fire followed by a 36-hour cool-down period in which the package is exposed to a 100°F ambient temperature and insolation (solar heat flux). The 36-hour cool-down period is of sufficient length to allow the package temperatures to reach their peak values. The results of the transient HAC thermal analysis are presented in Table 3.4.3-1.

Table 3.4.3-1. Temperature Results, Hypothetical Accident Conditions

Item	Peak Temperature (°F)	Time at Which Peak Temperature Occurs (Hours)
Material Basket	1045	13.0
HPI shielding (side)	670	11.0
HPI shielding (top)	599	9.0
HPI shielding (bottom)	618	11.0
Cask lid seal	508	6.2
Cask shielding (side)	570	0.6
Cask shielding (top)	529	7.1
Cask shell, puncture location	782	0.5
Cask shell, opposite side to puncture location	512	4.0
Overpack outer shell, puncture location	1,103	0.5
Overpack outer shell, opposite side to puncture location	1,337	0.5
Cask drain port (bottom)	612[a]	0.8
Cask test port (top)	608[b]	0.6
Cask vent port (lid)	520	7.1
HPI fill gas (average)	740	11.0
Cask fill gas (average)	571	7.1
HPI and Cask fill gas, combined (average)	585	8.0

Notes: a. The cask bottom port exceeds 600°F for approximately 0.34 hours during the HAC transient analysis.

b. The cask top port exceeds 600°F for approximately 0.17 hours during the HAC transient analysis.

Additionally, temperature-history plots of several package components are presented in Figure 3.4.3-1 through Figure 3.4.3-4 (Note: the steady-state starting temperatures are shown between time = -5 and 0 hours in these figures). As shown in these figures, the cool-down period of 36 hours is sufficient to allow all package temperatures to achieve their peak values. Finally, the temperature contours of the Model 2000 Transport Package with HPI for hypothetical accident conditions are shown in Figure 3.4.3-5.

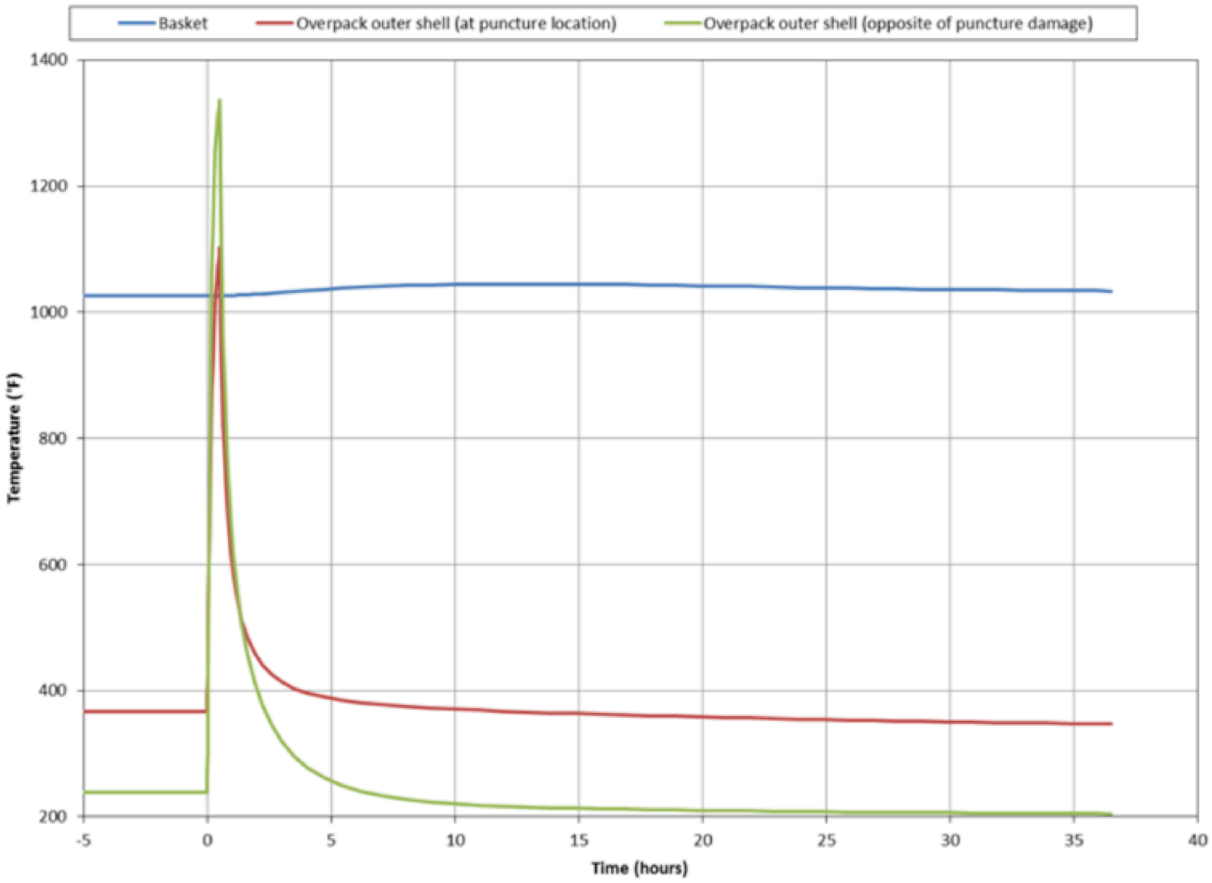

Figure 3.4.3-1. Temperature-History of the Material Basket and Overpack for HAC

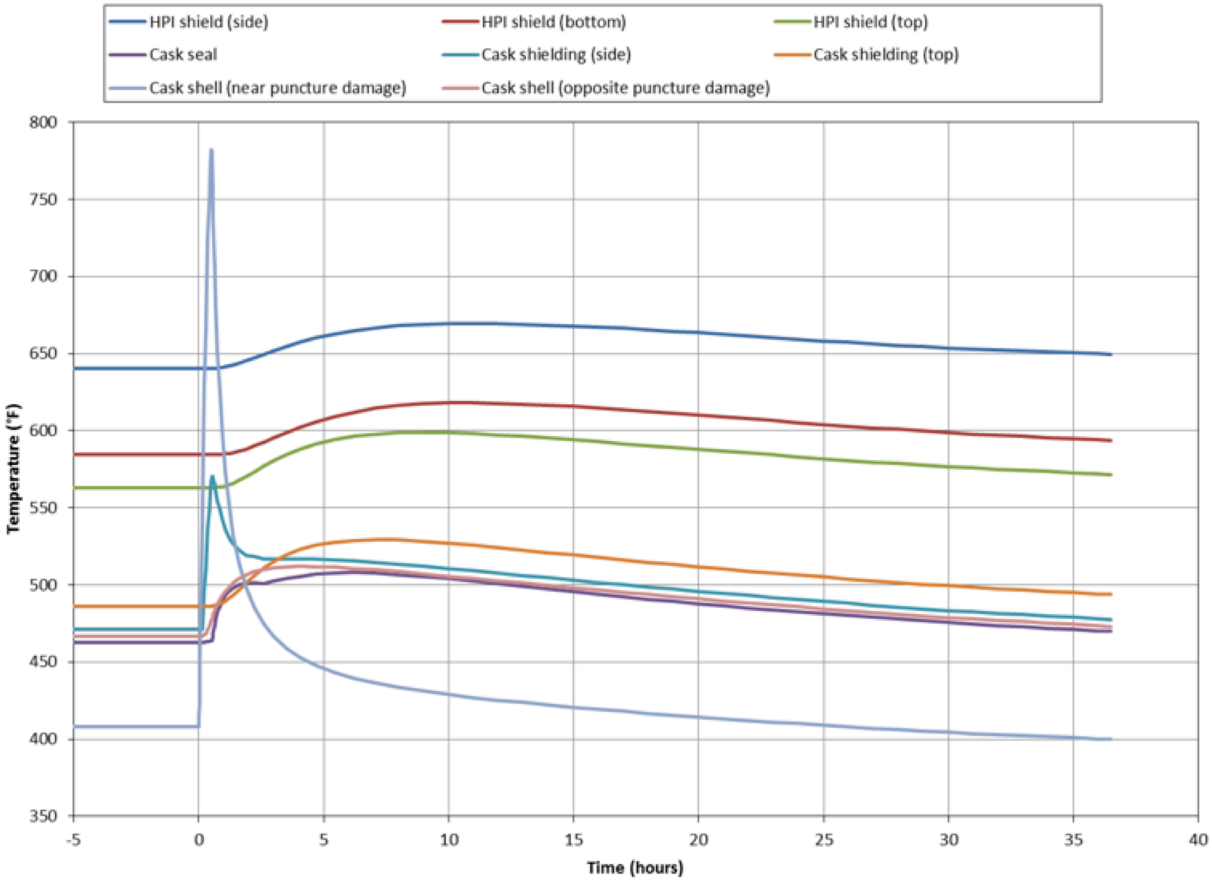

Figure 3.4.3-2. Temperature-History of the HPI and Cask for HAC

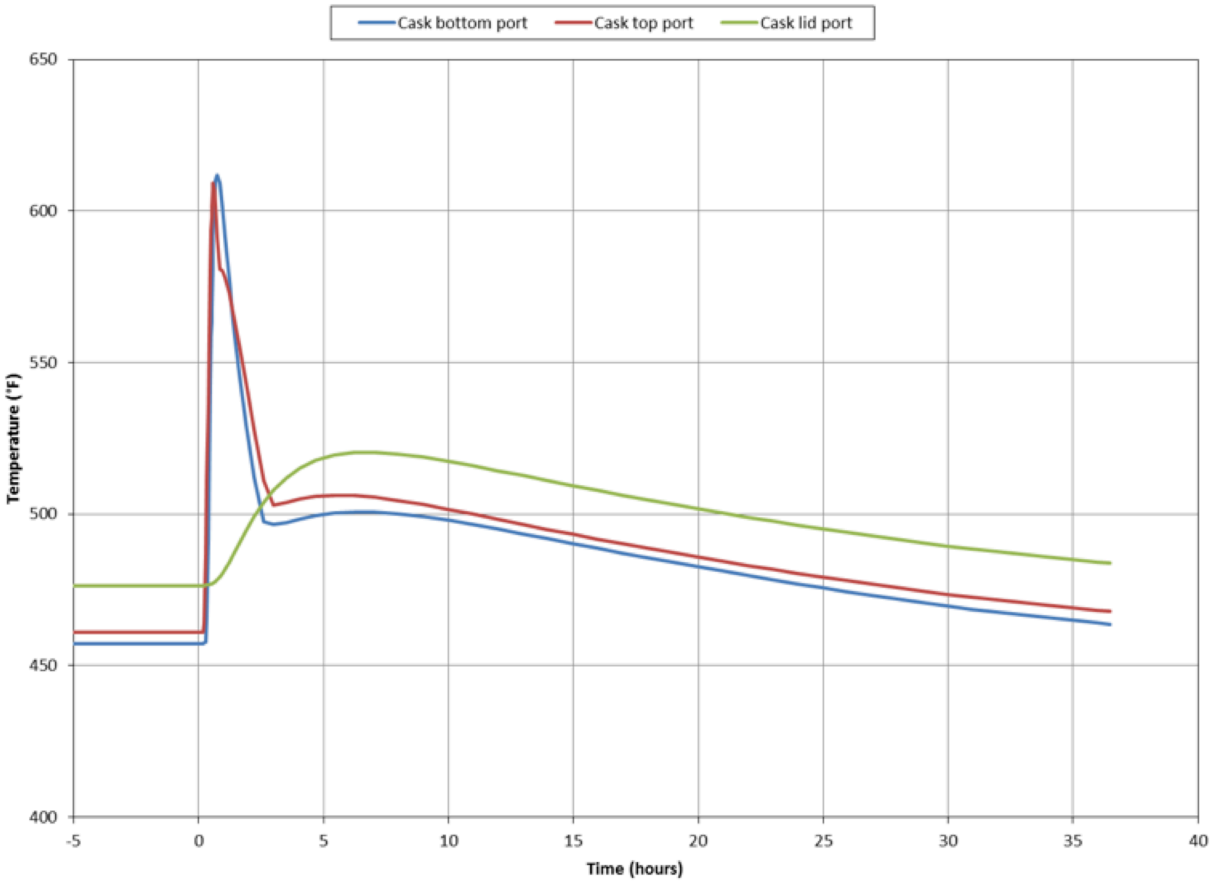

Figure 3.4.3-3. Temperature-History of the Cask Ports for HAC

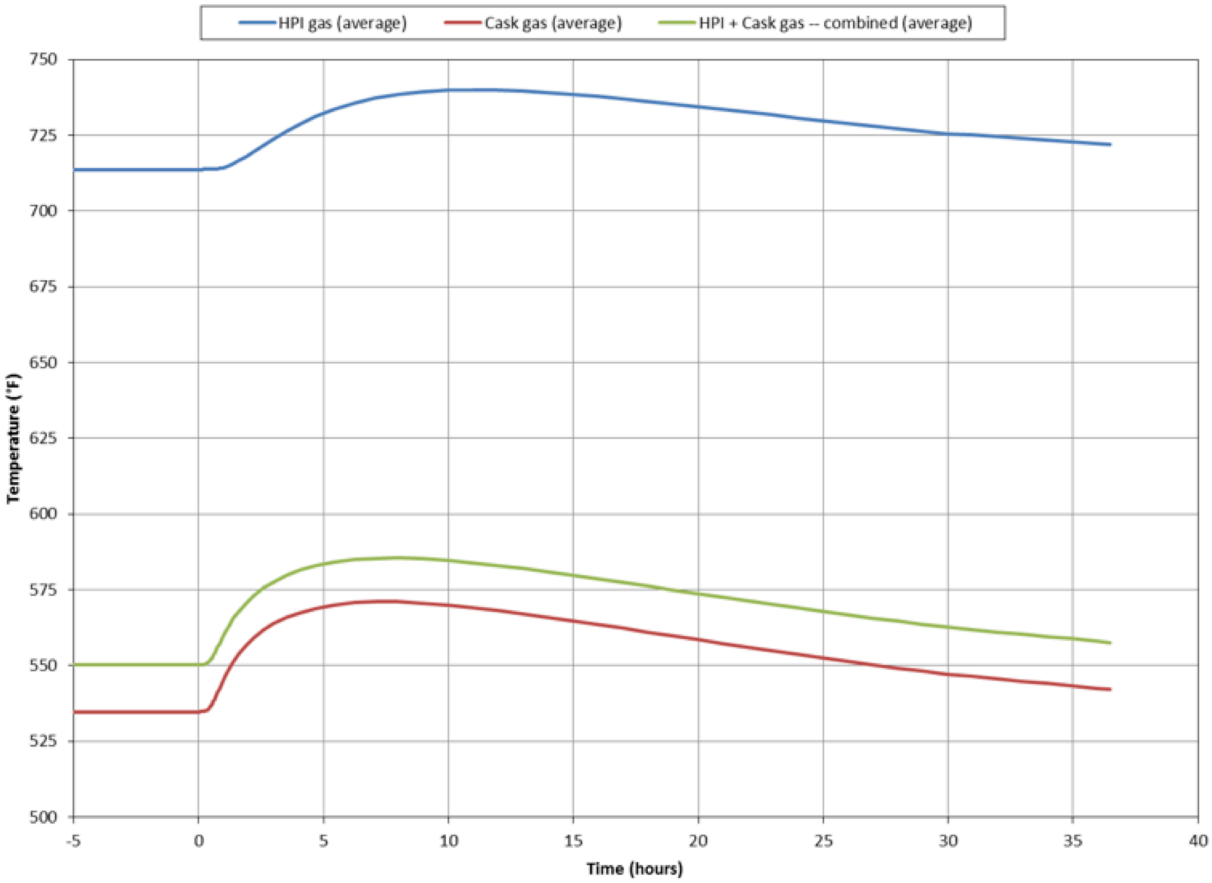

Figure 3.4.3-4. Temperature-History of the HPI and Cask Fill Gases

(Note: Volumetric Average Temperature)

[[

]]

Figure 3.4.3-5. Temperature Contours During HAC 30-Minute Fire and Cool-Down

HAC Thermal Contact Resistance Sensitivity Study

Similar to the NCT thermal conductivity resistance sensitivity study, to assess the effect that using the mixed thermal resistance levels have on package temperatures, the analyses for HAC is repeated with all of the thermal resistance levels set to "low" (i.e., perfect contact). The results of this analysis is compared with the results from Table 3.4.3-1, and presented in Table 3.4.3-2.

Table 3.4.3-2. Comparison of Mixed and Perfect Thermal Contact for HAC

Item	Peak temperature (°F)	
	Mixed Thermal Contact Resistance	Perfect Thermal Contact
Material basket	1,045	1,043
HPI shielding (side)	670	668
HPI shielding (top)	599	596
HPI shielding (bottom)	618	617
Cask lid seal	508	506
Cask shielding (side)	570	576
Cask shielding (top)	529	527
Cask shell, puncture location	782	795
Cask shell, opposite side to puncture location	512	511
Cask drain port (bottom)	612[a]	655[c]
Cask test port (top)	609[b]	613[d]
Cask vent port (lid)	520	518
Overpack outer shell, puncture location	1,103	1,094
Overpack outer shell, opposite side to puncture location	1,337	1,336
HPI fill gas (average)	740	738
Cask fill gas (average)	571	569
HPI and cask fill gases, combined (average)	585	584

Notes:
a. The cask bottom port exceeds 600°F for approximately 0.34 hours during the HAC transient analysis.
b. The cask top port exceeds 600°F for approximately 0.17 hours during the HAC transient analysis.
c. The cask bottom port exceeds 600°F for approximately 0.69 hours during the HAC transient analysis.
d. The cask top port exceeds 600°F for approximately 0.20 hours during the HAC transient analysis.

The same conclusion that was made for NCT thermal contact resistance can be made for HAC in that, in general, the package temperatures are lower when modeling the thermal contact as perfect as opposed to the mixed thermal contact levels. However, the cask drain port (bottom) and the cask test port (top) have peak temperatures that are higher when modeling the thermal contact as perfect. This is due to their proximity to the modeled puncture damage, which allows the heat from the fire to more readily enter the package.

It should be noted that the significant increase in the maximum temperature at the bottom port (drain port) for the perfect contact case is due to the perfect contact between the [[ ]] of the HPI and the bottom of the cask cavity. This perfect contact causes a significant increase in the heat driven out the bottom of the cask from the internal heat load. However, it should be considered that perfect contact between the HPI [[ ]] and the bottom of the cask is an unrealistic

scenario. For drainage purposes, there is a slight dish in the bottom of the Model 2000 cask cavity that will provide a significant separation between the HPI [[ ]] and the bottom of the cask. This separation, shown in Figure 3.4.3-6, will cause the temperature for the cask drain port (bottom) to be more accurately calculated with mixed thermal resistance.

[[

]]

Figure 3.4.3-6. Gap Between HPI [[ ]] and Cask Cavity Bottom (INCH)

3.4.3.2. HAC Maximum Pressure Calculation

During HAC, the average temperature of the cask fill gas (including the gas within the HPI) peaks at 585°F 11 hours after the end of the 30-minute fire. Using the ideal gas law, the cask internal pressure from gas expansion is:

$$\frac{P_1}{T_1} = \frac{P_2}{T_2}$$

$$P_2 = 14.7 \text{ psia} \times \left(\frac{585+460}{70+460}\right) = 29.0 \text{ psia} < 30 \text{ psia}$$

where,

P_1	=	14.7 psia	initial fill gas pressure,
T_1	=	70°F	initial fill gas temperature, and
T_2	=	585°F	average gas volume temperature during HAC.

The cask internal pressure during HAC is less than the design pressure of 30 psia. Therefore, no further evaluation is required.

3.4.4. Maximum Thermal Stresses

Section 2.7.4.3 discusses thermal stresses.

3.4.5. Accident Conditions for Fissile Material Packages for Air Transport

The Model 2000 Transport Package will not be transported by air.

3.5 Appendix

3.5.1. Model 2000 Transport Package with HPI and No Material Basket

This section evaluates the Model 2000 Transport Package with the HPI and no material basket, 1500 W, for both NCT and HAC using a subset of the finite element model described in the main text of this document. The evaluation presented in this section concludes that the temperatures and pressures generated in the Model 2000 Transport Package by 1500 W of decay heat results in package temperatures and pressures which are bounded by the 3000 W results.

3.5.1.1. Thermal Model with HPI and No Material Basket 1500 Watt Decay Heat

The model (see Figure 3.5.1-1) consists of the Overpack (with trapped air), cask, HPI, and cask fill gas. The contents are assumed to generate 1500 W of heat that is uniformly distributed on the internal surfaces of the HPI.

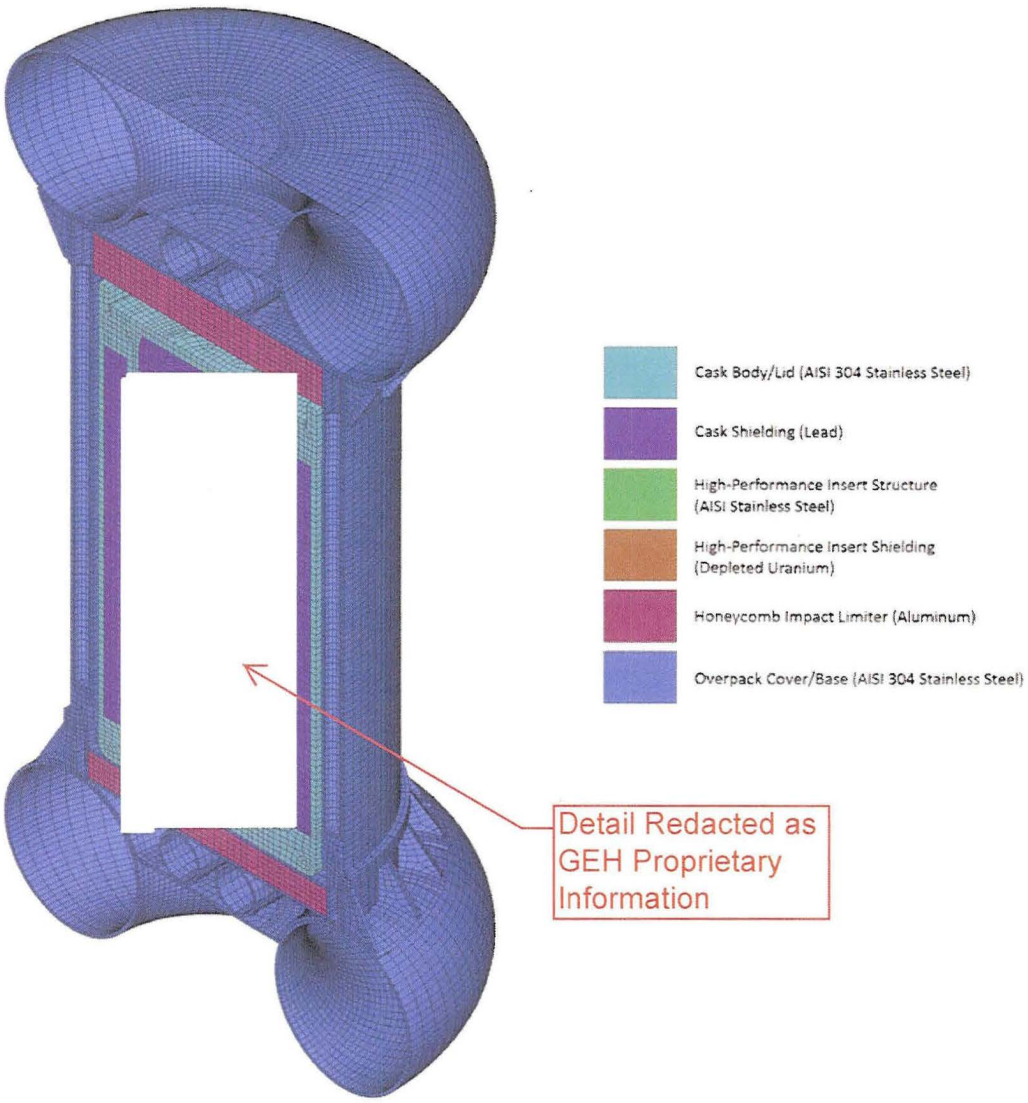

Figure 3.5.1-1. 3D FEA Model of the Model 2000 Transport Package with HPI and No Material Basket (Half Symmetry) - Elements Representing Air and Helium Not Shown for Clarity

$$q''_{gen} = \frac{Q}{A_{SURF152}} = \frac{1500\ W\left(\frac{3.4123\ Btu/h}{W}\right)}{2 \times 816.846194\ in^2} = 3.133\ \frac{Btu}{h\text{-}in^2}$$

where

$A_{SURF152}$ = the area of the SURF152 elements overlaid on the inner surface of the HPI (multiplied by 2 to account for the half-symmetry of the model).

The package is exposed to NCT and HAC using boundary conditions as described in the main text of this document. Additionally, the package is modeled with damage consistent with a side drop for HAC as described in the main text of this document. For HAC, the package is assumed to be

exposed to a 100°F ambient temperature with insolation prior to and following the 1,475°F fire, and is assumed to be exposed to a -20°F ambient temperature in shade prior to and following the 1,475°F fire.

3.5.1.2. NCT Temperature Results

The NCT thermal analysis results are presented in Table 3.5.1-1 (NCT, 100°F ambient temperature) and Table 3.5.1-2 (NCT cold conditions, -40°F and -20°F ambient temperatures). Table 3.5.1-3 provides a comparison of the component temperature and allowable. As the table shows, the cask lid seal and port temperatures are within the allowable limits for the [[ ]] seal material and port testing as specified in Chapter 4. Additionally, the steady-state temperature contours for NCT (100°F ambient temperature) are shown in Figure 3.5.1-2. As evident from Figure 3.5.1-3, no accessible surface of the package is greater than or equal to 185°F (maximum is less than 175°F) when exposed to a 100°F ambient temperature in shade.

Table 3.5.1-1. Model 2000 Transport Package with HPI (No Material Basket) Temperature Results, NCT (100°F Ambient Temperature in Shade and with Insolation)

Item	100°F Ambient Temperature, in Shade (°F)			100°F Ambient Temperature, with Insolation (°F)		
	Max	Min	Avg	Max	Min	Avg
HPI	390	254	---	420	289	---
HPI shielding (top)	356	346	352	388	378	383
HPI shielding (sides)	389	300	367	419	334	398
HPI shielding (bottom)	313	294	306	346	328	340
Cask (bottom, shells, top, lid)	296	223	---	331	261	---
Cask shielding (lid)	292	283	287	327	318	322
Cask shielding (sides)	280	242	267	316	279	303
Cask lid seal	282	269	---	317	305	---
Cask drain port (bottom)	243	223	---	279	261	---
Cask test port (top)	278	269	---	314	305	---
Cask vent port (lid)	288	284	---	323	319	---
Overpack base	239	136	---	275	158	---
Overpack cover	193	105	---	237	171	---
Overpack toroidal shell (top)	131	106	114	185	163	171
Overpack toroidal shell (bottom)	168	109	124	212	130	164
Overpack honeycomb impact limiter (top)	163	155	161	213	205	210
Overpack honeycomb impact limiter (bottom)	236	202	220	272	241	258
Cask fill gas	385	245	316	415	281	349

Table 3.5.1-2. Model 2000 Transport Package with HPI (No Material Basket) Temperature Results, -40°F & -20°F Ambient Temperatures in Shade

Item	-40°F Ambient Temperature, in Shade (°F)			-20°F Ambient Temperature, in Shade (°F)		
	Max	Min	Avg	Max	Min	Avg
HPI	305	147	---	317	162	---
HPI shielding (top)	268	258	263	280	270	276
HPI shielding (sides)	304	201	279	316	215	291
HPI shielding (bottom)	216	195	208	230	209	222
Cask (bottom, shells, top, lid)	199	110	---	213	126	---
Cask shielding (lid)	195	185	189	208	199	203
Cask shielding (sides)	182	134	164	195	150	179
Cask lid seal	183	171	---	197	184	---
Cask drain port (bottom)	135	110	---	150	126	---
Cask test port (top)	179	171	---	193	184	---
Cask vent port (lid)	190	187	---	204	200	---
Overpack base	130	1	---	145	21	---
Overpack cover	64	-36	---	83	-16	---
Overpack toroidal shell (top)	-7	-35	-26	13	-15	-6
Overpack toroidal shell (bottom)	41	-33	-14	59	-12	6
Overpack honeycomb impact limiter (top)	29	19	25	48	39	45
Overpack honeycomb impact limiter (bottom)	127	82	107	142	100	123
Cask fill gas	301	137	221	312	152	234

Table 3.5.1-3. NCT Temperature Summary and Comparison with Allowable Temperatures

Item	NCT Temperatures (°F)	Allowable Temperature (°F)
HPI Shielding (Depleted Uranium)	419 (max)	2071
Cask lid seal	317 (max)	400 [b]
Cask Shielding (Lead)	327 (max)	622
Honeycomb Impact Limiters	272	350
Cask Drain Port (Bottom)	279	612 [a]
Cask Test Port (Top)	314	
Cask Vent Port (Lid)	323	
Overpack Outer Surface	175	185

Notes: See Table 3.1.3-1 for allowable temperature referencing;
[a] Temperature limit applies to the port plug containment boundary
[b] See Section 4

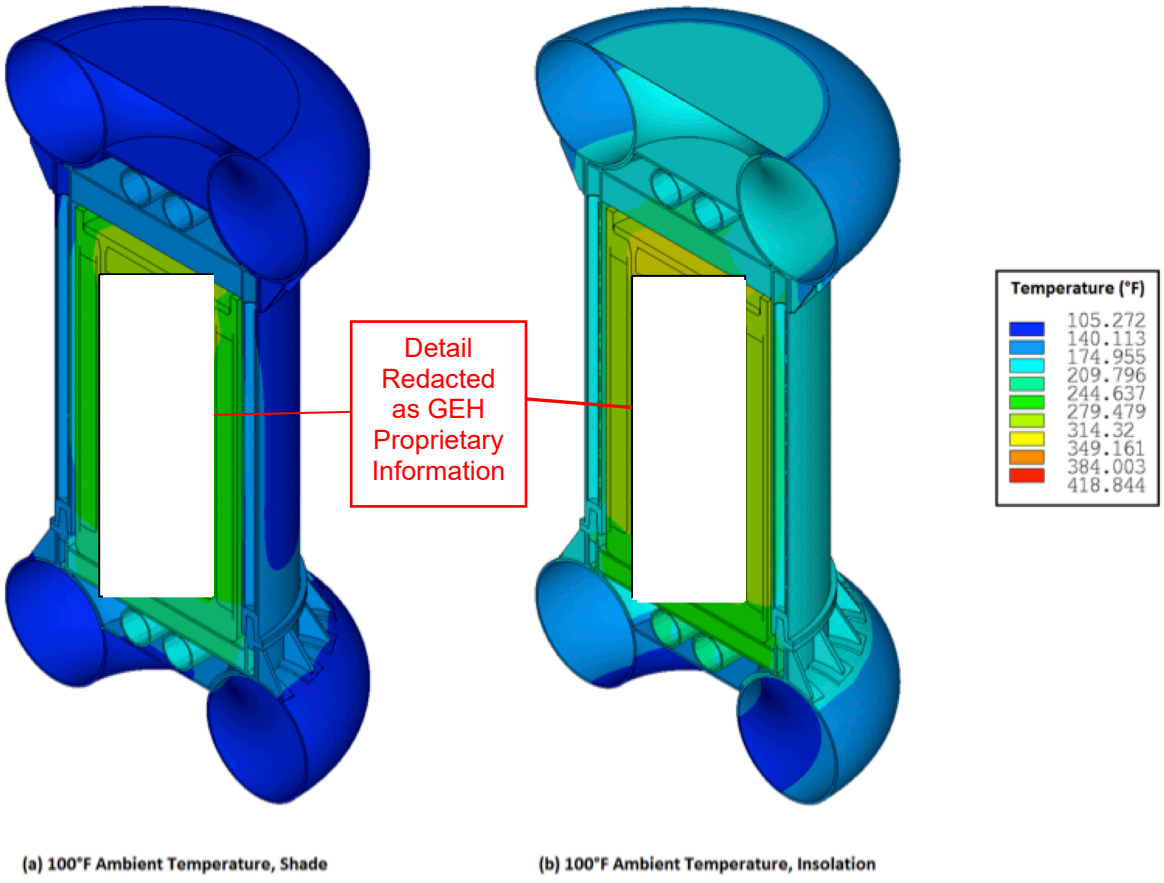

Figure 3.5.1-2. Package Temperature Contours for NCT with 100°F Ambient Temperature in Shade and with Insolation

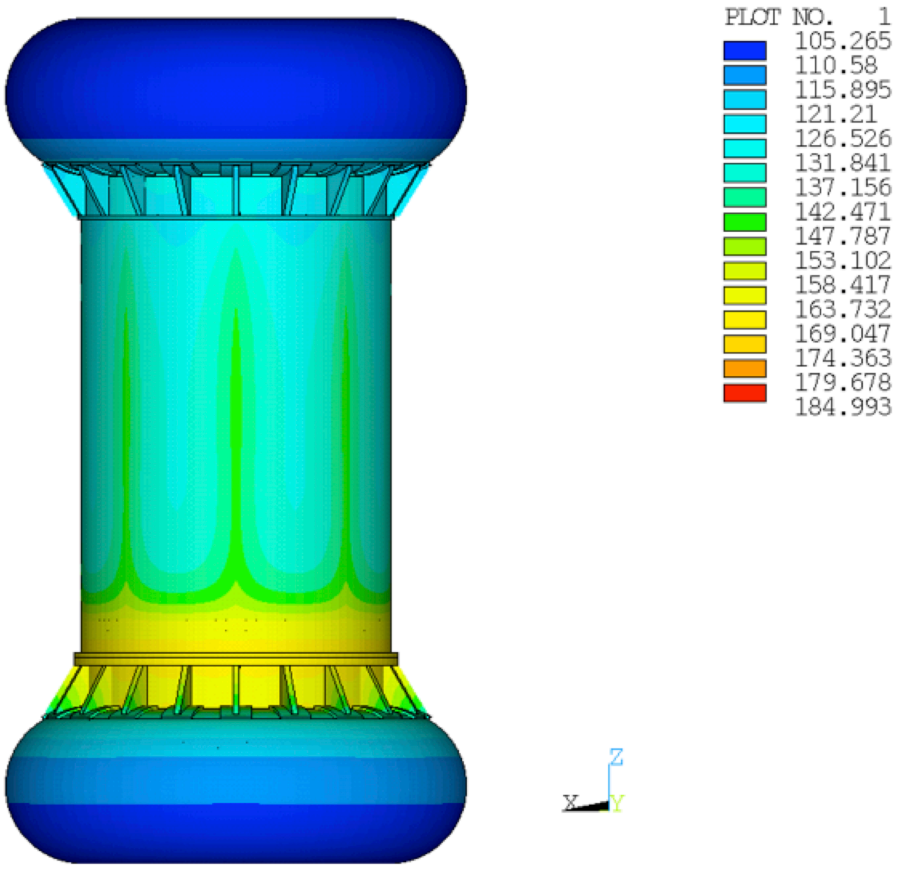

Figure 3.5.1-3. Package Exterior Surface Temperature Contours for NCT with 100°F Ambient Temperature in Shade

3.5.1.3. HAC Temperature Results

The HAC thermal analysis results are presented in Table 3.5.1-4. The table presents the temperature results for both hot and cold pre/post fire conditions. Table 3.5.1-5 provides a comparison of the component temperature and allowable. As the table shows, the cask lid seal and port temperatures are within the allowable limits for the [[ ]] seal material as specified in Chapter 4.

Table 3.5.1-4. Model 2000 Transport Package with HPI (No Material Basket) Temperature Results, HAC

Item	Fire with 100°F and Insolation Pre/Post Fire		Fire with -20°F and Shade Pre/Post Fire	
	Peak Temp. (°F)	Time at Which Peak Temp. Occurs (hours)	Peak Temp. (°F)	Time at Which Peak Temp. Occurs (hours)
HPI shielding (side)	482	12.3	389	16.5
HPI shielding (top)	439	10.3	338	13.5
HPI shielding (bottom)	446	12.3	348	15.5
Cask lid seal	389	2.2	275	10.5
Cask shielding (side)	456	0.6	344	0.6
Cask shielding (top)	396	8.3	287	10.5
Cask shell, puncture location	704	0.5	621	0.5
Cask shell, opposite side to puncture location	385	5.6	273	8.5
Overpack outer shell, puncture location	1,063	0.5	1,017	0.5
Overpack outer shell, opposite side to puncture location	1,330	0.5	1,314	0.5
Cask drain port (bottom)	537	0.8	435	0.8
Cask test port (top)	515	0.6	406	0.6
Cask vent port (lid)	392	8.3	283	10.5
Cask fill gas (average)	421	9.3	319	12.5

Table 3.5.1-5. HAC Temperature Summary and Comparison with Allowable Temperatures

Item	HAC Temperatures (°F)	Allowable Temperature (°F)
HPI Shielding (Depleted Uranium)	482 (max)	2071
Cask lid seal	389 (max)	400 [[ ]]
Cask Shielding (Lead)	456 (max)	622
Cask Drain Port (Bottom)	537	612[a]
Cask Test Port (Top)	515	
Cask Vent Port (Lid)	392	

Notes: See Table 3.1.3-1 for allowable temperature referencing;
[a] See Chapter 4

3.5.1.4. Thermal Contact Resistance Study

The thermal contact resistance levels in this model are modified to simulate perfect contact, and the NCT (100°F ambient with insolation) and HAC (100°F ambient with insolation during pre-fire and post-fire) analyses are performed and compared with those that include mixed thermal contact resistances. The results of these studies are presented in Table 3.5.1-6 (NCT) and Table 3.5.1-7 (HAC). As shown in Table 3.5.1-6, the simulation with perfect thermal contact results in component temperatures being lower than their mixed thermal contact counterparts.

The simulation for HAC with perfect thermal contact results in most component temperatures being lower than their mixed thermal contact counterparts while other component temperatures are higher for the case with perfect thermal contact. The item exhibiting the greatest sensitivity in the HAC study is the cask drain port (increased temperature of 50°F). However, as discussed in Section 3.4.3.1, there is a slight dish in the bottom of the Model 2000 cask cavity that will provide a significant separation between the HPI [[ ]] and the bottom of the cask. This separation, shown in Figure 3.4.3-6, will cause the temperature for the cask drain port (bottom) to be more accurately calculated with mixed thermal resistance. Therefore, a maximum temperature of 537°F is predicted for the drain port.

Table 3.5.1-6. Model 2000 Transport Package with HPI (No Material Basket) Temperature Results, 100°F Ambient Temperature with Insolation, NCT, Thermal Contact Resistance Study

Item	Mixed Contact Resistances (°F)			Perfect Contact (°F)		
	Max	Min	Avg	Max	Min	Avg
HPI	420	289	---	415	283	---
HPI shielding (top)	388	378	383	384	374	379
HPI shielding (sides)	419	334	398	414	327	393
HPI shielding (bottom)	346	328	340	341	322	334
Cask (bottom, shells, top, lid)	331	261	---	326	253	---
Cask shielding (lid)	327	318	322	322	314	317
Cask shielding (sides)	316	279	303	312	272	298
Cask lid seal	317	305	---	313	301	---
Cask drain port (bottom)	279	261	---	273	253	---
Cask test port (top)	314	305	---	310	301	---
Cask vent port (lid)	323	319	---	318	315	---
Overpack base	275	158	---	269	157	---
Overpack cover	237	171	---	235	170	---
Overpack toroidal shell (top)	185	163	171	184	162	170
Overpack toroidal shell (bottom)	212	130	164	208	130	164
Overpack honeycomb impact limiter (top)	213	205	210	210	202	207
Overpack honeycomb impact limiter (bottom)	272	241	258	268	236	254
Cask fill gas	415	281	349	411	275	344

Table 3.5.1-7. Model 2000 Transport Package with HPI (No Material Basket) Temperature Results, 100°F Ambient with Insolation During Pre- and Post-Fire, HAC, Thermal Contact Resistance Study

Item	Mixed Contact Resistances		Perfect Contact	
	Peak Temp. (°F)	Time at Which Peak Temp. Occurs (hours)	Peak Temp. (°F)	Time at Which Peak Temp. Occurs (hours)
HPI shielding (side)	482	12.3	480	12.2
HPI shielding (top)	439	10.3	438	10.2
HPI shielding (bottom)	446	12.3	446	12.2
Cask lid seal	389	2.2	389	2.2
Cask shielding (side)	456	0.6	463	0.2
Cask shielding (top)	396	8.3	395	8.2
Cask shell, puncture location	704	0.5	718	0.5
Cask shell, opposite side to puncture location	385	5.6	384	5.5
Overpack outer shell, puncture location	1,063	0.5	1,054	0.5
Overpack outer shell, opposite side to puncture loc.	1,330	0.5	1,330	0.5
Cask drain port (bottom)	537	0.8	587	0.7
Cask test port (top)	515	0.6	519	0.9
Cask vent port (lid)	392	8.3	390	7.2
Cask fill gas (average)	421	9.3	420	9.2

3.6 References

3-1 U.S. NRC, 10 CFR 71, "Packaging and Transportation of Radioactive Material," Washington D.C.

3-2 ANSYS®, "Mechanical, Revision 14.0," November 2011.

3-3 Incropera, Frank P., and DeWitt, David P., "Fundamentals of Heat and Mass Transfer," Fifth Edition, John Wiley & Sons, Inc., New York, 2002.

3-4 Hexcel Corporation, "HexWeb Honeycomb Attributes and Properties,", 2016.

3-5 GE Hitachi Nuclear Energy, "Model 2000 Cask Containment Boundary Testing," Test Specification 003N1962, Revision 0 (2015), or latest revision.

3-6 Editors H.K Hammond III and H.L Mason, “Precision Measurement and Calibration, Selected NBS Papers on Radiometry and Photometry,” Editors H.K Hammond III and H.L Mason, Ed.: National Bureau of Standards (NBS), 1971, Volume 7.

3-7 Robert Siegel and John R. Howell, "Thermal Radiation Heat Transfer, Third Edition," Hemisphere Publishing Corporation, New York, 1992.

3-8 Parker Hannifin Corporation. (2014) Parker O-Ring Handbook, 50th Anniversary Edition.

3-9 Lienhard IV, John H., and Lienhard V, John H., "A Heat Transfer Textbook," Fourth Edition, Phlogiston Press, Cambridge, Massachusetts, 1981.

3-10 Guyer, Eric C., Editor, "Handbook of Applied Thermal Design," McGraw-Hill, New York, 1989.

4 CONTAINMENT

This section demonstrates the ability of the Model 2000 Transport Package to meet the containment requirements of 10 CFR 71. The containment system for the Model 2000 Transport Package consists of the cask alone. The other components (e.g., overpack, high performance insert (HPI)) are not part of the containment system. The entire containment boundary, including containment welds and base metals (as shown in Figure 4.1.3-1), are leakage rate tested for fabrication, maintenance, and periodically as defined in Chapter 8.

4.1 Description of Containment System

The cask design has been evaluated to support 3000 W decay heat as stated in Section 1.2.2.3. However, for the purposes of this chapter, the allowable contents are limited to 1500 W decay heat.

4.1.1. Containment Vessel

Figure 1.2-1 shows the containment vessel (cask) for the Model 2000 Transport Package. The containment boundary for the cask is shown in Figure 4.1.3-1. The cask is constructed of a steel-clad lead cylinder with a stainless steel forging at each end. The cask lid is placed within the upper forging to protect the seal area during the accident conditions. Refer to Section 2.2 for information regarding the materials of construction of the cask.

4.1.2. Closure

The cask lid connects to the cask body by fifteen 1.25-inch diameter ASTM A540, Grade B22 or ASME SA540 socket head screws, which compress the cask lid seal. The screws are equally spaced on a 32.25-inch diameter bolt circle. Each screw is tightened to 720±30 ft-lb of torque, as shown in Section 2.12.4. The cask lid closure evaluation is presented in Section 2.4.3. The stress analysis of these screws is given in Section 2.12.4. These analyses show that positive closure is maintained during all conditions.

4.1.3. Containment Penetrations

The Model 2000 cask has three penetrations or ports. One port, located two inches from the bottom of the cask, serves as a drain for the cask cavity. This port is made by a series of offset ½-inch drilled holes through the 6-inch thick steel forging. The second penetration is located approximately in the center of the cask lid. It is made of 3/8-inch diameter tubing, shown as Item 13 - [[ ]], in the Model 2000 Transport Package Licensing Cask Drawings 101E8718 and 105E9520, respectively (see Section 1.3.1), spiraled through the lead and welded at both ends to the steel flanges that make up the lid. The combined use of these two ports provides means to eliminate water from the cask cavity collected during underwater operations. The third penetration or port is used to test the adequacy of the cask lid closure seal after each loading operation.

A ½ NPT hex socket head pipe plug followed by 1¾-12 UNC cap close each of these penetrations (see Figure 4.1.3-2). The closure of pipe plug is designed for leaktightness as defined in

ANSI N14.5-1997, Section 2.1 (Reference 4-1). Dimensions and components of the port seals are provided in the Model 2000 cask licensing drawings included in Section 1.3.1. Additional information is provided in Section 4.1.3.3.

4.1.3.1. Welds

All cask welds are [[ ]] to ensure structural and containment integrity. Each weld is liquid penetrant tested on the root and final passes. In addition, the welds are helium leak tested as required in Chapter 8.

[[

]]

Figure 4.1.3-1. Cask Containment Boundary

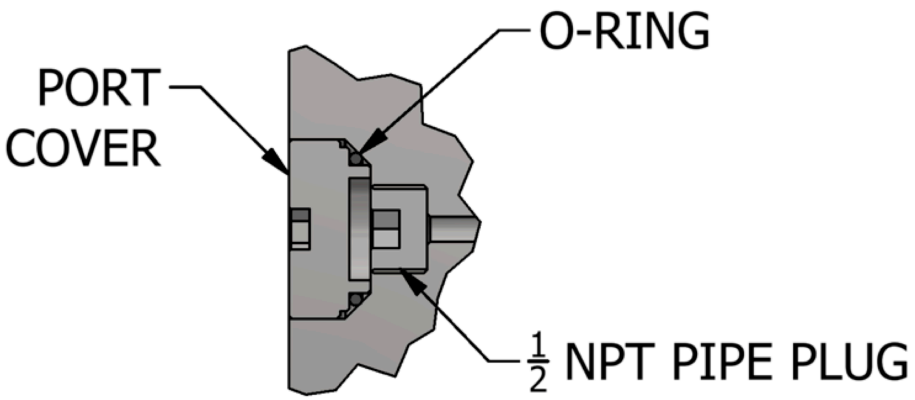

Figure 4.1.3-2. Cask Port Configuration (Assembled View)

4.1.3.2. Cask Lid Closure Seal

The cask lid seal (Parker Gask-O-Seal design) consists of a [[ ]] thick metal retainer with two concentric [[ ]] seals on the top and two concentric [[ ]] seals on the bottom (4 total), as seen in Figure 4.1.3-3. The surfaces of the Model 2000 cask body and the lid flanges have an electropolished finish to ensure that they are clean sealing surfaces for the [[ ]]. As the load from bolting the lid down is applied, the [[ ]] seals are compressed between the cask body flange and cask lid flange, and the seals deform to occupy the free volume in the metal retainer. A [[
]] are used as the seal material.

[[

]]

Figure 4.1.3-3. Cask Lid Seal Design

4.1.3.3. Cask Port Seals

The containment boundary for each port is at the respective pipe plug. As illustrated in Figure 4.1.3-1, the port O-rings and port covers are outside the containment boundary. An exploded view of these components is shown in Figure 4.1.3-4. For the cask port seals, an [[ ]] is used as the O-ring seal material. See cask licensing drawings in Section 1.3.1 for more detailed information. For details of the pipe plug installation controls, see Chapter 7.

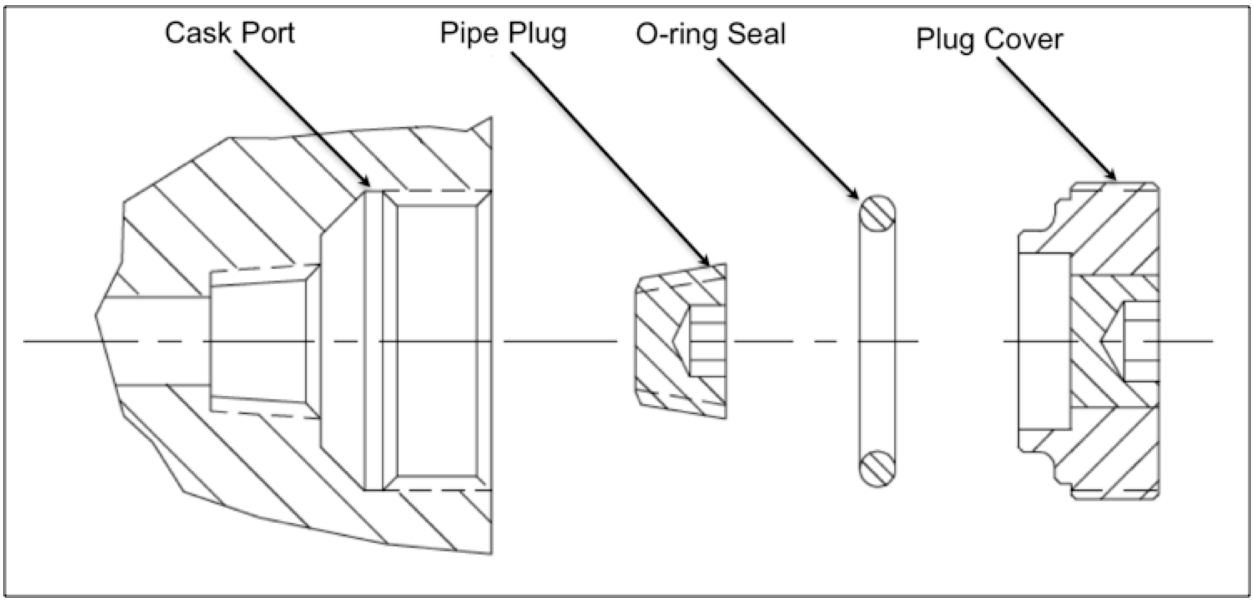

Figure 4.1.3-4. Cask Port Configuration (Exploded View)

4.2 Containment Under Normal Conditions of Transport

The Model 2000 cask containment is designed so that no release of radioactive materials will occur under the NCT, and there will not be any significant increase in external radiation or reduction in package effectiveness. This conclusion is supported by the analyses in Chapters 2 and 3 and the various component qualification tests.

The cask withstands pressures and temperatures in excess of those encountered in routine transport and normal conditions of transport. The maximum average cask fill gas temperature is determined to be 349°F in Section 3.5.1. This temperature value is based on helium occupying the entire cavity volume. The maximum pressure encountered under NCT, 22.4 psia (calculated using the formula in Section 3.3.2.1 with T_2=349°F), is bounded by the 30 psia cask design pressure. The structural evaluation presented in Chapter 2 shows low stress values throughout the cask structure, especially in the seal area under NCT. The maximum cask lid seal temperatures are bounded by the operational limit of 400°F, which is qualified for the cask seal (Reference 4-2). Additionally, cask port temperatures are bounded by the operational limit of 612°F, thus containment integrity is maintained (Reference 4-2).

4.3 Containment Under Hypothetical Accident Conditions

As seen in Section 3.5.1.3, the maximum average cask fill gas temperature in the cask cavity for HAC is 421°F. This temperature is based on helium occupying the entire cavity volume. The maximum pressure encountered during HAC (24.4 psia - calculated using the formula in Section 3.4.3.2 with T_2=421°F) is bounded by the 30 psia cask design pressure. Temperatures at the cask lid closure seal region and cask vent port are bounded by the 400°F design temperature of the seal material (see Table 3.5.1-5 and Reference 4-2). Temperatures at the drain port and test port exceed the seal material allowable temperature by 137°F and 115°F respectively. This is considered acceptable because: (a) the port O-rings and port covers are outside the containment boundary as illustrated in Figure 4.1.3-1, and (b) the duration of HAC maximum temperatures at these ports is short, < 1 hour per Table 3.5.1-4, resulting in minor material degradation. The analytical evaluations under HAC presented in Chapter 2 show that the stresses throughout the cask structure are below the failure criteria for the material.

4.4 Leakage Rate Tests for Type B Packages

The maximum temperature at the cask lid seal region is bounded by 400°F and the maximum temperature at the penetrations or port areas are bounded by 612°F. The internal pressure in the cask cavity may increase to 24.4 psia due to rise in the temperature. The Model 2000 cask is loaded dry or underwater. If loaded underwater, the cavity must be vacuum dried to remove any residual moisture.

Regardless of how the cask is loaded, a leak test is performed after it is loaded. To perform the leak test, helium is introduced into the cavity to a pressure of 15 psig. The preshipment, fabrication, periodic, and maintenance leakage rate tests are performed in accordance with ANSI N14.5 (Reference 4-1) standards. At the conclusion of the pre-shipment test, the pressure is released. Therefore, it can be assumed that helium remains inside the cavity. The peak average fill gas temperature is 421°F under hypothetical accident conditions.

Full-scale acceptance testing of the cask lid closure seal [[ ]] was performed at maximum pressure at ambient temperature. Full-scale acceptance testing of the port NPT fittings was performed at maximum pressure with both maximum (612°F) and minimum (5°F) temperature predictions in accordance with ANSI N14.5 standards (Reference 4-1). The 5°F minimum test temperature bounds the lowest temperature at the port O-rings (21°F) as stated in Section 3.3.1.2. The seal material for both the cask lid seal and port O-rings [[
]] is suitable for conditions less than -40°F. The maximum internal pressure of 24.4 psia is less than the design pressure of 30 psia. Therefore, the Model 2000 Transport Package design pressure is a conservative design basis for the shipment of the 1500 W decay heat content.

4.5 References

4-1 American National Standards Institute (ANSI), "American National Standard for Radioactive Materials – Leakage Tests on Packages for Shipment," ANSI N14.5, 1997.

4-2 GE Hitachi Nuclear Energy, "Model 2000 Cask Containment Boundary Testing," Test Specification 003N1962, Revision 0 (2015), or latest revision.

5 SHIELDING EVALUATION

This chapter outlines the Model 2000 cask shielding analysis, and demonstrates compliance with the external radiation requirements of 10 CFR 71, "Packaging and Transport of Radioactive Material" (Reference 5-1). This shielding evaluation was performed to demonstrate that the Model 2000 Transport Package with the high performance insert (HPI) provides sufficient shielding, such that the external radiation limits are satisfied under Normal Conditions of Transport (NCT) and Hypothetical Accident Conditions (HAC).

5.1 Description of Shielding Design

5.1.1. Design Features

The Model 2000 cask is a cylindrical lead lined cask used for transporting Type B quantities of radioactive materials. For any shipments of radioactive material in the Model 2000 cask, the use of the HPI is required, and all contents must be confined inside the HPI cavity. The radiation shielding design features of the Model 2000 with the HPI are the lead and Stainless Steel (SS) in the Model 2000 cask and the depleted uranium (DU) and SS in the HPI. Narrative descriptions of the HPI, Model 2000 cask, and Model 2000 overpack are provided in Section 1.2. The radiation shielding design features of the Model 2000 with the HPI are provided in Table 5.1-1, including nominal dimensions, materials of construction, and densities of the materials that provide gamma shielding.

Table 5.1-1. Model 2000 Transport Package Shielding Design Features

Model 2000 Component	Part	Component	Thickness (in)	Thickness (cm)	Material of Construction	Material Density (lb/in^3)	Material Density (g/cm^3)
HPI	Top Plug	Inner Shell	[[		[[ ]]	0.29	8.000
		DU			DU	[[	]]
		Outer Shell			[[ ]]	0.29	8.000
	HPI Body	Inner Shell			[[ ]]	0.29	8.000
		DU			DU	[[	]]
		Outer Shell			[[ ]]	0.29	8.000
	Bottom [[ ]]	Inner Shell			[[ ]]	0.29	8.000
		DU			DU	[[	]]
		Outer Shell		]]	[[ ]]	0.29	8.000
Cask	Cask Lid	Lid Flange	1.75	4.445	SS304	0.29	8.000
		Lead	5.37	13.64	Lead	0.41	11.34
		Inner Plate	1.50	3.810	SS304	0.29	8.000
	Cask Body (Side)	Cavity Shell	1.00	2.540	SS304	0.29	8.000
		Lead	4.00	10.16	Lead	0.41	11.34
		Cask Shell	1.00	2.540	SS304	0.29	8.000

Model 2000 Component	Part	Component	Thickness (in)	Thickness (cm)	Material of Construction	Material Density (lb/in^3)	Material Density (g/cm^3)
	Cask Body (Bottom)	Cask Bottom[a]	5.88	14.92	SS304	0.29	8.000
Overpack[b]	Overpack (Top)	Top Plate	0.50	1.270	SS304	0.29	8.000
		End Plate	0.50	1.270	SS304	0.29	8.000
	Overpack (Side)	Inner Shell	0.50	1.270	SS304	0.29	8.000
		Outer Shell	0.50	1.270	SS304	0.29	8.000
	Overpack (Bottom)	Support Plate	0.50	1.270	SS304	0.29	8.000
		Bottom Plate	0.50	1.270	SS304	0.29	8.000
		End Plate	0.50	1.270	SS304	0.29	8.000

Notes: [a] Due to [[ ]] the minimum thickness is used.
[b] Credit for shielding provided by the cask overpack is only taken for NCT analyses.
General: All dimensions based on component licensing drawings in Section 1.3.1.

5.1.2. Summary Table of Maximum Radiation Levels

Table 5.1-2 and Table 5.1-3 present the maximum calculated NCT and HAC dose rates, at the appropriate locations for exclusive use shipment of the Model 2000 Transport Package with the HPI. The calculated NCT and HAC dose rates are reported for each of the two content types described in Section 5.2, as well as the overall maximum dose rates from all contents. The 1-meter transportation index dose rate limits are not applicable as the Model 2000 cask will only be shipped exclusive use. The Model 2000 cask will only be shipped in the upright position, thus the 2-meter and occupied position (cab) dose rates are calculated at the appropriate distances from the side of the cask. Dose rates are limited to 90% of the regulatory limit at each location to provide additional assurance that any small uncertainties in the source term or cask modeling will not result in external dose rates exceeding the respective regulatory limit.

Table 5.1-2. Maximum NCT Dose Rates

Contents	Radiation	Package Surface mSv/hr (mrem/hr)			2-meter mSv/hr (mrem/hr)	Cab mSv/hr (mrem/hr)
		Top	Side	Bottom	Side	Side
1	Gamma	0.1026 (10.26)	1.7999 (179.99)	0.1651 (16.51)	0.0251 (2.51)	0.0044 (0.44)
2	Gamma	0.1799 (17.99)	0.8578 (85.78)	0.3832 (38.32)	0.0162 (1.62)	0.0028 (0.28)
Overall Maximum		0.1799 (17.99)	1.7999 (179.99)	0.3832 (38.32)	0.0251 (2.51)	0.0044 (0.44)
10 CFR 71.47(b)(2) Limit		2 (200)	2 (200)	2 (200)	0.1 (10)	0.02 (2)

Contents:
1 – Irradiated hardware and byproducts
2 – Cobalt-60 isotope rods

Table 5.1-3. Maximum HAC Dose Rates

Contents	HAC	1 Meter from Package Surface mSv/hr (mrem/hr)		
	Radiation	Top	Side	Bottom
1	Gamma	0.1335 (13.35)	0.3421 (34.21)	0.0841 (8.41)
2	Gamma	0.5843 (58.43)	1.6951 (169.51)	0.3454 (34.54)
Overall Maximum		0.5843 (58.43)	1.6951 (169.51)	0.3454(34.54)
10 CFR 71.51(a)(2) Limit		10 (1000)	10 (1000)	10 (1000)

Contents:
1 – Irradiated hardware and byproducts
2 – Cobalt-60 isotope rods

5.2 Source Specification

The allowable contents for the Model 2000 cask are: 1) irradiated hardware and byproducts and 2) cobalt-60 isotope rods. The irradiated hardware and byproduct and cobalt-60 isotope rod contents have photon source terms for determining package external dose rates. Due to the thick layers of shielding provided by the HPI and Model 2000 cask, external dose rate contributions from charged particles (alpha and beta particles) and their secondary particles from interactions (i.e., bremsstrahlung) are negligible.

Irradiated Hardware and Byproducts

The irradiated hardware and byproduct contents are irradiated components from typical reactor operation. These contents include:

1. Hardware: Irradiated metals composed of materials such as SS, carbon steels, nickel alloys, and zirconium alloys. Examples include:
   - Bundle components: water rods, spacers, and upper/lower tie plates
   - Reactor internals: jet pump beams, core shroud samples
2. Irradiated Byproducts: Irradiated control rod blades with the following neutron poison materials:
   - Hafnium
   - Boron Carbide

Cobalt-60 Isotope Rods

The radioactive material in the isotope rod contents is in the form of pellets or cylindrical solid rods with the source(s) evenly distributed and encapsulated in normal or special form. The isotope rods are loaded into a commercial or research reactor to irradiate the cobalt source pellets. After discharge from the reactor, the isotope rods are loaded into the Model 2000 cask for transport. These [[ ]] prior to loading into the HPI. Herein for the cobalt-60 isotope rod contents, the term ‘rod’ refers to a full-length rod, in its form as it is irradiated in a reactor; and the term [[ ]] in its form as it is loaded and shipped in the Model 2000 Transport Package.

5.2.1. Gamma Source

5.2.1.1. Irradiated Hardware and Byproducts

To calculate a gamma energy spectrum, the ORIGEN-S module distributed in the SCALE6.1 code package (Reference 5-2) was used. With the ORIGEN-S methodology, a problem dependent cross section library is generated by interpolating between cross sections in the SCALE pre-generated libraries.

For the irradiated hardware and byproduct contents, the gamma source strength and spectra are based on the individual radionuclides in a given shipment. Multiple ORIGEN-S irradiation calculations were used to identify the radionuclides that could be in a shipment of irradiated hardware and byproduct. Table 5.2-1 provides a list of radionuclides that may be present in irradiated hardware and byproduct contents that contribute to external dose rates. Other radionuclides which may be present in irradiated hardware and byproducts but do not emit significant gammas were excluded from Table 5.2-1. However, all radionuclides that may be present in irradiated hardware and byproducts are considered when determining the total decay heat of the payload as described in Section 5.5.3.

External dose rates are calculated individually for 1 Ci of activity with the energy spectrum from each of the listed radionuclides. The energy spectrum for each radionuclide is from the ORIGEN-S Data Library origen.rev04.mpdkxgam.data (Reference 5-2). The dose rate contribution from a specific radionuclide at a regulatory dose rate location is calculated by multiplying the total activity for the radionuclide by its respective dose rate per curie multiplier. The total dose rate from a payload of irradiated hardware and byproduct is calculated by summing the dose rate contributions from each radionuclide included in the shipment. Details of the ORIGEN-S irradiated hardware and byproduct source term calculations and the energy spectra for each radionuclide of interest are provided in Section 5.5.1.

Table 5.2-1. Irradiated Hardware and Byproduct - Radionuclides Significant to External Dose Rates

Radionuclides
Sc-46
Cr-51
Mn-54
Co-58
Fe-59
Co-60
Zn-65
Nb-92m
Nb-94
Zr/Nb-95
Sb-124
Sb-125
Sb-126
Cs-134
Cs-137 (Ba-137m)
Hf-175
Hf-181
Ta-182

5.2.1.2. Cobalt-60 Isotope Rods

The primary gamma source in the cobalt-60 isotope rod content is from the cobalt-60 source pellets. Dose rate contributions from the small quantities of radionuclides in crud that has built up on the rods while in the reactor is negligible due to insignificant gammas emitted. The cask external dose rates are dominated by the quantity of cobalt-60 in the isotope rods, and any dose rate contributions from any radionuclides in the rod cladding can be accounted for as irradiated hardware (see Section 5.4.4.3 for further explanation). Table 5.2-2 provides the energy spectrum and gamma source strength for cobalt-60 used for dose rate calculations. The energy spectrum is from the ORIGEN-S data library origen.rev04.mpdkxgam.data (Reference 5-2). All energy lines less than 0.1 MeV are considered negligible and are neglected from the energy spectrum. The source strength is based on the cobalt-60 activity equivalent to the thermal limit of 1500 W. The watt/curie (W/Ci) conversion factor is based on the ORIGEN-S decay library origen.rev03.decay.data (Reference 5-2). The values from this library and the calculation of a W/Ci conversion factor for multiple radionuclides are presented in Section 5.5.3. Using the W/Ci conversion factor presented in Section 5.5.3, the equivalent activity for 1500 W is 97,250 Ci of cobalt-60.

Table 5.2-2. Isotope Rod Source Term (97,250 Ci Cobalt-60)

Energy (MeV)	Relative Intensity	Source Strength (γ/sec)
0.347	7.500E-05	2.699E+11
0.826	7.600E-05	2.735E+11
1.173	9.985E-01	3.593E+15
1.333	9.998E-01	3.598E+15
2.159	1.200E-05	4.318E+10
2.506	2.000E-08	7.197E+07
Total	1.998E+00	7.191E+15

5.2.2. Neutron Source

5.2.2.1. Irradiated Hardware and Byproducts / Cobalt-60 Isotope Rods

There is no applicable neutron source term for the irradiated hardware and byproduct or cobalt-60 isotope rod contents.

5.3 Shielding Model

5.3.1. Configuration of Source and Shielding

The following subsections describe the MCNP6 shielding model geometry and source configuration for the dose rate calculations of each of the described content types of the Model 2000 cask.

5.3.1.1. MCNP6 Source Distribution

An individual source geometry is used in the MCNP6 shielding model for each of the Model 2000 cask contents. The source geometry for each content type is based on the respective content specifications and the source term calculation.

Irradiated Hardware and Byproducts

Due to the uncertainty in the form and activity distribution of irradiated hardware or byproduct contents, both the NCT and HAC MCNP6 shielding model conservatively assumes that all the activity is concentrated into a single point. Therefore, the use of the HPI material basket is not required for irradiated hardware and byproduct shipments. However, use of the HPI material basket for shipments of irradiated hardware and byproducts is optionally allowable because the material basket 12-inch line source is bounded by the shielding results obtained from the point source model, as long as all dose rates and thermal limits are satisfied. The source locations of the point sources in the MCNP6 shielding models for the irradiated hardware and byproduct dose rate calculations are shown in Figure 5.3-1.

Cobalt-60 Isotope Rods

For the cobalt-60 isotope rod content, the NCT source geometry is a single 12-inch line source, across which the photon source activity is distributed uniformly. There is variation in the distribution of cobalt-60 activity in the HPI cavity with a shipment of cobalt-60 isotope [[ ]] and loading of the rods into the HPI. Section 5.5.2 provides a discussion of the distribution of activity in the HPI cavity for the cobalt-60 isotope rod contents, and the basis for a 12-inch line source for NCT dose rate calculations.

For the HAC MCNP6 shielding model source geometry, the structural components in the cask cavity were conservatively assumed to fail. Therefore, all source activity was concentrated into a single point. The source locations for the NCT model 12-inch line source and the HAC model point source are shown in Figure 5.3-1. The MCNP6 12-inch line source modeling limitation imposed during the NCT evaluations requires that the HPI material basket be present for cobalt-60 isotope rod shipments.

5.3.1.2. MCNP6 Source Locations

The sources for the MCNP6 dose rate calculations are modeled in the HPI cavity in the position that results in the highest dose rate for the respective regulatory dose rate location. This limiting source position changes based on the geometry of the source and the direction of interest. Figure 5.3-1 provides two depictions of the Model 2000 cask with the HPI. This figure shows the positions for any point or line sources in the HPI cavity for all dose rate calculations.

The source positions for side dose rate locations are located at the bottom corner of the HPI cavity, at the interface of the HPI body and the HPI bottom [[ ]]. This is the most restrictive location for side dose rates because in this area the [[ ]], due to the step at this interface. For the HAC side 1-meter dose rate, the calculated dose rate is higher with a point source in the bottom corner than in the top corner of the HPI cavity, despite the slump in the lead column.

The line source positions for top and bottom dose rate locations are centered in the HPI cavity so that particles emitted at any location along the line source can travel at any angle in the direction of interest, unimpeded before entering the respective [[ ]]. For a line source pushed to the side against the HPI body, there is a reduction in the calculated dose rates for the top and bottom.

[[

]]

Figure 5.3-1. MCNP6 Point / Line Source Locations

5.3.1.3. MCNP6 NCT Shielding Model Geometry

The MCNP6 NCT model geometry used for the dose rate calculations in this shielding analysis is a detailed three-dimensional model of the HPI, the Model 2000 cask, and the overpack. Table 5.3-1 provides the relevant dimensions of the MCNP6 shielding model including the modeled thicknesses of each material. This table along with Table 5.1-1 allow for a quick review of the most significant dimensions of the shielding model geometry. All HPI shield dimensions are at the minimum (except cavity radius which is nominal), per the respective licensing drawings, with the fabrication tolerances subtracted from the nominal values. The model dimensions for the Model 2000 cask and overpack use predominantly nominal dimensions with some areas of reduced thickness. For example, for the [[ ]], the cask bottom is considered to be flat at the minimum thickness. The majority of the material thicknesses prescribed by the Model 2000 cask and overpack licensing drawings have tolerances based on American Society for Testing and Materials (ASTM) specifications, as the component dimensions are based on ASTM SS stock plate. Per ASTM A480 (Reference 5-3), for plates up to 10 inches in thickness, the tolerance under the specified thickness is 0.01 inches. These plate thicknesses are modeled at the specified nominal plate value.

Table 5.3-1. Relevant MCNP6 Shielding Model Dimensions

Model 2000 Component	Part	Parameter	Dimension (cm)	Dimension (in)
Cask	Cask Lid	Lid Flange (t_{SS1})	3.810	1.500
		Lead (t_{Pb})	13.64	5.370
		Inner Plate (t_{SS2})	4.445	1.750
	Cask Side	Cavity Radius (r_{cavity})	33.66	13.25
		Cavity Shell	2.540	1.000
		Lead (t_{Pb})	10.16	4.000
		Cask Shell (t_{SS2})	2.540	1.000
		Lead (h_{pb}[c])	141.9	55.87
	Cask Bottom	Cask Bottom (t_{SS})	14.94[a]	5.880[a]
		Cavity Height (h_{cavity})	137.5	54.13
HPI	HPI Top Plug	Inner Shell (t_{SS1})	[[	
		DU (t_{DU})		
		Outer Shell (t_{SS2})		
	HPI Body Side	Cavity Radius (r_{cavity})		
		Inner Shell (t_{SS1})		
		DU (t_{DU})		
		Outer Shell (t_{SS2})		
	HPI [[ ]]	Inner Shell (t_{SS1})		
		DU (t_{DU})		
		Outer Shell (t_{SS2})		]]
Overpack	Top	Top Plate (t_{SS1})	1.270	0.500
		End Plate (t_{SS2})	1.270	0.500
	Side	Inner Shell (t_{SS1})	1.270	0.500
		Outer Shell (t_{SS2})	1.270	0.500
	Bottom	Support Plate (t_{SS1})	1.270	0.500
		Bottom Plate (t_{SS2})	1.270	0.500
		End Plate (t_{SS3})	1.270	0.500

Notes: [a] Cask Bottom modeled flat, with thickness equal to the 6.13" height [[ ]].
[b] Minimum DU thicknesses considered with tolerance gaps explicitly modeled.
[c] Lead column height.
[d] Nominal value

The NCT shielding model for photon dose rate calculation is shown in Figure 5.3-2. The materials for the HPI, cask, and overpack are defined as prescribed in Section 5.3.2.

[[

]]

Figure 5.3-2. NCT MCNP6 Shielding Model

The NCT model conservatively neglects the additional shielding provided by the HPI material basket and rod holders for the cobalt-60 isotope rod contents. Due to the use of 12-inch vertical line sources for the cobalt-60 isotope rod contents, the HPI material basket is required for the cobalt-60 isotope rod contents in the upright position. The material basket is not required for shipments of irradiated hardware and byproducts because a point source was used for the shielding analysis.

5.3.1.4. MCNP6 HAC Shielding Model Geometry

For HAC, the MCNP6 shielding model only includes the HPI and the Model 2000 cask, with dimensions as prescribed in Table 5.3-1. This model conservatively assumes the removal of the overpack. The HAC model also includes the slump in the lead column of the Model 2000 cask body. In Section 2.12.2, the maximum deformation in the lead column is calculated to be 3.56 mm.

This value is rounded up to 4 mm for this analysis. It is determined in Chapter 2 that the overpack provides adequate protection from HAC to the cask body. More specifically, in Section 2.12.1 it is stated that when the cask is dropped 30 feet followed by a drop of 40 inches onto a rigid pin 6 inches in diameter, no gross deformations of the cask are predicted. The MCNP6 HAC shielding model is shown in Figure 5.3-3.

[[

]]

Figure 5.3-3. HAC MCNP6 Shielding Model

5.3.1.5. MCNP6 Tallies

To calculate the particle flux at the regulatory dose rate locations of interest, multiple arrangements of cell tallies are modeled at each location. The void cells that are added to the model for particle tallying allow for dose rates to be calculated at the multiple locations of interest, without having

an effect on the calculated flux. All of the tally cells are modeled as small 1 cm thick volumes, to ensure that the calculated flux is not averaged over too large of a region.

Figures 5.3-4 and 5.3-5 provide depictions of the tally cells used in the MCNP6 shielding analysis models, with the tally cells highlighted in yellow. All tally cells are 1 cm thick and relatively small in size, in order to ensure that the flux calculation is not averaged over a large area, and dose rates are representative of the sampled region.

[[

]]

Figure 5.3-4. NCT MCNP6 Tallies with 10% Margin to the Regulatory Limit

[[

]]

Figure 5.3-5. HAC MCNP6 Tallies with 10% Margin to the Regulatory Limit

5.3.2. Material Properties

The material compositions used for photon dose rate calculations are listed in Tables 5.3-2 through 5.3-5. There is negligible difference between the two types of SS in terms of shielding effectiveness. However, both types are included for accuracy to the actual materials of construction. The densities and material compositions for both stainless steel types are from Pacific Northwest National Lab (PNNL) report PNNL-15870 Revision 1 (Reference 5-4). The densities of the lead and DU materials are based on the minimum specified densities for these materials in the respective component licensing drawings in Section 1.3.1.

Table 5.3-2. Type 304 Stainless Steel Material Composition

	Element	Photon ZA	Mass Fraction
Elemental Composition	C	6000	4.00E-04
	Si	14000	5.00E-03
	P	15000	2.30E-04
	S	16000	1.50E-04
	Cr	24000	1.90E-01
	Mn	25000	1.00E-02
	Fe	26000	7.02E-01
	Ni	28000	9.25E-02
Density (g/cm^3)	8.0		

Table 5.3-3. [[ ]] Material Composition

	Element	Photon ZA	Mass Fraction
Elemental Composition	C	6000	4.10E-04
	Si	14000	5.07E-03
	P	15000	2.30E-04
	S	16000	1.50E-04
	Cr	24000	1.70E-01
	Mn	25000	1.01E-02
	Fe	26000	6.69E-01
	Ni	28000	1.20E-01
	Mo	42000	2.50E-02
Density (g/cm^3)	8.0		

Table 5.3-4. Lead Material Composition

Elemental Composition	**Element**	**Photon ZA**	**Mass Fraction**
	Pb	82000	1.00E+00
Density (g/cm^3)	11.34		

Table 5.3-5. Depleted Uranium Material Composition

Elemental Composition	**Element**	**Photon ZA**	**Mass Fraction**
	U	92000	1.00E+00
Density (g/cm^3)	[[ ]]		

5.4 Shielding Evaluation

5.4.1. Methods

5.4.1.1. Computer Codes

The shielding calculations for this analysis were completed using MCNP6 Version 1.0 (Reference 5-5). MCNP6 is a general-purpose, continuous-energy, generalized-geometry, time-dependent, coupled neutron/photon/electron Monte Carlo transport code. MCNP6 was used in the photon only transport mode to calculate external dose rates for the Model 2000 cask for each of the content types considered. Photon dose rate calculations used the MCNP6 photoatomic data library MCPLIB84, which compiles data from the ENDF/B-VI.8 data library (Reference 5-6).

5.4.1.2. MCNP6 Variance Reduction

Due to the thick layers of photon shielding provided by the Model 2000 cask and the HPI, multiple variance reduction techniques are used for the MCNP6 photon dose rate calculations. MCNP6 variance reduction parameters for weight windows, exponential transform, and source biasing were all used as necessary to aid in the statistical convergence of the MCNP6 photon dose rate calculations.

5.4.1.3. Irradiated Hardware, Byproduct, and Cobalt-60 Isotope Rod Dose Rate Calculation

To calculate a dose rate response $\mathrm{R(r,X)}$ for an individual radionuclide X, the MCNP6 calculated photon flux $\phi(\mathrm{r,X})$ is multiplied by the dose rate conversion factor $\mathcal{R}$ as well as a per curie multiplier and the total number of gammas per decay of the respective radionuclide $\mathrm{I(X)}$.

$$\mathrm{R(r,X)}\left[\frac{\frac{\mathrm{mrem}}{\mathrm{hr}}}{\mathrm{Ci}}\right] = \phi(\mathrm{r,X})\left[\frac{\frac{\gamma}{\mathrm{cm}^2}}{\mathrm{emitted}\,\gamma}\right]\cdot 3.7\mathrm{e}10\left[\frac{\frac{\mathrm{decays}}{\mathrm{sec}}}{\mathrm{Ci}}\right]\cdot \mathrm{I(X)}\left[\frac{\mathrm{emitted}\,\gamma}{\mathrm{decay}}\right]\cdot \mathcal{R}\left[\frac{\frac{\mathrm{mrem}}{\mathrm{hr}}}{\frac{\gamma}{\mathrm{cm}^2\cdot\mathrm{sec}}}\right] \tag{5-1}$$

$$\sigma_{\mathrm{R}}(\mathrm{r,X}) = \mathrm{R(r,X)}\cdot \mathrm{fsd(r,X)} \tag{5-2}$$

To account for statistical uncertainty, the two standard deviations are added to the calculated MCNP6 dose rate per curie:

$$\mathrm{R}_{\sigma}(\mathrm{r,X})\left[\frac{\mathrm{mrem}}{\mathrm{hr}}\right] = \left(\mathrm{R(r,X)} + 2\cdot\sigma_{\mathrm{R}}(\mathrm{r,X})\right)\left[\frac{\frac{\mathrm{mrem}}{\mathrm{hr}}}{\mathrm{Ci}}\right] \tag{5-3}$$

The total dose rate $\mathrm{DR(r)}$ is calculated by summing the dose rate from the activity of each radionuclide:

$$\mathrm{DR(r)}\left[\frac{\mathrm{mrem}}{\mathrm{hr}}\right] = \sum_{\mathrm{X}} \mathrm{R}_{\sigma}(\mathrm{r,X})\left[\frac{\mathrm{mrem}}{\mathrm{hr}}\right]\cdot \mathrm{A(X)[Ci]} \tag{5-4}$$

where

R	MCNP6 dose rate per curie	σ	Standard deviation
r	Regulatory dose rate location	fsd	MCNP6 fractional standard deviation
X	Radionuclide X	R_σ	Dose rate per curie with 2σ uncertainty
ϕ	MCNP6 calculated flux	DR	Total dose rate
I	gammas/decay	A	Activity
$\mathcal{R}$	Flux-to-dose-rate conversion factor		

5.4.2. Input and Output Data

5.4.2.1. Input Data

Input data will be submitted separately.

5.4.2.2. Output Data

Output data will be submitted separately. The tally fluctuation chart and probability density function plot were studied for each MCNP6 tally to ensure proper tally bin convergence. This along with a check of the reported fsd for each tally bin and the additional statistical information reported for MCNP6 tallies ensured the reliability of all MCNP6 calculated dose rate results.

5.4.3. Flux-to-Dose-Rate Conversion

Consistent with NUREG-1609 Section 5.5.4.3 (Reference 5-7), the ANSI/ANS-6.1.1 1977 flux-to-dose-rate conversion factors (Reference 5-8) are used. The gamma conversion factors used in the MCNP6 input files are tabulated in Table 5.4-1.

Table 5.4-1. Gamma Flux-to-Dose-Rate Conversion Factors (ANSI/ANS-6.1.1 1977)

Gamma Energy (MeV)	Conversion Factor (mrem/hr)/(gammas/cm^2-s)
1.00E-02	3.96E-03
3.00E-02	5.82E-04
5.00E-02	2.90E-04
7.00E-02	2.58E-04
1.00E-01	2.83E-04
1.50E-01	3.79E-04
2.00E-01	5.01E-04
2.50E-01	6.31E-04
3.00E-01	7.59E-04
3.50E-01	8.78E-04
4.00E-01	9.85E-04
4.50E-01	1.08E-03
5.00E-01	1.17E-03
5.50E-01	1.27E-03
6.00E-01	1.36E-03
6.50E-01	1.44E-03
7.00E-01	1.52E-03
8.00E-01	1.68E-03
1.00E+00	1.98E-03
1.40E+00	2.51E-03
1.80E+00	2.99E-03
2.20E+00	3.42E-03
2.60E+00	3.82E-03
2.80E+00	4.01E-03
3.25E+00	4.41E-03
3.75E+00	4.83E-03
4.25E+00	5.23E-03
4.75E+00	5.60E-03
5.00E+00	5.80E-03
5.25E+00	6.01E-03
5.75E+00	6.37E-03
6.25E+00	6.74E-03
6.75E+00	7.11E-03
7.50E+00	7.66E-03
9.00E+00	8.77E-03
1.10E+01	1.03E-02
1.30E+01	1.18E-02
1.50E+01	1.33E-02

5.4.4. External Radiation Levels

The maximum external radiation levels are determined individually for each of the two content types. The limiting dose rate location for all content types is the NCT side package surface. That is, for each of the two contents, the maximum allowable quantity of material is limited by the NCT side surface dose rate. The external radiation levels resulting from each of the two content types are summarized below.

5.4.4.1. Irradiated Hardware and Byproducts

For the irradiated hardware and byproduct contents, the resulting external dose rates are calculated by calculating the dose rate per curie in MCNP6 for each radionuclide individually, using the source spectra listed in Tables 5.5-3 through 5.5-20. The 2σ statistical uncertainty is added on to the calculated dose rate per curie as shown in Equation 5-3. The resulting values from these calculations for NCT and HAC are presented in Tables 5.4-2 and 5.4-3.

Table 5.4-2. Irradiated Hardware and Byproduct Dose Rate per Curie Results - NCT

Radionuclide	Dose Rate (mrem/hr/Ci)				
	Top Surface	Side Surface	Bottom Surface	2-meter	Cab
Co-58	1.356E-05	2.444E-04	2.169E-05	3.375E-06	5.945E-07
Co-60	4.183E-04	9.437E-03	6.237E-04	1.211E-04	2.078E-05
Cr-51	3.981E-15	1.648E-20	5.556E-20	2.125E-22	3.509E-23
Cs-134	1.584E-05	3.433E-04	2.402E-05	4.504E-06	7.780E-07
Cs-137	9.341E-10	3.713E-08	2.822E-09	4.381E-10	7.404E-11
Fe-59	1.239E-04	2.894E-03	1.853E-04	3.649E-05	6.292E-06
Hf-175	1.642E-13	1.917E-15	3.513E-16	1.167E-17	1.891E-18
Hf-181	1.968E-11	2.116E-11	3.427E-12	2.749E-13	4.721E-14
Mn-54	2.294E-07	9.856E-06	4.279E-07	1.116E-07	1.904E-08
Nb-92m	4.559E-05	8.088E-04	7.216E-05	1.128E-05	1.974E-06
Nb-94	5.561E-07	2.214E-05	9.703E-07	2.519E-07	4.293E-08
Sb-124	1.973E-03	3.462E-02	3.176E-03	4.809E-04	8.336E-05
Sb-125	1.440E-10	3.334E-09	3.261E-10	4.139E-11	7.082E-12
Sb-126	6.649E-06	1.526E-04	1.009E-05	1.955E-06	3.399E-07
Sc-46	4.123E-05	1.111E-03	6.179E-05	1.353E-05	2.327E-06
Ta-182	1.343E-04	3.273E-03	1.997E-04	4.080E-05	6.989E-06
Zn-65	2.023E-05	5.398E-04	3.014E-05	6.581E-06	1.131E-06
Zr-95	5.015E-08	2.505E-06	1.181E-07	2.816E-08	4.790E-09
Nb-95	5.015E-08	2.505E-06	1.181E-07	2.816E-08	4.790E-09

Table 5.4-3. Irradiated Hardware and Byproduct Dose Rate per Curie Results - HAC

Radionuclide	Dose Rate (mrem/hr/Ci)		
	Top 1-meter	Side 1-meter	Bottom 1-meter
Co-58	1.795E-05	4.460E-05	1.155E-05
Co-60	6.008E-04	1.743E-03	3.552E-04
Cr-51	1.268E-13	5.043E-20	9.455E-19
Cs-134	2.252E-05	6.356E-05	1.340E-05
Cs-137	3.023E-09	9.383E-09	3.140E-09
Fe-59	1.806E-04	5.370E-04	1.071E-04
Hf-175	1.676E-12	4.820E-16	7.744E-16
Hf-181	1.493E-10	6.868E-12	5.073E-12
Mn-54	4.057E-07	2.046E-06	3.326E-07
Nb-92m	5.907E-05	1.450E-04	3.671E-05
Nb-94	9.502E-07	4.548E-06	7.240E-07
Sb-124	2.568E-03	6.144E-03	1.618E-03
Sb-125	6.258E-10	9.213E-10	4.006E-10
Sb-126	9.516E-06	2.875E-05	5.919E-06
Sc-46	6.274E-05	2.115E-04	3.852E-05
Ta-182	1.976E-04	6.138E-04	1.176E-04
Zn-65	3.066E-05	1.026E-04	1.860E-05
Zr-95	9.528E-08	5.459E-07	1.039E-07
Nb-95	9.528E-08	5.459E-07	1.039E-07

The resulting dose rate at any regulatory dose rate location can be calculated, for a cask loading of irradiated hardware or byproducts with a defined radionuclide inventory, by multiplying the activity of each radionuclide by the respective dose rate per curie for the given location and summing the dose rate contributions from each radionuclide, as shown in Equation 5-4. Repeating this dose rate calculation for each regulatory dose rate location determines the total external dose rates for the Model 2000 Transport Package. This process is completed and recorded in the Irradiated Hardware and Byproduct Loading Table. The use of the Irradiated Hardware and Byproduct Loading Table is described in Section 5.5.4.

The maximum activity of each radionuclide, individually, is limited by the minimum of either the activity equivalent to the 1500W thermal limit of the cask or the activity resulting in an NCT side surface dose rate equal to 90% of the regulatory limit (180 mrem/hr). The maximum activity limit for each radionuclide individually is presented in Table 5.4-4. These limits are based on the dose rate per curie limits in Tables 5.4-2 and 5.4-3, and the decay heat W/Ci values in Table 5.5-24. The maximum possible dose rates for each regulatory location are summarized in Table 5.4-5. These values are calculated using the activity limits in Table 5-4.4 and the dose rate per curie values in Tables 5.4-2 and 5.4-3, for each radionuclide.

Table 5.4-4. Maximum Activities for Irradiated Hardware and Byproduct Individual Radionuclides

Radionuclide	Activity Limit (Ci)	Basis[a,b]
Co-58	2.508E+05	Thermal
Co-60	1.907E+04	Dose Rate
Cr-51	6.899E+06	Thermal
Cs-134	1.472E+05	Thermal
Cs-137	3.009E+05	Thermal
Fe-59	6.219E+04	Dose Rate
Hf-175	6.369E+05	Thermal
Hf-181	3.465E+05	Thermal
Mn-54	3.011E+05	Thermal
Nb-92m	2.225E+05	Dose Rate
Nb-94	1.438E+05	Thermal
Sb-124	5.199E+03	Dose Rate
Sb-125	4.742E+05	Thermal
Sb-126	8.108E+04	Thermal
Sc-46	1.192E+05	Thermal
Ta-182	5.499E+04	Dose Rate
Zn-65	3.334E+05	Dose Rate
Zr-95	1.525E+05	Thermal
Nb-95	3.127E+05	Thermal

Notes: [a] Thermal – 1500 W thermal limit.

[b] Dose Rate – 180 mrem/hr NCT side surface dose rate limit.

Table 5.4-5. Maximum External Dose Rates - Irradiated Hardware and Byproducts

Location	NCT Top Surface	NCT Side Surface	NCT Bottom Surface	NCT 2-meter	NCT Cab	HAC Top 1-meter	HAC Side 1-meter	HAC Bottom 1-meter
Dose Rate (mrem/hr)	10.26	179.99	16.51	2.51	0.44	13.35	34.21	8.41
Regulatory Limit (mrem/hr)	200	200	200	10	2	1000	1000	1000

5.4.4.2. Cobalt-60 Isotope Rods

For the cobalt-60 isotope rod contents, the resulting external dose rates are calculated using the dose rate per curie in MCNP6 for cobalt-60, with the cobalt-60 source energy spectrum listed in Table 5.2-2. The 2σ statistical uncertainty is added on to the calculated dose rate per curie as shown in Equation 5-3. The resulting values from these calculations for NCT and HAC are presented in Tables 5.4-6 and 5.4-7.

Table 5.4-6. Cobalt-60 Isotope Rod Dose Rate per Curie Results – NCT

Radionuclide	Dose Rate (mrem/hr/Ci)				
	Top Surface	Side Surface	Bottom Surface	2-meter	Cab
Co-60	1.850E-04	8.821E-04	3.940E-04	1.664E-05	2.921E-06

Table 5.4-7. Cobalt-60 Isotope Rod Dose Rate per Curie Results - HAC

Radionuclide	Dose Rate (mrem/hr/Ci)		
	Top 1-meter	Side 1-meter	Bottom 1-meter
Co-60	6.008E-04	1.743E-03	3.552E-04

The resulting dose rate at any regulatory dose rate location can be calculated, for a cask loading of cobalt-60 isotope rod [[ ]], by filling out the cobalt-60 isotope rod loading table.

To determine the maximum possible dose rate at each regulatory location, the dose rate per curie values in Tables 5.4-6 and 5.4-7 are multiplied by the cobalt-60 activity equivalent to the 1500 W thermal limit (97,250 Ci). The results of this calculation are presented in Table 5.4-8.

Table 5.4-8. Maximum External Dose Rates – Cobalt-60 Isotope Rods

Location	NCT Top Surface	NCT Side Surface	NCT Bottom Surface	NCT 2-meter	NCT Cab	HAC Top 1-meter	HAC Side 1-meter	HAC Bottom 1-meter
Dose Rate (mrem/hr)	17.99	85.78	38.32	1.62	0.28	58.43	169.51	34.54
Regulatory Limit (mrem/hr)	200	200	200	10	2	1000	1000	1000

5.4.4.3. Combined Contents

There is the possibility of a shipment that includes combined contents such as a combined content of cobalt-60 isotope rods with irradiated hardware. For this case the Cobalt-60 Isotope Rod Loading Table (in Chapter 7) is confirmed for the isotope rod contents and any radionuclide activity in the rod cladding or additional irradiated hardware shipped with the isotope rods is confirmed in the Irradiated Hardware and Byproduct Loading Table (in Chapter 7). The resulting thermal and dose rate contributions from radionuclides in the hardware and cladding are summed with the thermal and dose rate contributions from the cobalt-60 isotope rods in the Combined Contents Loading Table (in Chapter 7).

5.5 Appendices

5.5.1. ORIGEN-S Irradiated Hardware and Byproduct Source Term Calculation

The radionuclides that are significant to the irradiated hardware and byproduct dose rate calculations, were determined with multiple ORIGEN-S (Reference 5-2) irradiation calculations. For the irradiation case there are two significant inputs; the composition of the material that is being irradiated and the neutron flux that the material is exposed to. For determining the source term, the quantity of material is irrelevant for the determination of which radionuclides are generated. A generic thermal neutron flux of 1E+14 $n/s \cdot cm^2$ is assumed for the irradiation cases. For the material compositions of the irradiated hardware/byproducts, there are six materials considered. These materials along with their compositions are listed in Table 5.5-1. The materials selected include multiple SS, a nickel alloy, a zirconium alloy, as well as hafnium and boron carbide. The materials listed in parenthesis in Table 5.5-1, are included as they are similar in

composition to the material listed. The materials listed contain elements expected in any irradiated hardware or byproduct contents. Thus, the resulting total radionuclide inventory from the ORIGEN-S calculations is comprehensive. The basis for each ORIGEN-S input is 1 kg of the respective material being irradiated. Because elements for each material are entered into the ORIGEN-S input in grams, Table 5.5-1 lists the gram amount of each element per kilogram of the material. While an increase or decrease in the flux or a variation in the material composition entered for the irradiation case would result in a change to the relative activity of the radionuclides generated, the purpose of the ORIGEN-S source term calculations is not to determine the inventory of each radionuclide, but simply to identify which radionuclides may be present in irradiated hardware/byproduct contents. The quantity of each radionuclide that is significant to dose rate calculations must be entered into the Irradiated Hardware and Byproduct Loading Table to calculate the maximum external dose rates. The quantity of each radionuclide that is significant to the thermal calculations must also be entered into the Irradiated Hardware and Byproduct Loading Table to calculate the total thermal content.

The radionuclides calculated from the ORIGEN-S irradiation cases are listed in Table 5.5-2. This table also includes some radionuclides that may be included on the hardware or byproduct contents in the form of surface contamination, as these contents may be exposed to a reactor environment. Radionuclides in cells that are highlighted are considered significant to dose rate calculations. The selection of significant radionuclides is based on the energy of the gamma emissions and half-lives. A radionuclide is considered insignificant to dose rate calculations if it has no gamma emissions greater than 0.3 MeV, or if it has a half-life less than 3 days. All shipments of irradiated hardware and byproducts are required to include a decay time of 30 days prior to shipment. Thus, for any radionuclide with a half-life less than 3 days, there are more than 10 half-lives of decay time prior to shipment.

Tables 5.5-3 through 5.5-20 provide the energy spectra for all radionuclides considered significant to the irradiated hardware and byproduct dose rate calculations. These radionuclide energy spectra are from the ORIGEN-S Data Library origen.rev04.mpdkxgam.data (Reference 5-2). Any gamma lines under 0.1 MeV are neglected from the listed radionuclide spectra. Though Cs-137 does not emit any significant gammas, the gamma emission of its short-lived daughter Ba-137m is used as its representative spectrum. Also, because Nb-95 is the daughter of Zr-95, the energy spectra of the two radionuclides are combined and only one set of dose rate calculations is performed for both radionuclides. Thus, the dose rates calculated for this combined spectrum account for one decay of each radionuclide. This calculates an appropriate dose rate for Zr-95, as it accounts for the decay of its daughter Nb-95. However, this spectrum results in a conservative dose rate for Nb-95, as the calculated dose rate includes the contribution from its parent radionuclide as well. The resulting dose rates from this combined spectrum are used to calculate external dose rates for activities of both Zr-95 and Nb-95, individually.

Table 5.5-1. Irradiated Hardware and Byproduct Irradiation Materials

Material	Symbol	Element ID No.	wt %	g/kg material	# nuclides
SS304 (SS302, SS304L)	C	60000	0.0800	0.8000	10
	N	70000	0.1000	1.0000	
	Si	140000	0.7500	7.5000	
	P	150000	0.0450	0.4500	
	S	160000	0.0300	0.3000	
	Cr	240000	19.000	190.00	
	Mn	250000	2.0000	20.000	
	Fe	260000	67.495	674.95	
	Co	270000	0.0800	0.8000	
	Ni	280000	10.420	104.20	
SS CF3M (SS316)	C	60000	0.0300	0.300	8
	Si	140000	2.0000	20.000	
	Cr	240000	19.000	190.00	
	Mn	250000	1.5000	15.000	
	Fe	260000	62.970	629.70	
	Co	270000	0.0800	0.8000	
	Ni	280000	11.920	119.20	
	Mo	420000	2.5000	25.000	
SS348H	C	60000	0.0700	0.7000	11
	Si	140000	1.0000	10.000	
	P	150000	0.0450	0.4500	
	S	160000	0.0300	0.3000	
	Cr	240000	18.000	180.00	
	Mn	250000	2.0000	20.000	
	Fe	260000	64.555	645.55	
	Co	270000	0.2000	2.0000	
	Ni	280000	13.000	130.00	
	Nb	410000	1.0000	10.000	
	Ta	730000	0.1000	1.0000	
Inconel-718 (Inconel X-750)	B	50000	0.0060	0.0600	16
	C	60000	0.0800	0.8000	
	Al	130000	0.5000	5.0000	
	Si	140000	0.3500	3.5000	
	P	150000	0.0150	0.1500	
	S	160000	0.0150	0.1500	
	Ti	220000	0.9000	9.0000	
	Cr	240000	19.000	190.00	
	Mn	250000	0.3500	3.5000	
	Fe	260000	14.934	149.34	
	Co	270000	1.0000	10.000	
	Ni	280000	54.000	540.00	
	Cu	290000	0.3000	3.0000	
	Nb	410000	2.7500	27.500	
	Mo	420000	3.0500	30.500	
	Ta	730000	2.7500	27.500	

Material	Symbol	Element ID No.	wt %	g/kg material	# nuclides
Zircaloy-2 (Zircaloy-4)	O	80000	0.1200	1.2000	6
	Cr	240000	0.1000	1.0000	
	Fe	260000	0.2000	2.0000	
	Ni	280000	0.0800	0.8000	
	Zr	400000	97.800	978.00	
	Sn	500000	1.7000	17.000	
Boron Carbide (B_4C)	B	50000	78.261	782.61	2
	C	60000	21.739	217.39	
Hafnium	Hf	720000	100.00	1000.0	1

Table 5.5-2. Irradiated Hardware and Byproduct Radionuclides

H-3	Co-58m	Sr-91	Tc-99[a]	**Sb-125**	Lu-177m
C-14	**Co-60**	Y-89m	Tc-99m	**Sb-126**	Yb-175
Na-24	Co-60m	Y-90	Tc-101	Te-125m	Yb-177
Si-31	Co-61	Y-90m	Ru-106a	I-129[a]	Ta-180
P-32	Ni-57	Y-91	In-113m	**Cs-134[a]**	**Ta-182**
P-33	Ni-59	Y-91m	In-114	**Cs-137 (Ba-137m) [a]**	Ta-183
S-35	Ni-63	Y-92	In-114m	La-140[a]	W-181
Ca-45	Ni-65	Nb-91m	In-115m	Ba-140[a]	W-183m
Sc-46	Fe-55	**Nb-92m**	Sn-113	Ce-144[a]	W-185
Sc-47	**Fe-59**	**Nb-94**	Sn-113m	Hf-173	Re-186
Sc-48	Cu-64	**Nb-95**	Sn-117m	**Hf-175**	Np-237[a]
V-49	Cu-66[a]	Nb-96	Sn-119m	Hf-177m	Pu-238[a]
V-52[a]	**Zn-65**	Nb-95m	Sn-121	Hf-180m	Pu-239[a]
Cr-51	Zr-89	Nb-97	Sn-121m	**Hf-181**	Pu-240[a]
Cr-55[a]	**Zr-95**	Nb-97m	Sn-123	Lu-173	Pu-241[a]
Mn-54	Zr-97	Mo-93	Sn-123m	Lu-174	Am-241[a]
Mn-56	Sr-87m	Mo-93m	Sn-125	Lu-174m	Cm-242[a]
Co-57	Sr-89	Mo-99	Sb-122	Lu-176m	Cm-243[a]
Co-58	Sr-90[a]	Mo-101	**Sb-124**	Lu-177	Cm-244[a]

Notes: [a] Radionuclides not calculated in ORIGEN-S calculations, but included from previous shipments. Only present in small quantities in surface contamination.

Table 5.5-3. Sc-46 Gamma Emission Energy Spectrum

Total Photons/Disintegration	
2.000E+00	
Energy	**Intensity**
0.889	1.00E+00
1.121	1.00E+00
2.010	1.30E-07

Table 5.5-4. Cr-51 Gamma Emission Energy Spectrum

Total Photons/Disintegration	
9.910E-02	
Energy	**Intensity**
0.320	9.91E-02

Table 5.5-5. Mn-54 Gamma Emission Energy Spectrum

Total Photons/Disintegration	
9.998E-01	
Energy	**Intensity**
0.511	5.600E-09
0.835	9.998E-01

Table 5.5-6. Co-58 Gamma Emission Energy Spectrum

Total Photons/Disintegration	
1.305E+00	
Energy	**Intensity**
0.511	2.98E-01
0.811	9.95E-01
0.864	6.86E-03
1.675	5.17E-03

Table 5.5-7. Fe-59 Gamma Emission Energy Spectrum

Total Photons/Disintegration	
1.041E+00	
Energy	**Intensity**
0.143	1.02E-02
0.189	9.00E-06
0.192	3.08E-02
0.335	2.70E-03
0.382	1.80E-04
1.099	5.65E-01
1.292	4.32E-01
1.482	5.90E-04

Table 5.5-8. Co-60 Gamma Emission Energy Spectrum

Total Photons/Disintegration	
1.998E+00	
Energy	**Intensity**
0.347	7.5000E-05
0.826	7.6000E-05
1.173	9.9850E-01
1.333	9.9983E-01
2.159	1.2000E-05
2.506	2.0000E-08

Table 5.5-9. Zn-65 Gamma Emission Energy Spectrum

Total Photons/Disintegration	
5.289E-01	
Energy	**Intensity**
0.511	2.84E-02
0.345	2.53E-05
0.771	2.68E-05
1.116	5.00E-01

Table 5.5-10. Nb-92m Gamma Emission Energy Spectrum

Total Photons/Disintegration	
1.02E+00	
Energy	**Intensity**
0.511	1.28E-03
0.449	1.63E-05
0.561	2.23E-05
0.913	1.78E-02
0.934	9.91E-01
1.132	5.15E-05
1.848	8.52E-03

Table 5.5-11. Nb-94 Gamma Emission Energy Spectrum

Total Photons/Disintegration	
1.997E+00	
Energy	**Intensity**
0.703	9.98E-01
0.871	9.99E-01

Table 5.5-12. Zr/Nb-95 Gamma Emission Energy Spectrum

Total Photons/Disintegration	
1.99E+00	
Energy	**Intensity**
0.204	2.80E-04
0.562	1.50E-04
0.724	4.43E-01
0.757	5.44E-01
0.766	9.98E-01

Table 5.5-13. Sb-124 Gamma Emission Energy Spectrum

Total Photons/Disintegration					
1.878E+00					
Energy	**Intensity**	**Energy**	**Intensity**	**Energy**	**Intensity**
0.148	3.91E-05	0.766	1.21E-04	1.566	1.37E-04
0.190	6.36E-05	0.775	9.39E-05	1.580	3.81E-03
0.210	5.48E-05	0.791	7.39E-03	1.622	4.09E-04
0.254	1.61E-04	0.817	7.29E-04	1.691	4.76E-01
0.292	8.70E-05	0.857	2.38E-04	1.721	9.51E-04
0.336	7.43E-04	0.899	1.72E-04	1.852	6.45E-05
0.371	3.81E-04	0.968	1.88E-02	1.919	5.45E-04
0.400	1.39E-03	0.977	8.32E-04	2.016	9.49E-04
0.444	1.89E-03	1.045	1.83E-02	2.040	6.42E-04
0.469	4.99E-04	1.054	4.89E-05	2.080	2.05E-04
0.481	2.37E-04	1.087	3.78E-04	2.091	5.49E-02
0.526	1.38E-03	1.264	4.13E-04	2.099	4.57E-04
0.530	4.21E-04	1.301	3.43E-04	2.108	4.33E-04
0.572	1.90E-04	1.326	1.58E-02	2.172	2.05E-05
0.603	9.78E-01	1.355	1.04E-02	2.183	4.24E-04
0.632	1.05E-03	1.368	2.62E-02	2.284	8.02E-05
0.646	7.42E-02	1.376	4.83E-03	2.294	3.20E-04
0.662	2.93E-04	1.385	6.26E-04	2.324	2.44E-05
0.709	1.35E-02	1.437	1.22E-02	2.455	1.47E-05
0.714	2.28E-02	1.445	3.30E-03	2.682	1.65E-05
0.723	1.08E-01	1.489	6.72E-03	2.694	3.03E-05
0.736	5.57E-04	1.526	4.09E-03	2.808	1.47E-05
0.736	7.14E-04				

Table 5.5-14. Sb-125 Gamma Emission Energy Spectrum

Total Photons/Disintegration			
8.628E-01			
Energy	**Intensity**	**Energy**	**Intensity**
0.111	1.04E-05	0.408	1.84E-03
0.117	2.63E-03	0.428	2.96E-01
0.133	8.58E-06	0.444	3.06E-03
0.173	1.91E-03	0.463	1.05E-01
0.176	6.84E-02	0.490	1.36E-05
0.179	3.37E-04	0.491	4.74E-05
0.199	1.28E-04	0.497	3.20E-05
0.204	3.17E-03	0.503	3.85E-05
0.208	2.48E-03	0.539	1.39E-05
0.209	4.50E-04	0.601	1.76E-01
0.228	1.31E-03	0.607	4.98E-02
0.315	4.03E-05	0.617	5.33E-05
0.321	4.16E-03	0.636	1.12E-01
0.332	2.52E-05	0.653	2.66E-05
0.367	7.99E-05	0.671	1.79E-02
0.380	1.52E-02	0.693	4.59E-07
0.402	6.22E-05		

Table 5.5-15. Sb-126 Gamma Emission Energy Spectrum

Total Photons/Disintegration			
4.304E+00			
Energy	**Intensity**	**Energy**	**Intensity**
0.149	3.98E-03	0.667	9.96E-01
0.209	4.98E-03	0.675	3.69E-02
0.224	1.39E-02	0.695	9.96E-01
0.278	2.39E-02	0.697	2.89E-01
0.297	4.48E-02	0.721	5.38E-01
0.297	4.98E-03	0.857	1.76E-01
0.415	8.33E-01	0.954	1.20E-02
0.415	9.96E-03	0.958	4.98E-03
0.556	1.69E-02	0.990	6.77E-02
0.574	6.67E-02	1.036	9.96E-03
0.593	7.47E-02	1.061	3.98E-03
0.620	8.96E-03	1.064	8.96E-03
0.639	8.96E-03	1.213	2.39E-02
0.656	2.19E-02	1.477	2.79E-03

Table 5.5-16. Cs-134 Gamma Emission Energy Spectrum

Total Photons/Disintegration	
2.228E+00	
Energy	**Intensity**
0.243	2.72E-04
0.327	1.62E-04
0.475	1.48E-02
0.563	8.34E-02
0.569	1.54E-01
0.605	9.76E-01
0.796	8.55E-01
0.802	8.69E-02
0.847	3.00E-06
1.039	9.90E-03
1.168	1.79E-02
1.365	3.02E-02

Table 5.5-17. Cs-137 (Ba-137m) Gamma Emission Energy Spectrum

Total Photons/Disintegration	
8.990E-01	
Energy	**Intensity**
0.662	8.99E-01

Table 5.5-18. Hf-175 Gamma Emission Energy Spectrum

Total Photons/Disintegration	
8.683E-01	
Energy	**Intensity**
0.114	2.94E-03
0.161	2.27E-04
0.230	6.83E-03
0.319	1.68E-03
0.343	8.40E-01
0.353	2.28E-03
0.433	1.44E-02

Table 5.5-19. Hf-181 Gamma Emission Energy Spectrum

Total Photons/Disintegration	
1.466E+00	
Energy	**Intensity**
0.133	4.33E-01
0.136	5.85E-02
0.137	8.61E-03
0.346	1.51E-01
0.476	7.03E-03
0.482	8.05E-01
0.615	2.33E-03
0.619	2.50E-04

Table 5.5-20. Ta-182 Gamma Emission Energy Spectrum

Total Photons/Disintegration					
1.456E+00					
Energy	**Intensity**	**Energy**	**Intensity**	**Energy**	**Intensity**
0.100	1.42E-01	0.830	1.41E-04	1.189	1.65E-01
0.110	1.07E-03	0.892	5.74E-04	1.221	2.72E-01
0.114	1.87E-02	0.928	6.14E-03	1.224	2.36E-03
0.116	4.44E-03	0.960	3.50E-03	1.231	1.16E-01
0.122	2.36E-05	1.002	2.09E-02	1.257	1.51E-02
0.152	7.02E-02	1.036	6.70E-05	1.274	6.60E-03
0.156	2.67E-02	1.044	2.39E-03	1.289	1.37E-02
0.179	3.12E-02	1.113	4.45E-03	1.343	2.57E-03
0.198	1.46E-02	1.121	3.52E-01	1.374	2.22E-03
0.222	7.57E-02	1.157	7.33E-03	1.387	7.29E-04
0.229	3.64E-02	1.158	2.89E-03	1.410	3.96E-04
0.264	3.61E-02	1.181	8.74E-04	1.453	3.07E-04
0.351	1.13E-04				

5.5.2. Cobalt-60 Isotope Rod Activity Distribution

The cobalt-60 isotope rod shielding analysis utilizes 12-inch long line sources, which distribute the activity of the source uniformly across the line. Distribution of the cobalt-60 activity into a longer line source results in a lower external dose rate, and greater concentration of the cobalt-60 activity into a shorter line source results in a higher external dose rate. Thus, in order to demonstrate compliance with the regulatory dose rate limits for the cobalt-60 isotope rod contents, two requirements must be met. First, it must be shown that the dose rate contribution from all cobalt-60 source activity in a single shipment is less than the regulatory limit. Second, it must also be shown that the distribution of the activity in any single shipment of isotope rod [[ ]] is distributed axially, such that the uniform line source used in the shielding analysis is bounding of the actual axial distribution of activity.

For the cobalt-60 isotope rod shielding analysis, there are two source geometries considered. The first source geometry is referred to as the 'bounding' source geometry, which concentrates all of the cobalt-60 activity into a single 12-inch line source that is located in the most restrictive location for dose rate calculations in the given direction (top, side, or bottom). For side dose rate calculations with the bounding source geometry, dose rates are calculated with the source at both the bottom (Case 1) and top (Case 2) of the HPI cavity to determine the bounding source location.

The second geometry, referred to as the 'Realistic' source geometry distributes the cobalt-60 activity into [[ ]] of the HPI material basket. This source geometry provides a more realistic radial distribution of the source, as rod [[ ]] will be distributed throughout the basket during shipment, while still condensing the source axially to 12-inches. The array of line sources for the realistic arrangement is pushed against the top of the HPI for the top dose rate calculations, and is at the bottom of the HPI for bottom and side dose rate calculations. Figure 5.5-1 shows a cross section of the HPI material basket, with locations of the line sources used in the MCNP6 model.

[[

]]

Figure 5.5-1. HPI Material Basket with 'Realistic' Source Geometry Locations

A list of all source geometries analyzed is provided in Table 5.5-21 and a depiction of each source geometry is presented in Figures 5.5-2 through 5.5-8. The 'realistic' dose rate calculations are only included to quantify the margin in the bounding dose rates. For the demonstration of compliance with the normal and hypothetical accident condition dose rate limits, the reported dose rates are based on the more restrictive 'bounding' source geometries.

Table 5.5-21. Cobalt-60 Isotope Rod Shielding Analysis Case Summary

NCT Dose Rate Calculation Locations	Source Arrangement	Source Arrangement Figure
Bottom Surface	Realistic	5.5-2
	Bounding	5.5-3
Top Surface	Realistic	5.5-4
	Bounding	5.5-5
Side Surface	Realistic	5.5-6
	Bounding – 1	5.5-7
	Bounding – 2	5.5-8
2-meter	Realistic	5.5-6
	Bounding – 1	5.5-7
	Bounding – 2	5.5-8
Cab	Realistic	5.5-6
	Bounding – 1	5.5-7
	Bounding – 2	5.5-8

[[

]]

Figure 5.5-2. 'Realistic' Source Arrangement for Bottom Dose Rates

[[

]]

Figure 5.5-3. 'Bounding' Source Arrangement for Bottom Dose Rates

[[

]]

Figure 5.5-4. 'Realistic' Source Arrangement for Top Dose Rates

[[

]]

Figure 5.5-5. 'Bounding' Source Arrangement for Top Dose Rates

[[

]]

Figure 5.5-6. 'Realistic' Source Arrangement for Side Dose Rates

[[

]]

Figure 5.5-7. 'Bounding' Source Arrangement for Side Dose Rates – Case 1

[[

]]

Figure 5.5-8. 'Bounding' Source Arrangement for Side Dose Rates – Case 2

Table 5.5-22 lists the peak dose rate per curie calculated at each NCT regulatory dose rate location for each source geometry included in the cobalt-60 isotope rod shielding analysis, and the overall maximum calculated dose rate for each regulatory dose rate location. All maximum calculated dose rates were calculated with the 'bounding' source geometries, where the activity is concentrated into a single line. Also, the line source at the bottom of the HPI cavity calculated higher side dose rates than at the top.

Table 5.5-22. Cobalt-60 Isotope Rod Shielding Analysis NCT Dose Rate Results

NCT Dose Rate Location	Source Arrangement	Dose Rate (mrem/hr/Ci)	Maximum Location Dose Rate (mrem/hr/Ci)
Bottom Surface	Realistic	3.555E-04	3.940E-04
	Bounding	3.940E-04	
Top Surface	Realistic	1.780E-04	1.850E-04
	Bounding	1.850E-04	
Side Surface	Realistic	4.422E-04	8.821E-04
	Bounding	8.821E-04	
	Bounding	8.168E-04	
2-meter	Realistic	1.254E-05	1.664E-05
	Bounding	1.664E-05	
	Bounding	1.348E-05	
Cab	Realistic	2.277E-06	2.921E-06
	Bounding	2.921E-06	
	Bounding	2.331E-06	

Table 5.5-23 lists the maximum calculated dose rate at each NCT regulatory dose rate location using the dose rate per curie values calculated in Table 5.5-22 and the total cobalt-60 activity resulting in the dose rate equal to the 90% of regulatory limit for the respective location. This activity is 204,000 Ci, which results in an NCT side surface dose rate of 180 mrem/hr. Although a cobalt-60 activity of 204,000 Ci is not permitted in the Model 2000 cask due to the thermal limit, this table is included to demonstrate at this activity, no regulatory dose rate limits are exceeded.

Table 5.5-23. Cobalt-60 Isotope Rod Shielding Analysis Maximum NCT Dose Rates

Dose Rate Location	Dose Rate per Curie (mrem/hr/Ci)	Dose Rate[a] (mrem/hr)
Bottom Surface	3.940E-04	80.4
Top Surface	1.850E-04	37.7
Side Surface	8.821E-04	180.0
2-meter	1.664E-05	3.4
Cab	2.921E-06	0.6

Notes: [a] Based on an activity of 204,000 Ci cobalt-60

In Table 5.5-23 it is demonstrated that external dose rates resulting from any cobalt-60 isotope rod activity up to 204,000 Ci are less than the regulatory dose rate limits. It still must be demonstrated that the activity in any single shipment of isotope rod [[ ]] is distributed axially, such that the uniform line source used in the shielding analysis is bounding of the actual axial distribution

of activity. The exact axial activity profile of the cobalt-60 isotope rod [[ ]] is variable due to differences in the neutron flux profiles when irradiated in a commercial or research reactor. To determine that the uniform source in the MCNP6 shielding analysis is bounding of the distribution of activity in a shipment of rod [[ ]], it should first be considered that the source geometry is a single 12-inch line source. Modeling the source in this way assumes that all cobalt-60 activity loaded into the cavity is concentrated into a single line, with a uniform distribution. With all activity in a single line at the most restrictive location of the HPI cavity, any radial distribution of activity is bounded. Thus, the only variation in the source distribution that can cause the external dose rates to increase is in one direction (axially). So, it can be demonstrated that the source distribution of the contents in an actual shipment are bounded, by determining that there is no axial location in the HPI cavity where the concentration of activity is greater than what was analyzed in the MCNP6 analysis.

With the source arrangement of a single 12-inch line, no external dose rates will exceed the regulatory limits for any activity up to 204,000 Ci. By dividing the activity of 204,000 Ci evenly across the 12-inch uniform MCNP6 source, the result is a source that is concentrated in the axial direction to an activity of 17,000 Ci in each inch of the line source. Thus, it can be demonstrated that the activity distribution in the MCNP6 shielding model bounds the total activity distribution in the HPI cavity by determining for the package contents, the total activity in any axial 1-inch increment of the HPI cavity is not greater than 17,000 Ci. If for an actual shipment, there is a total activity of less than or equal to (≤) 17,000 Ci in any axial 1-inch increment of the HPI cavity, there is a greater distribution of the activity in the contents than in the MCNP6 source and the MCNP6 source is bounding.

5.5.3. Radionuclide Decay Heat Conversion Factors

In addition to demonstrating compliance with the regulatory dose rate requirements, filling out the Irradiated Hardware and Byproduct Loading Table also demonstrates compliance with the thermal limit of the Model 2000 cask. One characteristic of every radionuclide is a given Q-value, which is the quantity of energy emitted per decay (MeV/Decay). By assuming that all energy emitted is deposited locally in the HPI material basket or the HPI body, the radionuclide decay heat in W/Ci can be calculated. All radionuclides considered in the irradiated hardware and byproduct contents are listed in Table 5.5-2 of Section 5.5.1, regardless of their significance to dose rate calculations. The Q-values for each of these radionuclides are provided in SCALE6.1 ORIGEN-S Decay library origen.rev03.decay.data (Reference 5-2). Table 5.5-24 lists all of the irradiated hardware and by-product radionuclides with their ORIGEN-S library identification number, Q-value, and the calculated decay heat. Radionuclide Q-values are converted to decay heat values as shown in Equation 5-5.

$$\text{Decay Heat}\left[\frac{\text{W}}{\text{Ci}}\right] = \text{Q}\left[\frac{\text{MeV}}{\text{disintegration}}\right] \cdot 1.60217 \cdot 10^{-13}\left[\frac{\text{J}}{\text{MeV}}\right] \cdot 3.7 \cdot 10^{10}\left[\frac{\frac{\text{disintegrations}}{\text{s}}}{\text{Ci}}\right] \quad (5\text{-}5)$$

Table 5.5-24. Isotope Decay Heat Data

Isotope	ORIGEN-S Radionuclide ID	Q-Value (MeV/Decay)	Decay Heat (W/Ci)
H-3	10030	5.6900E-03	3.373E-05
C-14	60140	4.9470E-02	2.933E-04
Na-24	110240	4.6769E+00	2.772E-02
Si-31	140310	5.9645E-01	3.536E-03
P-32	150320	6.9490E-01	4.119E-03
P-33	150330	7.6430E-02	4.531E-04
S-35	160350	4.8758E-02	2.890E-04
Ca-45	200450	7.6860E-02	4.556E-04
Sc-46	210460	2.1214E+00	1.258E-02
Sc-47	210470	2.7132E-01	1.608E-03
Sc-48	210480	3.5737E+00	2.118E-02
V-49	230490	4.4514E-03	2.639E-05
V-52	230520	2.5137E+00	1.490E-02
Cr-51	240510	3.6680E-02	2.174E-04
Cr-55	240550	1.1017E+00	6.531E-03
Mn-54	250540	8.4017E-01	4.981E-03
Mn-56	250560	2.5226E+00	1.495E-02
Co-57	270570	1.4380E-01	8.525E-04
Co-58	270580	1.0088E+00	5.980E-03
Co-58m	270581	2.4744E-02	1.467E-04
Co-60	270600	2.6006E+00	1.542E-02
Co-60m	270601	6.3045E-02	3.737E-04
Co-61	270610	5.6391E-01	3.343E-03
Ni-57	280570	2.0927E+00	1.241E-02
Ni-59	280590	6.9156E-03	4.100E-05
Ni-63	280630	1.7425E-02	1.033E-04
Ni-65	280650	1.1863E+00	7.032E-03
Fe-55	260550	5.8421E-03	3.463E-05
Fe-59	260590	1.3060E+00	7.742E-03
Cu-64	290640	3.1188E-01	1.849E-03
Cu-66	290660	1.1645E+00	6.903E-03
Zn-65	300650	5.8284E-01	3.455E-03
Zr-89	400890	3.5256E-01	2.090E-03
Zr-95	400950	8.5013E-01	9.835E-03[b]
Zr-97	400970	8.6426E-01	5.123E-03
Sr-87m	380871	3.8798E-01	2.300E-03
Sr-89	380890	5.8534E-01	3.470E-03
Sr-90	380900	1.9580E-01	1.161E-03
Sr-91	380910	1.3485E+00	7.994E-03
Y-89m	390891	9.0902E-01	5.389E-03
Y-90	390900	9.3302E-01	5.531E-03
Y-90m	390901	6.8000E-01	4.031E-03
Y-91	390910	6.0617E-01	3.593E-03
Y-91m	390911	5.5554E-01	3.293E-03
Y-92	390920	1.7017E+00	1.009E-02
Nb-91m	410911	1.2634E-01	7.489E-04
Nb-92m	410921	9.7526E-01	5.781E-03
Nb-94	410940	1.7599E+00	1.043E-02
Nb-95	410950	8.0900E-01	4.796E-03
Tc-101	431010	8.1600E-01	4.837E-03
Ru-106	441060	1.0030E-02	5.946E-05
In-113m	491131	3.9159E-01	2.321E-03
In-114	491140	7.7607E-01	4.601E-03
In-114m	491141	2.2277E-01	1.321E-03
In-115m	491151	3.3436E-01	1.982E-03
Sn-113	501130	2.9753E-02	1.764E-04
Sn-113m	501131	7.1749E-02	4.253E-04
Sn-117m	501171	3.1563E-01	1.871E-03
Sn-119m	501191	8.7589E-02	5.192E-04
Sn-121	501210	1.1582E-01	6.866E-04
Sn-121m	501211	3.7987E-02	2.252E-04
Sn-123	501230	5.3006E-01	3.142E-03
Sn-123m	501231	6.2147E-01	3.684E-03
Sn-125	501250	1.1357E+00	6.732E-03
Sb-122	511220	1.0098E+00	5.986E-03
Sb-124	511240	2.2351E+00	1.325E-02
Sb-125	511250	5.3352E-01	3.163E-03
Sb-126	511260	3.1205E+00	1.850E-02
Te-125m	521251	1.4546E-01	8.623E-04
I-129	531290	7.4338E-02	4.407E-04
Cs-134	551340	1.7185E+00	1.019E-02
Cs-137	551370	1.7945E-01	4.985E-03[a]
Ba-137m	561371	6.6140E-01	
La-140	571400	2.8438E+00	1.686E-02
Ba-140	561400	5.0041E-01	2.966E-03
Ce-144	581440	1.1059E-01	6.556E-04
Hf-173	721730	4.4558E-01	2.641E-03
Hf-175	721750	3.9728E-01	2.355E-03
Hf-177m	721771	1.5190E+00	9.005E-03
Hf-180m	721801	1.1148E+00	6.609E-03
Hf-181	721810	7.3010E-01	4.328E-03
Lu-173	711730	2.3057E-01	1.367E-03
Lu-174	711740	1.5804E-01	9.369E-04
Lu-174m	711741	1.6712E-01	9.907E-04
Lu-176m	711761	4.9032E-01	2.907E-03
Lu-177	711770	1.8133E-01	1.075E-03
Lu-177m	711771	2.4764E-01	1.468E-03
Yb-175	701750	2.0070E-01	1.190E-03
Yb-177	701770	6.2579E-01	3.710E-03
Ta-180	731800	1.0251E-01	6.077E-04
Ta-182	731820	1.5156E+00	8.985E-03
Ta-183	731830	6.3433E-01	3.760E-03
W-181	741810	5.1849E-02	3.074E-04
W-183m	741831	2.9876E-01	1.771E-03
W-185	741850	1.2690E-01	7.523E-04
Re-186	751860	3.5696E-01	2.116E-03

Isotope	ORIGEN-S Radionuclide ID	Q-Value (MeV/Decay)	Decay Heat (W/Ci)
Nb-96	410960	2.7140E+00	1.609E-02
Nb-95m	410951	2.4933E-01	1.478E-03
Nb-97	410970	1.1330E+00	6.716E-03
Nb-97m	410971	7.4336E-01	4.407E-03
Mo-93	420930	1.6143E-02	9.570E-05
Mo-93m	420931	2.4158E+00	1.432E-02
Mo-99	420990	5.4317E-01	3.220E-03
Mo-101	421010	1.9735E+00	1.170E-02
Tc-99	430990	5.5202E-02	3.272E-04
Tc-99m	430991	1.4222E-01	8.431E-04

Isotope	ORIGEN-S Radionuclide ID	Q-Value (MeV/Decay)	Decay Heat (W/Ci)
Np-237	932370	4.9445E+00	2.931E-02
Pu-238	942380	5.5899E+00	3.314E-02
Pu-239	942390	5.2433E+00	3.108E-02
Pu-240	942400	5.2522E+00	3.114E-02
Pu-241	942410	5.3555E-03	3.175E-05
Am-241	952410	5.6280E+00	3.336E-02
Cm-242	962420	6.2153E+00	3.684E-02
Cm-243	962430	6.1779E+00	3.662E-02
Cm-244	962440	5.9011E+00	3.498E-02

Notes: [a] Combined decay heat for Cs-137 and Ba-137m
[b] Decay heat calculated using summed Q-values from Zr-95 and Nb-95.

5.5.4. Irradiated Hardware and Byproduct Loading Table

In order to demonstrate compliance with the 10 CFR 71 (Reference 5-1) regulatory dose rate limits and the thermal limit of the cask, the Irradiated Hardware and Byproduct Loading Table must be confirmed for every shipment of irradiated hardware or byproducts in the Model 2000 cask. The use of this loading table is simple: for each of the radionuclides included in a shipment, enter the radionuclide into the table, enter the activity of the radionuclide, then calculate the decay heat and dose rate contribution at each regulatory location based on the dose rate per curie and decay heat values presented in Tables 5.4-2, 5.4-3 and 5.5-24.

Tables 5.5-25 through 5.5-27 provide radionuclide inventories for three hypothetical shipments of irradiated hardware, zirconium-95, and hafnium poison rods. The irradiated hardware radionuclide inventory presented in Table 5.5-25 lists the sample activities and percent-activity of the total content for a list of radionuclides based on a previous shipment of a piece of irradiated 304 SS in the Model 2000 cask with all of the radionuclide activities scaled up to higher activities. The zirconium and hafnium poison rod radionuclide inventories in Tables 5.5-26 and 5.5-27 are hypothetical radionuclide inventories, included only to provide additional examples.

Table 5.5-25. Example Irradiated SS304 Radionuclide Inventory

Nuclide	Ci/sample	% Activity	Total Activity (Ci)
H-3	6.75E-06	0.00%	4.605E-05
P-32	3.49E-04	0.00%	2.381E-03
S-35	8.26E-04	0.00%	5.635E-03
Cr-51	3.73E+00	2.12%	2.545E+01
Mn-54	5.60E+00	3.18%	3.821E+01
Fe-55	5.69E+01	32.35%	3.882E+02
Fe-59	3.32E-01	0.19%	2.265E+00
Co-58	2.85E+00	1.62%	1.944E+01
Co-60	1.01E+02	57.42%	6.891E+02
Ni-59	4.14E-02	0.02%	2.825E-01
Ni-63	5.42E+00	3.08%	3.698E+01
Zn-65	1.06E-02	0.01%	7.232E-02
Nb-93m	3.25E-04	0.00%	2.217E-03
Mo-99	6.13E-14	0.00%	4.182E-13
Tc-99m	5.94E-14	0.00%	4.053E-13
Total	175.89	100.00%	1200

Table 5.5-26. Example Zr-95 Radionuclide Inventory

Nuclide	Total Activity (Ci)
Zr-95	80,000

Table 5.5-27. Example Hf Poison Rod Radionuclide Inventory

Nuclide	% Activity	Total Activity (Ci)
Hf-175	4.21%	10,650
Hf-181	90.09%	228,000
Ta-182	5.70%	14,422
Total	100.00%	253,072

Tables 5.5-28 through 5.5-30 show the respective Irradiated Hardware and Byproduct Loading Tables for each of the hypothetical shipments outlined in Tables 5.5-25 through 5.5-27. These tables show that all three hypothetical shipments of irradiated hardware and byproduct contents comply with all dose rate and thermal criteria and would be acceptable for shipment.

Table 5.5-28. Example SS304 Irradiated Hardware and Byproduct Loading Table

Radio-nuclide	Activity (Ci)	Decay Heat (W)	NCT					HAC		
			DR_{surf}			DR_{2m}	DR_{cab}	DR_{1m}		
			Top	Side	Bottom			Top	Side	Bottom
Cr-51	25.40	5.53E-03	1.01E-13	4.19E-19	1.41E-18	5.41E-21	8.93E-22	3.23E-12	1.28E-18	2.41E-17
Mn-54	38.20	1.90E-01	8.77E-06	3.77E-04	1.63E-05	4.26E-06	7.27E-07	1.55E-05	7.82E-05	1.27E-05
Fe-55	388.20	1.34E-02	0.00E+00	0.00E+00	0.00E+00	0.00E+00	0.00E+00	0.00E+00	0.00E+00	0.00E+00
Fe-59	2.30	1.75E-02	2.81E-04	6.56E-03	4.20E-04	8.27E-05	1.43E-05	4.09E-04	1.22E-03	2.43E-04
Co-58	19.40	1.16E-01	2.64E-04	4.75E-03	4.22E-04	6.56E-05	1.16E-05	3.49E-04	8.67E-04	2.25E-04
Co-60	689.10	1.06E+01	2.88E-01	6.50E+00	4.30E-01	8.34E-02	1.43E-02	4.14E-01	1.20E+00	2.45E-01
Ni-63	37.00	3.82E-03	0.00E+00	0.00E+00	0.00E+00	0.00E+00	0.00E+00	0.00E+00	0.00E+00	0.00E+00
Total	-	10.970	0.289	6.514	0.431	0.084	0.014	0.415	1.203	0.245
Limit	-	1500	180	180	180	9	1.8	900	900	900
Criteria Met?	-	YES	YES	YES	YES	YES	YES	YES	YES	YES

Table 5.5-29. Example Zr-95 Irradiated Hardware and Byproduct Loading Table

Radionuclide	Activity (Ci)	Decay Heat (W)	NCT					HAC		
			DR_{surf}			DR_{2m}	DR_{cab}	DR_{1m}		
			Top	Side	Bottom			Top	Side	Bottom
Zr-95	80,000	787.0	4.01E-03	2.00E-01	9.45E-03	2.25E-03	3.83E-04	7.62E-03	4.37E-02	8.31E-03
Total	-	787.0	4.01E-03	2.00E-01	9.45E-03	2.25E-03	3.83E-04	7.62E-03	4.37E-02	8.31E-03
Limit	-	1500	180	180	180	9	1.8	900	900	900
Criteria Met?	-	YES	YES	YES	YES	YES	YES	YES	YES	YES

Table 5.5-30. Example Hf Poison Rod Irradiated Hardware and Byproduct Loading Table

Radionuclide	Activity (Ci)	Decay Heat (W)	NCT					HAC		
			DR_{surf}			DR_{2m}	DR_{cab}	DR_{1m}		
			Top	Side	Bottom			Top	Side	Bottom
Hf-175	10,650	25.1	1.75E-09	2.04E-11	3.74E-12	1.24E-13	2.01E-14	1.78E-08	5.13E-12	8.25E-12
Hf-181	228,000	986.8	4.49E-06	4.82E-06	7.81E-07	6.27E-08	1.08E-08	3.40E-05	1.57E-06	1.16E-06
Ta-182	14,422	129.6	1.94E+00	4.72E+01	2.88E+00	5.90E-01	1.01E-01	2.85E+00	8.85E+00	1.70E+00
Total	-	1141.5	1.94	47.20	2.88	0.59	0.10	2.85	8.85	1.70
Limit	-	1500	180	180	180	9	1.8	900	900	900
Criteria Met?	-	YES	YES	YES	YES	YES	YES	YES	YES	YES

5.5.5. Combined Content Shipments

There is the possibility of a shipment that includes multiple content types. To demonstrate compliance with all regulatory and cask requirements, the total thermal power and dose rate contributions from each content type must be determined. Using the procedure in Chapter 7 compliance is demonstrated for shipments of multiple content types.

For combinations of contents, the Loading Table of each content type must be confirmed and the total contribution to the thermal power and dose rates must be below the limit. Additionally, the requirements for each content type that are defined in Section 1.2.2.3 must be met.

5.6 References

5-1 U.S. NRC, 10 CFR 71, "Packaging and Transportation of Radioactive Material," Washington D.C.

5-2 Oak Ridge National Lab, "SCALE: A Comprehensive Modeling and Simulation Suite for Nuclear Safety Analysis and Design, ORNL/TM-2005/39, Version 6, Vols. I-III," ORNL/TM-2005/39, Version 6.1, June 2011.

5-3 American Society for Testing and Materials, "Standard Specification for General Requirements for Flat-Rolled Stainless and Heat-Resisting Steel Plate, Sheet, and Strip," ASTM A480, 2016.

5-4 R.J. McConn et al., "Compendium of Material Composition Data for Radiation Transport Modeling," PNNL-15870, Revision 1, March 2011.

5-5 T. Goorley, et al., "Initial MCNP Release Overview - MCNP6 Version 1.0," Los Alamos National Laboratory, LA-UR-13-22934, April 2013.

5-6 J. Conlin et al., "Listing of Available ACE Data Tables," Los Alamos National Laboratory, LA-UR-13-21822, Revision 4, June 2014.

5-7 U.S. Nuclear Ragulatory Commission, "Standard Review Plan for Transportation Packages for Radioactive Material," NUREG-1609, March 1999.

5-8 ANS 6.1.1 Working Group, M. E. Battat (Chairman), "American National Standard Neutron and Gamma-Ray Flux-to-Dose-Rate Factors," American Nuclear Society, ANSI/ANS-6.1.1-1977, March 1977.

6 CRITICALITY EVALUATION

As described in Section 1.2.2.3, the allowable contents for the Model 2000 Transportation Cask are: 1) irradiated hardware and byproducts and 2) cobalt-60 isotope rods. Therefore, a criticality evaluation is not required because fissile material is not an approved content of the Model 2000 Radioactive Material Transport Package.

7 OPERATING PROCEDURES

Instructions for use of the Model 2000 Transport Package are summarized below, beginning with Section 7.1. The instructions for detailed use are implemented administratively via site specific procedures. A pre-shipment engineering evaluation is implemented to ensure that the packaging, with its proposed contents, satisfies the applicable requirements of the package's license, certificate, or equivalent authorization. This evaluation includes, but is not limited to, the review of:

- Proposed contents' isotopic composition, quantities, and decay heat
- Proposed contents' form, weight, and geometry
- Shielding requirements
- Structural requirements
- Thermal requirements
- Shipping hardware (e.g., material basket and shoring devices)
- Compliance with the respective content requirements listed in Section 7.5.

7.1 Package Loading

Fully trained personnel using approved operating procedures shall carry out all loading operations at the facility. The general sequence is as follows:

- Use respective loading tables and guidance provided in Section 7.5 to ensure compliance with the authorized contents.
- Receive the empty Model 2000 Transport Package, including the HPI packaging and shoring hardware.
- Inspect cask and components for damage and prepare for loading.
- Load the contents directly into the HPI as required.
- Load the cobalt-60 isotope rods into the HPI material basket and load the material basket into the HPI.
- Install HPI and cask lids.
- If wet loaded, raise cask to allow draining of cask
- Install cask lid screws by hand, transfer cask to staging area and torque cask lid screws.
- Vacuum dry cask and perform pre-shipment leak test.
- Load the cask into the overpack and onto the trailer for transport.

7.1.1. Preparation for Loading

7.1.1.1. Packaging Receipt and Inspection

a. Position the Model 2000 transport vehicle for packaging inspection upon arrival.

b. Perform visual inspection for shipping damage.

7.1.1.2. Removal of the Packaging from the Transport Vehicle

a. Position the transport vehicle under an overhead crane.

b. Remove the packaging tie-downs.

c. Position the spreader bar or strongback and connect the appropriate slings and shackles.

d. Depending on site-specific procedure:

- Lift the overpack top section off the overpack base and place on the overpack stand,
- Lift the entire packaging free from the transport vehicle and set it down. Then lift the overpack top section from the overpack base and place on the overpack stand, or as instructed in the site-specific procedure to account for facility limitations.

7.1.1.3. Preparing to Load the Cask

a. Perform a visual inspection. Note any damage or unusual conditions to GEH. If functionality of the part is impaired, do not repair or replace without authorization from GEH.

b. Install cask ears. Torque the lifting ear screws to 600±20 ft-lb. If lifted by crane, inspect lifting slings.

c. Move the cask to the designated work area.

d. With proper radiological protection and monitoring, remove the cask lid and verify presence of the required HPI hardware.

e. If there is a spacer, it needs to remain with the HPI for reuse.

f. Visually inspect the cask and lid sealing surfaces for damage or foreign material. Report any damage to GEH; do not repair or replace without authorization from GEH.

g. Visually inspect the cask lid seal for damage. Gouges or cuts in the seal gasket areas are cause for replacement. Report any damage to GEH; do not repair or replace without authorization from GEH.

h. Place the cask lid seal over the alignment pins on the top of the cask.

i. Remove vent and drain port plugs and covers, and test port plug and cover, to allow filling and draining of cask. Report any damage to GEH; do not repair or replace without authorization from GEH.

7.1.2. Loading of Contents

7.1.2.1. Cobalt-60 Isotope Rods

The usage of the term 'rods' in this section refers to cobalt-60 isotope rods. This content type must be shipped according to the requirements in Section 7.5.2 or Section 7.5.3.

a. Remove the HPI top plug including spacer if installed.

b. [[ ]] the rods and load into additional shoring components (e.g., rod holders).

c. Load the rods with any additional shoring components into the HPI material basket. Depending on site-specific procedures, the HPI material basket may be loaded independently.

d. If the HPI material basket is loaded independently, load contents into the HPI.

e. After the HPI material basket and all contents and shoring are loaded into the HPI, lower the HPI top plug, including spacer if installed, over the alignment pins with the proper rigging.

f. Slowly lower the lid onto the cask over the guide pins with proper rigging. Closely watch this operation to ensure that the lid is properly aligned.

7.1.2.2. Irradiated Hardware and Byproducts

The usage of the term 'contents' in this section refers to irradiated hardware and byproducts. This content type must be shipped according to the requirements in Section 7.5.1 or Section 7.5.3.

a. The use of the HPI material basket is not required, but may be used as a shoring component.

b. Remove the HPI top plug, including spacer if installed.

c. Load the contents with any additional shoring components into the HPI. The HPI material basket may be used as shoring, but is not required.

d. After all contents and shoring are loaded into the HPI, lower the HPI top plug, including spacer if installed, over the alignment pins with the proper rigging.

e. Slowly lower the cask lid onto the cask over the guide pins with proper rigging. Closely watch this operation to ensure that the lid is properly aligned and seated.

7.1.3. Closing the Cask and Performing Leakage Tests

7.1.3.1. Removing the Cask from the Loading Area

a. Carefully monitor the cask radiation levels while removing the cask from the loading area.

b. Tighten the lid bolts so they are hand tight.

c. If the cask was loaded under water:

- Raise cask above level of pool to allow for water drainage.
- After the water has drained, vacuum-dry the cask cavity until 1 torr pressure is attained. Maintain the pressure in the cavity at or below 1 torr for at least 30 minutes.
- After the 30-minute hold time is reached, isolate the vacuum system from the cask by closing the valve between the vacuum pump(s) and the cask. With the vacuum pump valve(s) closed, disconnect the power to the vacuum pump(s) or shut off the vacuum pump power.
- Observe the pressure in the cavity, which must be maintained at or below 1 torr for at least an additional 5 minutes. This ensures that the pressure measurement is reliable and not due to the vacuum pump(s) pulling past a partially open valve.
- If the pressure rise should exceed 1 torr in the first 30-minute hold or in the second 5-minute hold with the system isolated, turn the vacuum drying system back on and open the cask valve(s) to continue the vacuum drying process.
- Filter the discharged gas of the vacuum pump(s) if necessary.

d. Decontaminate the cask exterior surfaces to a level consistent with 49 CFR 173.443 and 10 CFR 71.87.

7.1.3.2. Securing the Cask Lid

a. Torque the lid bolts to 720±30 ft-lb in a crisscross pattern to ensure equal compression of the seal.

b. Install the drain and vent plugs following the drying operation as applicable using proper thread sealant. The plugs are installed by applying proper thread sealant and inserted until leak tight.

7.1.3.3. Assembly Verification Pre-Shipment Leakage Testing

a. Perform leakage testing of the cask lid closure seal and vent port and drain port threaded pipe plugs in accordance with a procedure developed by an American Society for Nondestructive Testing (ASNT) Level III examiner.

b. Upon completion of the vacuum drying procedure, backfill the cask cavity with 2 ±1 psig helium. For leak testing, pressurize the cask cavity with 15 +1/-0 psig helium. Introduce helium by using the fitting at a cask port.

c. Set up and use the helium test instrument according to the written procedure and the manufacturer's instructions.

d. With the instrument calibrated, check the closure seal and the vent and drain threaded pipe plugs for indications of leakage.

e. If leakage is detected during either of the above checks, repair or replace the offending components and then re-test for leakage.

f. After leak testing is completed, vent the cask cavity to atmosphere. Assure helium vent hose is exhausted through an approved facility ventilation or high efficiency particulate air (HEPA) system.

7.1.4. Preparation for Transport

7.1.4.1. Preparing the Cask for Transport

a. Transport the cask to the overpack base and place the cask on the lower impact limiter base.

b. Remove the cask lifting ears or redundant ears from the cask and use approved tape to cover the ears' threaded holes for contamination control purposes.

c. Position the spreader bar over the overpack and connect the slings and shackles.

d. Slowly lower the overpack over the cask with the locating pins aligned.

e. Install the overpack bolts, securing the top section to the base section. Torque overpack screws to 100±5 ft-lb (dry) in 15 places (typ). An adhesive/sealant compound is applied to bolt threads prior to installation to prevent vibration loosening of bolts.

f. Position the package on the transport vehicle if required.

g. Remove the shackle and slings and tie down the package to the transport vehicle. The Model 2000 Transport Package does not have any parts or devices that would need to be rendered inoperable pursuant to 10 CFR 71.87(h).

h. Perform the radiological survey of the package and transport vehicle consistent with 10 CFR 71.47, 71.87 and 49 CFR 173.441, 173.443.

i. Measure and document the temperature of the overpack paying particular attention to the area around the bolting ring. If any temperature reading exceeds 185°F, install the protective personnel barrier around the package, in accordance with 10 CFR 71.43.

j. Apply the security seal to the overpack.

7.2 Package Unloading

Operations at the unloading facility are largely the reverse of loading operations. The unloading facility must provide fully trained personnel and shall be supplied with detailed operating procedures to cover all activities as required by 10 CFR 71.89.

7.2.1. Receipt of Package from Carrier

7.2.1.1. Package Receipt and Inspection

Repeat Steps 7.1.1 (a and b) and perform a radiological survey in accordance with the requirements of 10 CFR 20.205 or equivalent agreement state regulations.

7.2.1.2. Removal of the Package from the Transport Vehicle

a. Position the transport vehicle under an overhead crane.

b. Remove protective personnel barrier if required.

c. Remove the packaging tie-downs.

d. Position the spreader bar and connect the appropriate slings and shackles.

e. Depending on site-specific procedure:

- Lift the overpack top section off the overpack base and place on the overpack stand,
- Lift the entire packaging free from the transport vehicle and set down. Then lift the overpack top section from the overpack base and place on the overpack stand, or as instructed in the applicable site specific procedure.

7.2.1.3. Preparing to Unload Contents

a. Perform a visual inspection. Report any damage or unusual conditions to GEH; do not repair or replace without authorization from GEH. If functionality of the part is impaired, repair or replace as required.

b. Perform a radiological survey of the cask.

c. Install the cask lifting ears. Torque the cask ear to 600±20 ft-lb. Transport the cask to the unloading area.

d. With radiological monitoring and controlled ventilation in place, remove the vent plug and drain plugs.

e. Remove the lid bolts for unloading in either a storage basin or hot cell.

f. Remove the lid following the placing of the cask within a hot cell or storage basin.

g. If there is a spacer attached to the top plug, it must remain with the HPI top plug for reuse.

h. Remove the HPI top plug, including the spacer if attached.

i. If the cask is to be unloaded in air at a waste disposal site, prepare the cask for unloading following a procedure developed by the burial site and reviewed by GEH.

j. If the cask is unloaded in a hot cell or underwater, prepare the cask for unloading following a site-specific procedure, reviewed by GEH.

7.2.2. Removal of Contents

7.2.2.1. Co-60 Isotope Rods

The usage of the term ‘rods’ in this section refers to cobalt-60 isotope rods.

a. Obtain the list identifying the rods to be unloaded.

b. Verify the identification and location of the rods in the cask.

c. Transfer the rods, or shoring device such as rod holders if applicable, one at a time in accordance with the site's transfer procedure.

7.2.2.2. Unloading Irradiated Hardware

The usage of the term ‘contents’ in this section refers to irradiated hardware.

a. Unload cask contents in accordance with the site’s transfer procedure.

7.2.2.3. Installing the Cask Closure Lid

a. With proper rigging, slowly lower the HPI top plug over the alignment pins.

b. If spacer was provided with the HPI top plug, confirm it is secured to the HPI top plug.

c. With proper rigging, slowly lower the lid onto the cask over the guide pins. Closely watch this operation to assure that the lid is properly aligned.

7.2.2.4. Removing the Cask from the Unloading Area

a. Tighten the lid bolts hand-tight.

b. Remove the cask to the storage area.

7.2.2.5. Securing the Cask Lid

a. Repeat Section 7.1.3.2.

7.3 Preparation of Empty Packaging for Transport

The following operations are typically performed after transport of radioactive material.

7.3.1. Cask Cavity Inspection

a. Remove the lid from the empty cask.

b. Perform a radiological survey of the cavity to determine extent of any contamination.

c. Decontaminate the cavity to the limits of 49 CFR 173.428 if the cask is shipped as an empty container as defined in the regulation.

d. Visually inspect the cask and contents to ensure that moisture has been removed.

7.3.2. Installation of the Cask Closure Lid

a. With proper rigging, slowly lower the lid onto the cask over the guide pins. Closely watch this operation to assure that the lid is properly aligned.

b. Install the head bolts and torque to 720±30 ft-lb in a crisscross pattern to ensure equal compression of the seal.

c. Inspect the cask to verify that all drain, test, and vent plugs are properly installed.

7.3.3. Assembly Verification Leakage Testing

Leakage testing is not required to be performed on the empty container. As an option, leakage testing may be performed on an empty container prior to shipment for loading operations at a user facility, to assure a new seal performs as required.

7.3.4. Preparing the Empty Cask for Transport

Decontaminate the external surfaces of the cask to a level consistent with 49 CFR 173.427, "Empty Radioactive Materials Packaging".

7.4 Other Operations

There are no provisions required for any special operational controls (e.g., route, weather, mode, shipping time restrictions).

7.5 Appendix

The offeror is responsible for completing the loading table(s) in Sections 7.5.1 through 7.5.3 as necessary, as part of their pre-shipment evaluation review and approval process/system in advance of releasing the shipment in question.

7.5.1. Irradiated Hardware and Byproduct Loading Table

This section is included in order to provide clear instructions for using the Irradiated Hardware and Byproduct Loading Table. Figure 7.5.1-1 shows the Irradiated Hardware and Byproduct Loading Table with cells labeled for clear instruction for data entry. The Irradiated Hardware and Byproduct Loading Table shall be confirmed prior to any shipment of this content type.

It can be noted in this figure that:

- Column 1 is included to record each radionuclide in the Irradiated hardware or byproducts in a single shipment (with activity >1 Ci).
- Column 2 is included to record the activity of each radionuclide listed.
- Column 3 is included to demonstrate compliance with the thermal limits of the cask.
- Columns 4-11 are included to demonstrate compliance with regulatory dose rate limits for each location.
- Row A is filled out individually for each radionuclide in the shipment.
- Row B provides a summed total for each column.
- Row C provides the respective regulatory/cask limit for each column.
- Row D states whether the proposed shipment meets the respective regulatory/cask requirement. Cells in this row should be filled with either ‘YES’ or ‘NO’. Once the Irradiated Hardware and Byproduct Loading Table is filled out entirely, if all cells in Row D say ‘YES’, the shipment complies with all necessary activity, thermal, and dose rate criteria.
- Row E is included to record the personnel who filled out the loading table.

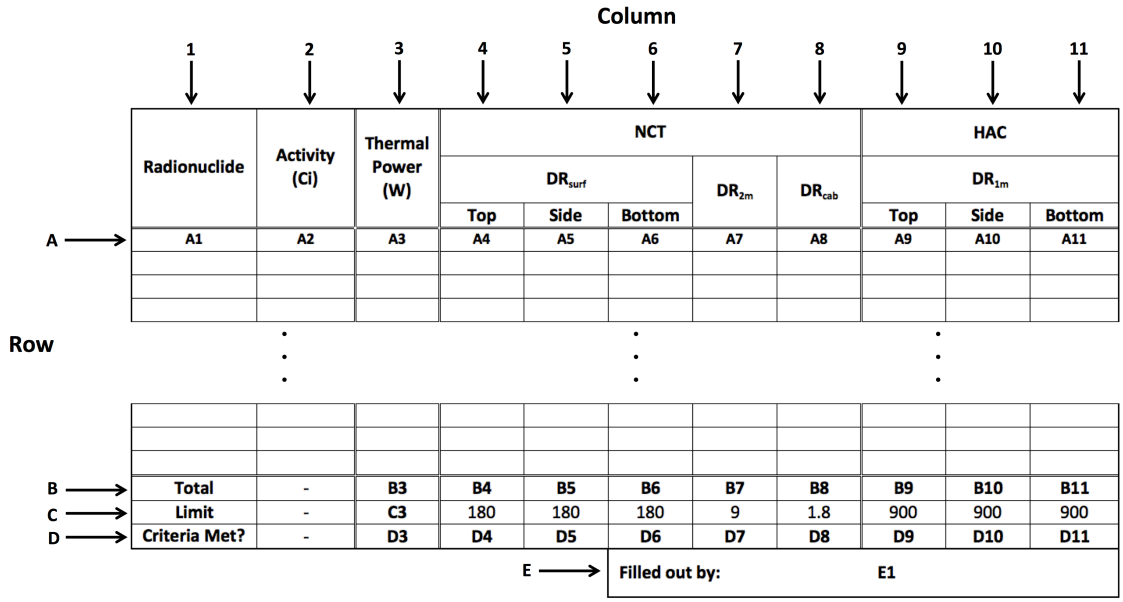

Figure 7.5.1-1. Irradiated Hardware and Byproduct Loading Table

The Irradiated Hardware and Byproduct Table is filled out using the following procedure. Cell labels are from Figure 7.5.1-1.

1. Enter the thermal limit of 1500 W for the shipment in Cell C3.
2. Starting in Cell A1 enter the first radionuclide into the loading table. This column should simply list the radionuclide name or abbreviation (e.g., enter either 'Cobalt-60' or 'Co-60').
    - Only radionuclides (alpha and beta emitters) with activity greater than 1 Ci must be entered into the loading table. Any neutron emitting radionuclides are limited to trace amounts, strictly from surface contamination of the hardware or byproducts are permitted for shipment. A list of radionuclides for consideration to include in the loading plan is provided in, but not limited to, Table 5.5-24.
    - Any radionuclide with all gamma emissions less than 0.3 MeV or a half-life less than 3 days is irrelevant to dose rate calculations, but should be entered in the table for thermal contributions. If the radionuclide is not included in Table 5.5-24, the thermal power multiplier can be calculated using Equation 5-5 and the Q-value for the radionuclide in the SCALE6.1 ORIGEN decay library origen.rev03.decay.data (Reference 7-2).
    - Any contents including radionuclides with an activity greater than 1 Ci that are not listed in Table 5.5-24, that also have gamma emissions greater than 0.3 MeV and a half-life greater than 3 days are not allowable for shipment.
3. In Cell A2 enter the activity in curies of the respective radionuclide.
4. In Cell A3, enter the thermal power for the radionuclide (in W). This value is calculated by multiplying the activity of the radionuclide (in Cell A2) by the thermal power multiplier of the radionuclide listed in Table 5.5-24.

5. In Cells A4 through A11, enter the dose rate contribution for the respective radionuclide (in mrem/hr) for the dose rate location of the appropriate column. This value is calculated by multiplying the activity of the radionuclide (in Cell A2) by the dose rate multiplier of the radionuclide for the respective dose rate location. Dose rate multipliers for all radionuclides that are significant to the shielding analysis are provided in Table 5.4-2 for NCT dose rates and Table 5.4-3 for HAC dose rates. Irradiated hardware and byproduct radionuclides listed in Table 5.5-2, but not in Table 5.4-2 or Table 5.4-3, are not relevant to dose rate calculations, thus cells A4 through A11 may be filled with a '0' for those radionuclides.

6. Repeat Steps 2 through 5 in the next row, filling in Columns 1 through 11, for every radionuclide that is included in the irradiated contents.

7. With the top portion of the loading table filled out, in Cell B3, sum the thermal power contributions from all radionuclides entered in Column 3 of the top portion of the loading table.

8. For Cells B4 - B11, sum the dose rate contributions from all radionuclides entered in the top portion of the loading table, for each column (e.g., for Cell B4 sum Column 4, for Cell B5, sum Column 5).

9. For Cells D3 through D11, if the respective value in Row B is less than or equal to the value in Row C, enter 'Yes', if the value in Row B is greater than the value in Row C enter 'No'.

10. If all cells in Row D say 'Yes', the proposed load of irradiated contents meet all thermal and dose rate criteria and are acceptable for shipment. If any cells in Row D say 'No', a limit has been exceeded and the proposed load of irradiated contents is not acceptable for shipment.

11. Upon completion of the Irradiated Hardware and Byproduct Table, the name of the personnel responsible for filling out the table is entered in Cell E1.

Model 2000 Irradiated Hardware and Byproduct Loading Table

Radionuclide	Activity (Ci)	Thermal Power (W)	NCT (mrem/hr)					HAC (mrem/hr)		
			$DR_{surface}$			DR_{2m}	DR_{cab}	DR_{1m}		
			Top	Side	Bottom			Top	Side	Bottom
Total	-									
Limit	-		180	180	180	9	1.8	900	900	900
Criteria Met?	-									

Filled out by:

7.5.2. Verification of Compliance for Cobalt-60 Isotope Rods

Compliance with the cask thermal and regulatory dose rate limits for the cobalt-60 isotope rod contents is demonstrated through a check of the peak activity limit across any rod and using the Cobalt-60 Isotope Rod Loading Table. The Cobalt-60 Isotope Rod Loading Table shall be confirmed prior to any shipment of this content type. It is determined that a batch of cobalt-60 isotope rods is acceptable for shipment in the Model 2000 Transport Package using the following procedure:

1. Verify that the peak activity in any axial 1-inch increment in the HPI cavity is in accordance with Section 5.5.2.
2. Determine if there is any additional significant radionuclide activity in the rod cladding or hardware components shipped with the isotope rods. If there are additional radionuclides in the rod cladding or additional hardware shipped with the isotope rods skip to Step 3. If there are no additional radionuclides other than the cobalt-60 in the isotope rods, check that the total activity of cobalt-60 in the cask is in the range specified:
   - 0 – 97,250 Ci (Thermal equivalent: 0 – 1,500 W)

   If the requirements in Step 1 and 2 are met, the load of cobalt-60 isotope rods meets all cask and regulatory requirements and is acceptable for shipment.
3. Enter 1500W for the thermal power limit into the 'Limit' row of the Cobalt-60 Isotope Rod Loading Table .
4. Enter the total cobalt-60 activity of the cobalt-60 isotope rod contents (in Ci).
5. Enter the thermal power for the cobalt-60 isotope rod contents (in W). This value is calculated by multiplying the activity of the isotope rods by the thermal power multiplier for cobalt-60 from Table 5.5-24.
6. In Cells A4 through A11, enter the dose rate contribution for the cobalt-60 isotope rod contents (in mrem/hr) for the dose rate location of the appropriate column. This value is calculated by multiplying the total activity of the isotope rods by the dose rate multiplier for the respective dose rate location. The dose rate multipliers for each dose rate location are provided in Table 5.4-6 for NCT dose rates and Table 5.4-7 for HAC dose rates.
7. Upon completion of the Cobalt-60 Isotope Rod Loading Table, the name of the personnel responsible for filling out the table is entered into the appropriate cell.
8. If the maximum dose rate is less than or equal to the dose rate limit, enter 'Yes' in the 'Criteria Met?' row, otherwise enter 'No'.
9. If all cells in the 'Criteria Met?' row of the Cobalt-60 Isotope Rod Loading Table say 'Yes', the cobalt-60 isotope rod contents meet all regulatory/cask criteria. Fill out the Irradiated Hardware and Byproduct Table per instructions in Section 7.5.1. This table should be filled out for any significant radionuclide activity in the rod cladding and any irradiated hardware included in the shipment. If there is a measurable thermal or dose rate contribution from

the irradiated hardware, also fill out the Combined Contents Loading Table per instructions in Section 7.5.3 to demonstrate that all regulatory/cask requirements are met for the combined contents.

Model 2000 Cobalt-60 Isotope Rod Loading Table

Content	Activity (Ci)	Thermal Power (W)	NCT (mrem/hr)					HAC (mrem/hr)		
			$DR_{surface}$			DR_{2m}	DR_{cab}	DR_{1m}		
			Top	Side	Bottom			Top	Side	Bottom
Cobalt-60 Isotope Rod										
Limit	-		180	180	180	9	1.8	900	900	900
Criteria Met?	-									

Filled out by:

7.5.3. Combined Contents

The Combined Contents Loading Table shall be confirmed prior to any shipment including multiple content types. For any shipment including multiple content types, compliance with regulatory/cask limits is demonstrated using the following procedure:

1. Fill out the Irradiated Hardware and Byproduct Loading Table per instructions in Section 7.5.1, as applicable.
2. Fill out the Cobalt-60 Isotope Rod Loading Table per instructions in Section 7.5.2, as applicable.
3. Enter 1500W for the thermal power limit into the 'Limit' row of the Combined Contents Loading Table .
4. Enter the thermal power and dose rate values from the 'Total' row of each applicable loading table from Steps 1 through 3 into the respective, 'Hardware/Byproduct', and 'Cobalt-60 Isotope Rod' rows in the Combined Contents Loading Table.
5. Sum the thermal powers and dose rate values from all content types in the 'Total' row of the Combined Contents Loading Table.
6. Verify that for each column the value in the 'Total' row is less than the value in the 'Limit' row. Record this verification by writing 'Yes' if the criteria is met, or 'No' if the criteria is not met.
7. If all cells in the 'Criteria Met?' row of the Irradiated Hardware and Byproduct Loading Table, and the Combined Contents Loading Table say 'Yes', the proposed load of combined contents meets all regulatory/cask criteria and is acceptable for shipment. If any cells in any of the three Tables say 'No', a limit has been exceeded and the proposed load of combined contents is not acceptable for shipment.
8. Upon completion of the Combined Contents Loading Table, the name of the personnel responsible for filling out the table is entered into the appropriate cell.

Model 2000 Combined Contents Loading Table

Content	Thermal Power (W)	NCT (mrem/hr)					HAC (mrem/hr)		
		DR_{surf}			DR_{2m}	DR_{cab}	DR_{1m}		
		Top	Side	Bottom			Top	Side	Bottom
Hardware / Byproduct									
Cobalt-60 Isotope Rods									
Total									
Limit		180	180	180	9	1.8	900	900	900
Criteria Met?									

Filled out by:

7.6 References

7-1 Oak Ridge National Lab, "SCALE: A Comprehensive Modeling and Simulation Suite for Nuclear Safety Analysis and Design, ORNL/TM-2005/39, Version 6, Vols. I-III," ORNL/TM-2005/39, Version 6.1, June 2011.

8 ACCEPTANCE TESTS AND MAINTENANCE PROGRAM

This chapter describes the acceptance tests and maintenance program to be used for the Model 2000 Transport Package, required by 10 CFR 71, Subpart G. The acceptance tests are prescribed to verify materials of construction, fabrication processes, and the transport package's design adequately meets the regulations, while the maintenance program outlined in this chapter assures the packaging's performance during its service life, in full compliance with this safety analysis report.

General information related to the Model 2000 Transport Package, including package design details and contents description, is presented in Chapter 1 of this safety analysis report. For package dimensions, refer to the licensing drawings provided in Section 1.3.1. Fabrication and examination of the Model 2000 Transport Package (i.e., cask and overpack), the high performance insert (HPI) assembly, and material basket assembly, conform to the requirements of ASME Section III, as delineated in Section 8.1.

Routine inspection (prior to each loading) consists of visual examination for physical damage of all surfaces and components. Periodic or annual inspection includes visual examination, penetrant inspection of welds, and replacement of damaged or worn components, as necessary.

8.1 Acceptance Test

The inspection and acceptance tests are specified in the fabrication specifications and engineering drawings for the Model 2000 Transport Package and are governed by GEH Quality Assurance Program QAP-1 (Reference 8-1). QAP-1 has been approved by the NRC (Docket Number 71-0170) (Reference 8-2).

8.1.1. Visual Inspections and Measurements

Visual examinations of all dimensions are conducted during fabrication to ensure that the packaging is fabricated and assembled in accordance with manufacturing drawings and specifications. All dimensions and tolerances specified on the drawings are confirmed by measurement. Fabrication deviations are addressed in compliance with QAP-1 for all components important to Safety Category A or B.

8.1.2. Weld Examinations

Visual examinations of all welds, including overpack torodial shells, are conducted during fabrication. In addition, all welds within the cask containment boundary are liquid penetration tested (root and final passes); also, the welds forming the toroidal shell are 100% radiographed. These inspections are performed to ensure no cracks, incomplete fusion, or lack of penetration, exists. Parts that do not meet the established criteria are repaired or replaced in accordance with written procedures. For Model 2000 Transport Package serial number (S/N) 2001, nondestructive examination (NDE) procedures and acceptance standards are based on the ASME Code, Section III, Subsection NG (Reference 8-3). All future fabrication will meet the requirements of the ASME Code, Section III as follows:

Cask assembly including ears (Reference 8-4):

- Materials per NB-2000, Certification NCA-3800
- Fabrication per NB-4000
- NDE per NB-5000
- Pressure testing per NB-6000

The following components of the cask assembly shall be excluded of the above requirements:

- Shielding lead and its installation
- [[ ]]
- Seals and test port components
- Electro-polishing
- Miscellaneous equipment (e.g., name plate and its screws, honeycomb, and thread inserts)

Overpack assembly per Subsection NF (Reference 8-5):

- Materials per NF-2000
- Fabrication per NF-4000
- NDE per NF-5000

HPI and material basket Importance to Safety Category B components and welds (Reference 8-5):

- Materials per NF-2000
- Forming, fittings, and aligning per NF-4200
- Welding per NF-4400
- Qualification of Weld Procedures and Personnel per NF-4300
- Examination per NF-5000

The shielding materials of the HPI shall be excluded of the above requirements.

8.1.3. Structural and Pressure Tests

The cask cavity is hydrostatically tested to ensure that it is tight, per the requirements of the ASME Boiler and Pressure Vessel Code, Section III, Subsection NB, NB-6200. The test pressure is 45 psia, 50% greater than the design pressure of 30 psia, per the requirement in 10 CFR 71.85(b).

8.1.4. Fabrication Leakage Tests

The fabrication leakage rate tests are performed in accordance with ANSI N14.5-1997, "American National Standard for Radioactive Materials – Leakage Tests on Packages for Shipment" (Reference 8-6) to ensure leaktightness of the cask welds and seals as follows. All leak testing

procedures are developed by an American Society for Nondestructive Testing (ASNT) Level III examiner per ASNT requirements.

During fabrication, maintenance, and periodic inspections, the cask containment boundary is tested to demonstrate whether it is leaktight in accordance with ANSI N14.5-1997. If the cask containment boundary is not demonstrated to be leaktight, the failed component is located, repaired or replaced, and reinspected. This applies to both the cask body and lid, as well as containment boundary components such as cask lid seal or port plugs.

8.1.5. Component and Material Tests

8.1.5.1. Valves, Rupture Discs, and Fluid Transport Devices

Component tests of valves, rupture discs and/or fluid transport devices are not applicable, because these parts do not exist in the Model 2000 Transport Package design.

8.1.5.2. Seal Testing

The procedure for testing the cask containment features is based on ANSI N14.5 and is conducted in accordance with the latest revision of the applicable GEH test specification. The justification for the [[ ]] retainer with four Parker Compound No. [[ ]] is as stated in Section 4.1.3. The port penetration containment boundary demonstration is documented in the test report summary, which demonstrates leak tightness for the port pipe plug with approved sealant. Test temperatures and pressures meet the HAC requirements as defined in Table 3.5.1-4.

The [[ ]] retainer with four Parker Compound No. [[ ]] is tested at room temperature. It is shown in the cold case analysis in Section 3.3.1.2, that with an internal wattage of 500 W, the minimum seal temperature at any of the seal regions is 21°F, with a minimum cask lid seal temperature of 45°F. These temperatures are clearly bounded by the minimum service temperature for [[ ]] (-70°F per Reference 1-2). The seal material is installed in a test flange and leak tested in accordance with ANSI N14.5. Seal material exceeding the allowable leak rate (leaktight per the ANSI N14.5 definition) is rejected. The test seal/flange joint used for the Parker Compound No. [[ ]] seal tests is a full-scale model in terms of flange and seal diameter with a representative cask body/lid joint fixture. The demonstration of the cask lid seal is documented in the test report summary.

8.1.5.3. Honeycomb Testing

The honeycomb energy absorber is tested in accordance with MIL-C-7438 latest revision (Reference 8-7), or equivalent. The test procedure determines the compressive properties of the honeycomb material in the direction normal to the plane of facings. The test produces a load deformation curve, and from this curve the compressive stress at proportional limit load is calculated. If the honeycomb material does not meet the required crush strength, the material is rejected.

8.1.6. Shielding Tests

The shielding material is inspected for integrity. A cobalt source placed inside the lead-shielded cask is surveyed from the outside of the cask with a gamma detection instrument. The cask outside surface is divided by radial lines 12° apart and by equally spaced circumferential lines along the vertical axis. Dose rate readings are taken over each of the 420 rectangular regions (~4 inches square); see Figure 8-1. If an area of void is detected, radiographic film is placed over this area to determine the size and location of the void. The criterion used to evaluate the effect of the void is that the dose rate may not exceed one and one-half times the mean dose rate. Any void area that does not meet the criteria shall be re-poured with lead.

The depleted uranium shielding in the HPI is cast and machined to a high precision, to the requirements of the licensing drawings. The shielding integrity of the HPI is determined during manufacturing, where voids in the depleted uranium are checked for using a visual inspection and the density is verified using the total volume and weight.

8.1.7. Thermal Tests

A thermal test is performed on the first unit built of the Model 2000 Transport Package to determine the thermal performance of the system versus what is predicted by the analysis. This test is only done for the 600 W and 2000 W cases. The 3000 W configuration testing is completed through analysis as described in Section 3. It should be noted that the cask design has been evaluated to support 3000 W decay heat as stated in Section 1.2.2.3. However, the allowable contents are limited to 1500 W decay heat.

8.1.7.1. Discussion of Test Setup

Two thermal tests are conducted, one each with a 600 W and a 2000 W heat source. The heat source is installed concentrically within the cask cavity. Thermocouples are strategically placed within the cavity and the external portions of the cask and overpack surfaces as schematically shown in Figure 8-2.

8.1.7.2. Test Procedure

The test is conducted with each of the heat sources in a controlled ambient environment to simulate normal conditions of transport. The temperature data are recorded every 30 minutes with a data acquisition system, permitting easy analysis and plotting of the results. Data are recorded until temperature remains significantly unchanged for a one-hour period.

8.1.7.3. Acceptance Criteria

The results of the thermal test are evaluated against the predicted thermal performances. If the evaluation shows a discrepancy, the analytical thermal model is corrected based on the test results and a new thermal analysis is conducted. If the new analysis results indicate deficiency in the thermal characteristics of the packaging, thermal barrier coating could be applied to the inner surface of the overpack structure as a corrective measure.

8.1.8. Miscellaneous Tests

No additional tests are required prior to the use of the packaging.

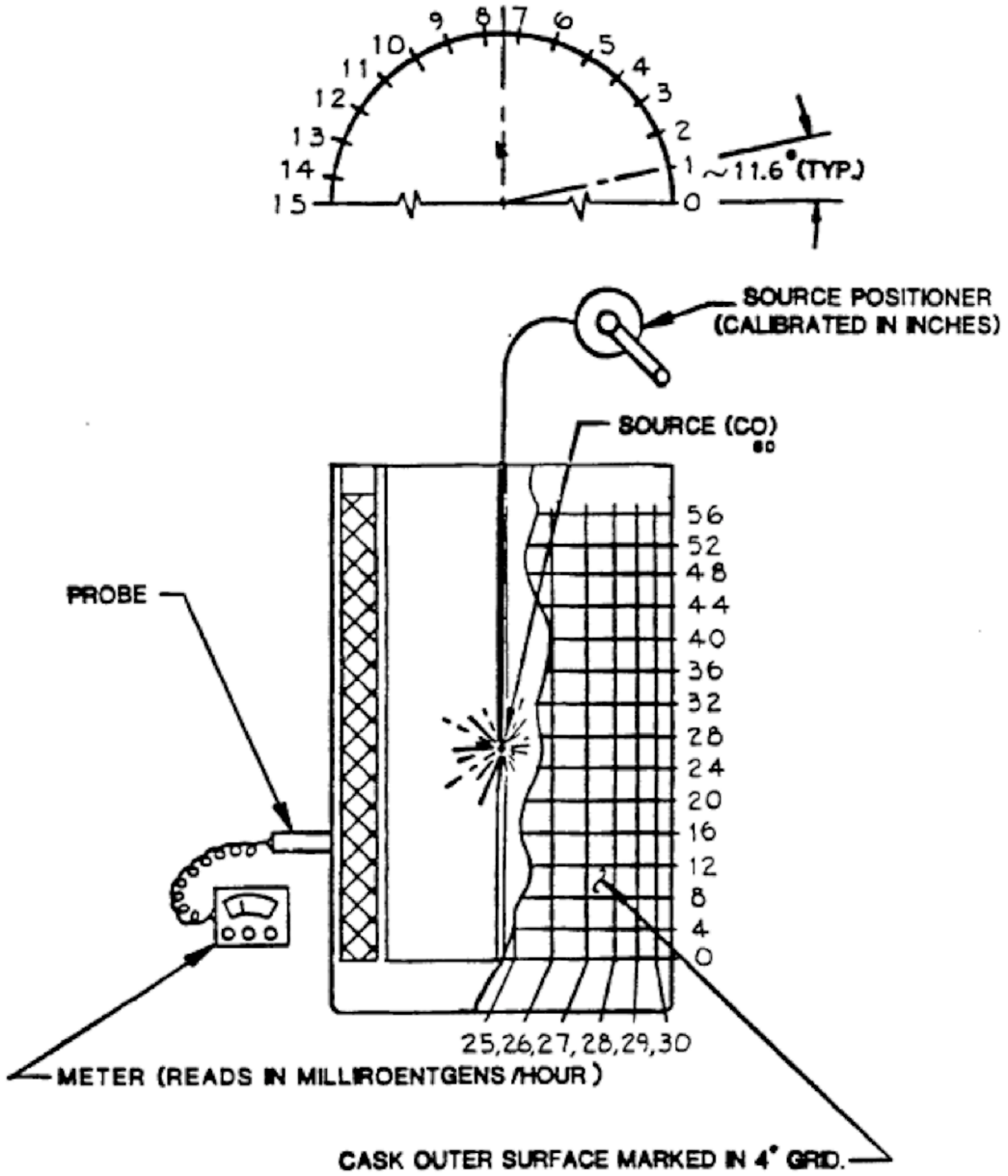

Figure 8-1. Cask Shielding Inspection Points

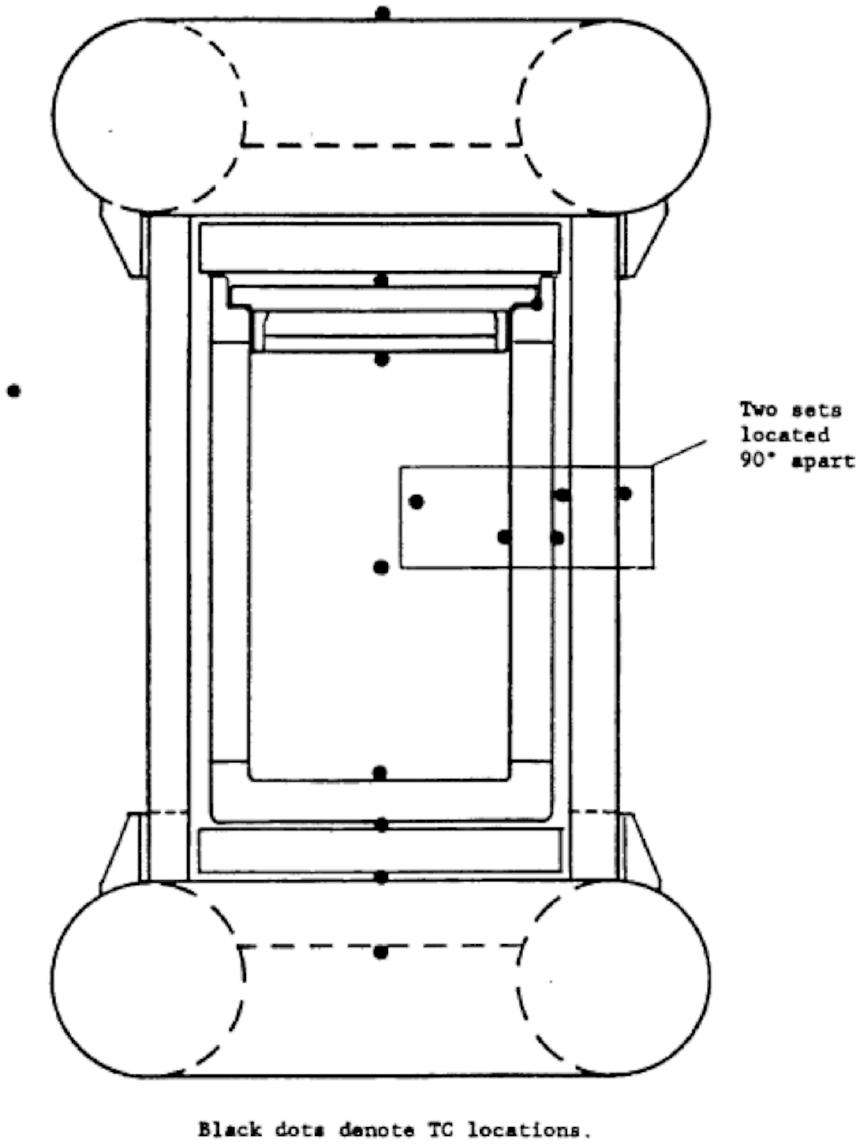

Figure 8-2. Thermocouple Locations

8.2 Maintenance Program

The cask maintenance program is described in detail in the GEH operations and maintenance specification for the Model 2000 Transport Package. The specification was developed to implement the requirements established in this chapter. Operators of the Model 2000 Transport Package may develop procedures of their own within the requirements of the GEH specification to include site-specific procedures.

Routine inspections are performed prior to each assembly and prior to each shipment. These inspections include visual checks of the packaging and any support structures or devices required to properly assemble the package. It also includes visual inspection of the cask and components and pressurization of the cask cavity. This pressurization is part of the leak check procedure. Additional, more detailed inspections are also performed every twelve (12) usages or at least once within the 12-month period prior to subsequent use, whichever comes first. The cask must be leak tested to 1×10^{-7} ref·cm^3/sec prior to its first use, after the third use, and at least once within the 12-month period prior to each shipment.

8.2.1. Structural and Pressure Tests

8.2.1.1. Routine Inspection

Prior to each loading and assembly operation, the cask and lid are inspected for physical damage, especially the bolt holes, vent ports and sealing surfaces. The cask lid closure bolts, port plugs, O-rings, and lid gasket are all inspected visually and for proper dimensions and identification. In addition, the cask lid closure bolts have a 190-use limit. As part of the leak check, the cask cavity is pressurized to 15 psig with helium and tested per the pre-shipment requirements listed in Section 8.2.2.1. The overpack, HPI assembly, and HPI material basket components are inspected for visible signs of damage.

8.2.1.2. Periodic Inspections

At least once within the 12-month period prior to each shipment, the following inspections are made. Any maintenance work required is identified on a maintenance check sheet.

The overpack is inspected for:

- Signs of excessive heat or fire.
- Punctures, holes, or other surface failures.
- Crushed sides or ends indicating a drop or severe impact.
- Defects resulting from normal or abnormal wear.
- Compression or damage to the honeycomb absorber material.
- Cracks or other damage to welds.
- Proper identification and damage to the bolts.

The cask is inspected for:

- Wear, corrosion or damage to the vent and drain port plugs, caps, and O-rings.
- Damage to sealing surfaces on the cask and lid.
- Damage or cracks to welds on the cask and lid.
- Proper identification or damage to the lid and ear bolts.

8.2.2. Leak Tests

The pre-shipment, periodic, and maintenance leak tests are all in accordance with ANSI N14.5 standards, with a reference air leakage rate (L_R) criterion of leaktight per the ANSI N14.5 definition of 1×10^{-7} ref·cm^3/sec. All leak testing procedures are developed by an ASNT Level III examiner per ASNT requirements.

8.2.2.1. Pre-Shipment

Prior to each shipment, leakage testing of the cask lid closure seal and vent and drain plugs may be performed with a helium Mass Spectrometer Leakage Detector (MSLD). The tests for the cask lid closure seal, vent port, and drain port are performed to ensure each containment boundary seal is leaktight, per the ANSI N14.5 definition (1×10^{-7} ref cm^3/sec).

8.2.2.2. Periodic

Prior to its first use, after the third use, and at least once within the 12-month period prior to each shipment, the cask lid closure seal and vent and drain plugs are tested to ensure each containment boundary seal is leaktight, per the ANSI N14.5 definition (1×10^{-7} ref cm^3/sec).

8.2.2.3. Maintenance

After any maintenance on the cask affecting a component of the containment boundary, such as a repair of a containment boundary weld, the affected component is leak tested per ANSI N14.5 standards, ensuring leaktightness ($< 1 \times 10^{-7}$ ref·cm^3/sec) of the component.

8.2.3. Component and Material Tests

There are no auxiliary cooling systems or other subsystems requiring maintenance.

8.2.3.1. Valves, Rupture Disks, and Gaskets on Containment Vessel

The cask lid closure seal is used until visual and/or leak test inspections identify the seal as defective. The O-rings on the three penetration caps are replaced when visual or leak test inspections identify them as defective, or during the periodic inspection, whichever comes first.

8.2.3.2. Shielding

The shielding materials are lead and depleted uranium. The initial tests for voids during fabrication and the required radiological surveys following each loading assure shielding integrity. If the results of surveys exceed the regulatory requirements, the contents are reduced or the shipment is not initiated.

8.2.4. Thermal Tests

Thermal testing is only performed following initial fabrication of the cask.

8.2.5. Miscellaneous Tests

No additional periodic tests are required.

8.3 Appendix

The only appendix information for Chapter 8 is provided in Section 8.4, References.

8.4 References

8-1 GE Hitachi Nuclear Energy, "Quality Assurance Program for Transport Packages for Radioactive Material (Docket 71-0170)," QAP-1, latest approved version.

8-2 U.S. Nuclear Regulatory Commission (NRC), "Quality Assurance Program Approval for Radioactive Material Packages, Number 0170, Revision 11," May 12, 2014.

8-3 American Society of Mechanical Engineers (ASME), Boiler and Pressure Vessel Code, Division I, Section III, Subsection NG, "Core Support Structures," 2010.

8-4 American Society of Mechanical Engineers (ASME), Boiler and Pressure Vessel Code, Division I, Section III, Subsection NB, "Class 1 Components," 2010 with addenda.

8-5 American Society of Mechanical Engineers (ASME), Boiler & Pressure Vessel Code, Division I, Section III, Subsection NF, "Component Supports," 2010.

8-6 American National Standards Institute (ANSI), "American National Standard for Radioactive Materials – Leakage Tests on Packages for Shipment," ANSI N14.5, 1997.

8-7 Military Specification, "Core Material, Aluminum, for Sandwich Construction," MIL-C-7438, or Equivalent.